A Genetic Study of Primary Angle-Closure Glaucoma and Nanophthalmos

Dr Mona S Awadalla, MBBS

Thesis is submitted for the degree of Doctor of Philosophy

Department of Ophthalmology

Faculty of Health Sciences, Flinders University

Adelaide, South Australia

January 2013

TABLE OF CONTENTS

SUMMARY

Glaucoma is a term describing a group of ocular disorders with multi-factorial etiology united by a clinically characteristic intraocular pressure-associated optic neuropathy. Collectively, they are the leading cause of irreversible blindness worldwide. Primary angle-closure glaucoma (PACG) is a subtype of glaucoma characterised by irido-trabecular contact and elevated intraocular pressure (IOP). Almost half of individuals who reach legal blindness due to glaucoma have PACG. PACG may be clinically divided into acute and chronic forms, and the pathogenesis is multifactorial. Short axial length and a “crowded” anterior segment are established risk factors in the development of PACG. Similar but more extreme clinical findings are found in a rare developmental disorder known as nanophthalmos. Recent studies have highlighted the heritable component of both nanophthalmos and PACG. The aim of this thesis was to further explore genetic risk factors in the development of nanophthalmos and PACG.

This study identified a novel variant c.577G>C located in exon 8 of *Transmembrane protein 98* (*TMEM98*) gene in a large family with autosomal dominant nanophthalmos, and reports variants of *Membrane frizzled-related protein* and *Protease serine 56* in two other families with nanophthalmos. These three genes were further analysed for association with PACG and borderline significance was identified, motivating further study on a larger cohort.

We then conducted a genome-wide association study (GWAS), which is an approach that involves scanning the whole genomes of many people to find genetic variations associated with a particular disease, on patients with PACG from two different cohorts available at the time of the study (Australia and Nepal). We chose different cohorts to investigate the differences in the allele frequencies and the genetic risks between these two cohorts. Unfortunately no significant single nucleotide polymorphisms (SNPs) reaching genome-wide significance were detected from this GWA study, so we aimed to build up the PACG cohort for the next larger GWAS.

Meanwhile, analyses of previously published candidate gene studies for PACG were undertaken. This study shows that common variation within *Matrix metalloproteinase-9*, and *Endothelial nitric oxide synthase* genes were significantly associated with PACG in the Australian cohort, while the *Hepatocyte growth factor* gene was associated with the disease in the Nepalese cohort. Finally, replication of three novel loci rs11024102 in *PLEKHA7* (*Pleckstrin homology domain containing, family A member 7*), rs3753841 in *COL11A1* (*Collagen, type XI, alpha 1*), and rs1015213 located between *PCMTD1* (*Protein-L-isoaspartate (D-aspartate) O-methyltransferase domain containing 1*) and *ST18* (*Suppression of tumorigenicity 18*) from a recent GWAS indicates replicated association of these candidate loci with PACG.

Data from this thesis advance understanding of the genes involved in the pathogenesis of nanophthalmos and PACG. It may assist in refining of the genetic screening programs to identify individuals at particularly high risk, especially in families with nanophthalmos, as they develop blindness at a younger age.

Identification of *TMEM98* as a gene for autosomal dominant nanophthalmos is also a finding of significance, which requires further functional work to unveil the role of this gene in the human eye.

Publications arising from data presented in this thesis:

Awadalla MS, Thapa SS, Burdon KP, Hewitt AW, Craig JE. The association of *Hepatocyte growth factor* (*HGF*) gene with primary angle-closure glaucoma in the Nepalese population. *Mol Vis*. 2011;17:2248-54.

Awadalla MS, Burdon KP, Kuot A, Hewitt AW, Craig JE. *Matrix metalloproteinase-9* genetic variation and primary angle-closure glaucoma in a Caucasian population. *Mol Vis*. 2011;17:1420-4.

Awadalla MS, Thapa SS, Burdon KP, Hewitt AW, Craig JE. A cross-ethnicity investigation of genes previously implicated in primary angle-closure glaucoma. *Mol Vis*. 2012;18:2247-54.

Awadalla MS, Thapa SS, Hewitt AW, Craig JE, Burdon KP. Association of *eNOS* with primary angle-closure glaucoma. *IOVS*. 2013;5:2108-14

Awadalla MS, Thapa SS, Hewitt AW, Burdon KP, Craig JE. Association of genetic variants with primary angle-closure glaucoma in two different populations. *PlosOne*. 2013; 8:e67903

Awadalla MS, Laurie K, Coote MA, Walland MJ, Casson RJ, Kuot A, Galanopoulos A, Souzeau E, Usher B, Burdon KP, Craig JE. Genetic variation of *MFRP* and *PRSS56* in families with nanophthalmos. *Clinical and Experimental Ophthalmology*. Submitted August 2013.

Awadlla MS, Burdon KP, Souzeau E, Landers J, Hewitt AW, Sharma S. Craig JE. A mutation in *TMEM98* in a large Caucasian kindred with autosomal dominant nanophthalmos linked to 17p12-q12. *JAMA ophthalmology*. Submitted August 2013.

SIGNED DECLARATION

I certify that this thesis does not incorporate without acknowledgment any material previously submitted for a degree or diploma in any university; and that to the best of my knowledge and belief it does not contain any material previously published or written by another person except where due reference is made in the text.

Mona S Awadalla

ACKNOWLEDGEMENTS

This thesis is dedicated to my amazing family. My father Prof Salaheldin Awadalla has been my inspiration since I was a little girl, I always dreamt to be like him. My appreciation goes to my beautiful mother for her endless encouragement and support. Together they taught me how to challenge life and to get the best out of it. Their emotional and financial support has enabled me to comfortably fulfil my passion for research. I thank my brothers Mohamed and Maged for being so supportive and for always being there for me in my ups and downs. They have provided utmost emotional encouragement and support for the last three years and also shared the joys of outcomes and successes of this project. To my fiancée Moataz, thank you for enlightening my life with your love, smile and kind heart.

Working on my PhD in the Department of Ophthalmology has been an overwhelming and rewarding experience. I have had the greatest honour to work under the supervision of Associate Professor Jamie Craig and Dr Kathryn Burdon. I strongly believe that anyone who has the chance to work with them is extremely lucky. To Jamie, you have been a steady influence throughout my PhD candidature with your support, care and encouragement in times of new ideas and difficulties. Thank you for being a person open to ideas, and for helping me to shape my research interests. To Kathryn, I cannot thank you enough for your tremendous support and always finding time for me. The outcome of the project in this timeframe would not be possible without you. Furthermore, I am grateful to my co-supervisors Professor Robert Casson and Professor David Mackey for their insightful comments in this thesis, and for their many motivating discussions.

Professor Douglas Coster is sincerely thanked for believing in my ambition when I first came to Flinders Eye Clinic as an ophthalmologist trainee in 2005, he encouraged me to always aim for the top. I am really grateful for his incredible generosity and support and for being my honorary father in Australia.

I thank all participants who contributed in this project. I am grateful to the ophthalmologists who assisted with recruitment of participants; Prof Robert Casson, Dr Mark Walland, Dr Guy D'Mellow, Dr Richard Mills, Dr Stewart Lake, Dr Michael Coote, Dr Deepa Taranath, Dr John Landers, Dr Erica Mancel, and Dr Anna Galanopoulos. Assistance for the recruitment of participants by Dr Suman Thapa from the Nepal eye clinic and Dr Alex Hewitt for recruiting the Normal South Australian cohort is highly appreciated.

The Department of Ophthalmology Centre for Clinical Research Excellence of Flinders Medical Centre, the FMC Foundation, the National Health and Medical Research Council (NH&MRC), Flinders University and the Ophthalmic Research Institute of Australia are acknowledged for their funding support.

I would love to thank Ms Emmanuelle Souzeau for her effort as a genetic counsellor and together with Ms Bronwyn Ridge for their effort in assisting with the recruitment of patients and data collection. The assistance I have received from the Ophthalmology laboratory group is appreciated: Mr Abraham Kuot, Ms Sarah Martin, Ms Alpana Dave, Ms Greta David, Mrs Kathleen Dowell, Mr Rhys Fogarty,

Ms Shari Javadiyan and Ms Kate Laurie. I also acknowledge Dr Stuart MacGregor at the Queensland Institute of Medical Research for conducting and analysing the genome-wide pooling data in chapter 3. As the thesis is the end result of team work, so the pleural personal pronoun “we” was used instead of the singular form. One sure thing is the rewarding experience I have received working in the Department of Ophthalmology, Flinders Medical Centre from everyone, particularly Dr Georgia Kaidonis, Dr Jude Fitzgerald, Dr David Dimasi, Dr Shiwani Sharma, Ms Deb Sullivan, Dr Miriam Keane, Mrs Lynda Saunders, Ms Anne Cazneaux, Ms Lyn Harding and Prof Keryn Williams.

Chapter 1

INTRODUCTION

Glaucoma

The term glaucoma was first used by the ancient Greeks to describe a form of ocular pathology that may, in fact, have been a cataract. A clear difference between cataract and glaucoma was not described until 1705. At the beginning of the 19th century a French physician (Dr A. Demours) showed that an increase in intraocular pressure (IOP) can lead to glaucoma. In 1973, Drance was the first to describe glaucoma as an optic neuropathy influenced by several risk factors. (Mantzioros 2006)

In modern nomenclature, Glaucoma is a term describing a group of ocular disorders with multi-factorial aetiology united by a clinically characteristic intraocular pressure-associated optic neuropathy. (Casson, Chidlow et al. 2012) It is not a single entity and is sometimes referred to in the plural as “the glaucomas”. All forms are potentially progressive and can lead to blindness. The different subtypes of glaucoma each vary in their pathophysiology and clinical presentation; (Morrison and Pollack 2003; Knaski 2008) however, an elevated IOP is present at some stage of the disease process in all forms of glaucoma except so-called, normal tension glaucoma.

Loss of vision from glaucoma is preventable but irreversible. In Australia, the cost of managing glaucoma exceeds AUS$50 million per year with the cost of glaucoma-related prescriptions alone increasing from $19 million per year in 1994 to $71 million per year in 2003. (Walland 2004)

Classification of Glaucomas

Glaucomas are classified by the anatomy and appearance of the irido-corneal angle, located at the junction between the iris and cornea in the anterior chamber, into two main groups: open-angle glaucoma, and angle-closure glaucoma.

Primary open-angle glaucoma (POAG) is the most common form of glaucoma worldwide. POAG shows normal structure of the anterior chamber of the eye with normal anterior chamber depth (ACD), and a wide open irido-corneal angle (**Figure 1.1.a**). (Yong, John et al. 2009) Primary angle-closure glaucoma is caused by anatomical narrowing of the anterior chamber angle, and is characterized by irido-trabecular contact, an elevated IOP and glaucomatous optic neuropathy (GON) (**Figure 1.1.b**).

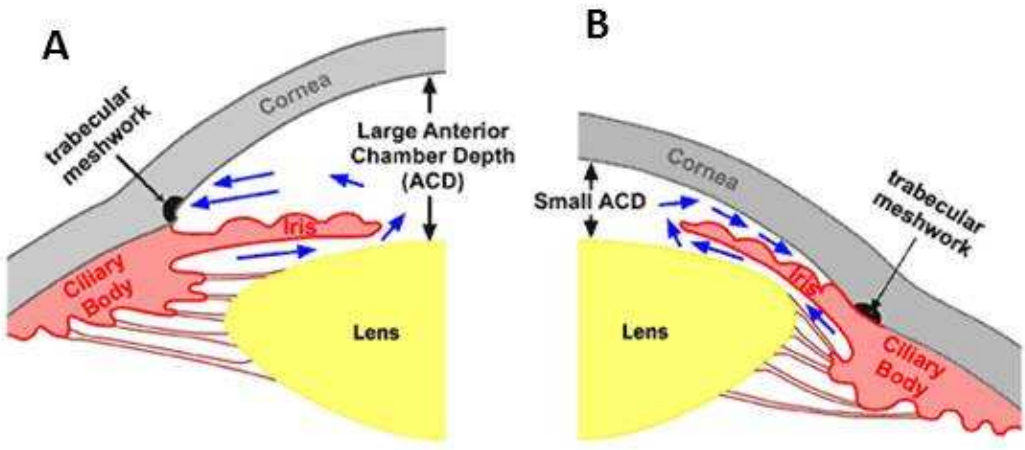

Figure 1.1. Structure of the anterior chamber of the eye. POAG (A) the drainage angle formed between the cornea and the iris is wide open ~40˚.The anterior chamber depth is large. PACG (B) the iris and trabecular meshwork in contact (irido-trabecular contact) blocking the flow of aqueous. Note the anterior chamber depth is shallow. (Adapted from http://www.medrounds.org)

Primary Angle-Closure Glaucoma

PACG has been classified into three categories following the International Society of Geographical and Epidemiological Ophthalmology (ISGEO) classification as described by Foster and colleagues; (Foster, Buhrmann et al. 2002)

- Primary angle-closure suspect (PACS) has an "occludable" angle on gonioscopy with IOP less than or equal to 21 mmHg and no glaucomatous damage.
- Primary angle-closure (PAC) is defined by the presence of peripheral anterior synechiae (adhesion of the iris to the cornea), or elevated IOP greater than 21 mmHg without evidence of optic disc damage.
- Primary angle-closure glaucoma (PACG) is the presence of glaucomatous optic neuropathy with irido-trabecular contact.

PACG is further subdivided into acute, subacute and chronic clinical forms. The acute type is characterized by a sudden severe elevation of IOP with corneal oedema and associated severe ocular pain. There may be an ischaemic component to the optic neuropathy and this subtype is visually devastating without emergency reduction of the IOP.

The subacute form is characterized by peripheral anterior synechiae and a history of periodic unilateral headache, blurred vision and coloured halos, and may resolve without treatment. (Sihota and Agarwal 1998)

Chronic PACG is usually asymptomatic and its diagnosis relies on gonioscopy, which makes it more likely to go undetected. (Quigley, Congdon et al. 2001) It is characterized by a chronically elevated IOP with irido-trabecular contact and the presence of glaucoma optic neuropathy. (Foster, Buhrmann et al. 2002)

The pathogenesis of PACG is complicated and involves anatomical, physiological and/or environmental factors. Whether a particular anatomically predisposed eye will develop PACG is quite unpredictable. (Hung and Chou 1979) Wang et al, showed that only 10% of individuals with narrow-angles developed PACG. (Wang, Wu et al. 2002) Different studies have divided PACG into three categories according to the mechanism of action; (Ningli, Wenbin et al. 1997; Wang, Wu et al. 2002; Huang and Barocas 2004)

1. Pupillary block: The term pupillary block has been used to define any of the various mechanisms which interfere with the forward flow of aqueous humor through the pupil. (Shaffer 1973) It is the most frequent and clinically treatable type, is usually associated with increased lens curvature, short zonule-iris distance and formation of iris bombe. It is associated with acute and sub-acute attacks. Permanent resolution may be achieved by iridectomy or laser iridotomy.
2. Non-pupillary blocking: may be associated with a classic plateau iris configuration or may occur without characteristic plateau features. In plateau iris, the iris root is angulated forward and centrally by anterior located ciliary processes. The iris appears flat by gonioscopy, and the central anterior chamber is not shallow. Plateau iris is found in up to 30%

of PACG patients who had laser iridotomy. (Kumar, Tantisevi et al. 2009)

3. Multi-mechanism: Several factors are involved such as pupillary block, crowding of the anterior chamber, especially in the presence of an enlarging lens due to cataract, and an anatomically anteriorly positioned iris.

Incidence of primary angle-closure glaucoma

Glaucoma is the leading cause of irreversible blindness worldwide and it is estimated that 80 million people will be affected by 2020. (Quigley and Broman 2006) Blindness is reported to be 25% more likely in people with PACG than POAG worldwide. (Foster and Johnson 2001) PACG is reported to be the cause of blindness for about half of blind glaucoma patients, and it has high visual morbidity rates, particularly in Asian individuals. The number of patients with PACG is expected to rise by approximately 5 million people, from 16 million over the next decade. (Casson 2008)

PACG has been shown to be the most common cause of bilateral blindness in Singapore, China and India. (Quigley, Congdon et al. 2001) In contrast, Caucasian populations have an overall prevalence of approximately 0.4%. (Day, Baio et al. 2012) The prevalence of acute PACG in Caucasians living in Israel was noted to be higher than other Caucasian populations, indicating that environmental factors may be involved. (Ivanisevic, Erceg et al. 2002)

Risk factors

PACG has anatomical risk factors: short axial length, small corneal diameter, thick anteriorly positioned crystalline lens, and hyperopic refractive error. (Salmon 1999) A shallow anterior chamber depth (ACD) is the most important risk factor, because it is consistently present, and is a heritable trait. (Alsbirk 1976; Alsbirk 1992; Aung, Nolan et al. 2005) It shows an association with older age, gender (more shallow in females) and race (more common in Eskimos and Asians). (Salmon 1999) The parents of affected individuals will often be deceased, whilst children will be too young to manifest disease.

Casson has suggested that the reason for the shallow anterior chamber found in certain people of Asian extraction is that this trait originated in *H. sapiens* in north-east Asia as an anatomical adaptation to resist corneal freezing and that their descendants possess the trait. (Casson 2008)

Aging plays a role in the disease development as the crystalline lens gets thicker and displaces the iris forward leading to apposition of the trabecular meshwork, relative pupil block and development of peripheral anterior synechiae as found in chronic angle-closure glaucoma. (Bonomi, Marchini et al. 2000)

Glaucoma in Nanophthalmos

Nanophthalmos (interchangeably referred to as simple microphthalmia) and posterior microphthalmia (PM) are two rare subtypes of microphthalmia. Microphthalmia is a developmental eye disorder of bilaterally small eyes, and is

characterised by the axial length of the globe being more than 2 standard deviations smaller than the normal range (< 20 mm in adults). (Vingolo, Steindl et al. 1994) The cornea and lens are typically of normal size, (Sundin, Dharmaraj et al. 2008) causing high lens to eye volume ratio and severe hyperopia (farsightedness) of +7.00 dioptres or more. (Othman, Sullivan et al. 1998) In patients with nanophthalmos, the decrease in the anterior chamber's dimensions cause the iridocorneal angle to be typically narrow, and abnormal thickening of the scleral connective tissue is often observed. (**Figure 1.2**) (Sundin, Leppert et al. 2005; Sundin, Dharmaraj et al. 2008) The abnormal structure of the anterior chamber observed in nanophthalmos differs from posterior microphthalmia where the anterior chamber is of normal dimensions (Spitznas, Gerke et al. 1983; Khairallah, Messaoud et al. 2002; Khan 2006) and patients with posterior microphthalmia do not tend to develop angle-closure glaucoma. (Khairallah, Messaoud et al. 2002) Recently, a study has revealed that eyes with posterior microphthalmia have corneal steepening proportional to the degree of the short axial length, suggesting that both nanophthalmos and posterior microphthalmia are not a distinct phonotype but they represent a spectrum of high hyperopia. (Nowilaty, Khan et al. 2013)

The worldwide prevalence of all microphthalmias is approximately 1-5 per 10,000 births. (Eurocat work group 2010; International Clearing House for Birth Defects Surveillance and Research 2010)

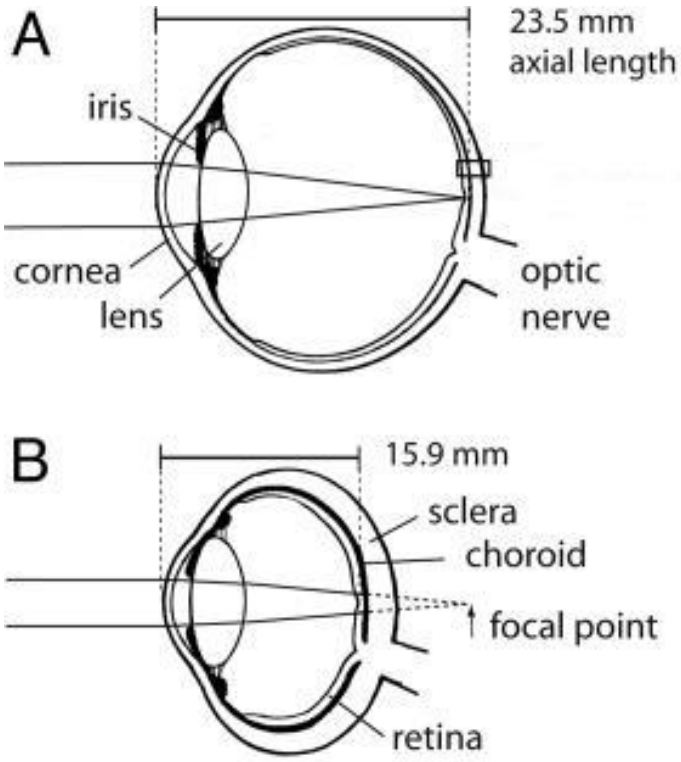

Figure 1.2. Morphological features of nanophthalmos. A diagram of the eye in sagittal section, showing the difference between (A) Normal eye, and (B) eye with Nanophthalmos. (Sundin, Leppert et al. 2005)

The aetiologies of different types of microphthalmia are varied and includes teratogens, foetal alcohol syndrome and intra-uterine infection (Kallen, Robert et al. 1996) but most cases are considered to be due to genetic defects. (Verma and Fitzpatrick 2007) Nanophthalmos is often reported in conjunction with other systemic abnormalities including cardiac defects and facial clefts. (Kallen, Robert et al. 1996)

Secondary complications from microphthalmia result from the small eye being required to accommodate a normal sized retina, causing loss of the foveal pit from

slippage between the retina and retinal pigment epithelium (RPE) and the formation of macular folds. (Sundin, Leppert et al. 2005) Retinal detachment can also occur due to the accumulation of fluid between the RPE and retina, driven by the thickened sclera, which reduces the flow through choroidal vessels. (Sundin, Leppert et al. 2005)

Development of angle-closure glaucoma in patients with nanophthalmos most commonly results from the forward displacement of the iris towards the cornea, with obstruction of the irido-corneal angle and formation of peripheral anterior synechiae (PAS). (Singh, Simmons et al. 1982)

Investigation of Angle-Closure Glaucoma

With more than 50% of patients with PACG undiagnosed, the rate of detecting early asymptomatic cases should be increased through encouraging family members of an affected individual to be screened and examined, as PACG tends to run in families. (Green, Kearns et al. 2007) Public health education, screening and early diagnosis are important ways to avoid permanent blindness. (Flanagan 1998) This will help to monitor the disease progression, to initiate timely treatment and postpone the complications.

First-degree relatives of PACG cases should be screened from the age of 40 years. If the initial assessment is normal, it has been recommended that 2-year interval reviews should be done until the age of 50 years then annual review thereafter. (Kanski 2007)

To diagnose a patient with angle-closure glaucoma, we should assess;

Visual field. Humphery perimetery is used for assessment of visual field. Early changes of glaucomatous damage show asymmetrical defects between both eyes which develop to nasal scotoma, paracentral scotoma, arcuate scotoma, ring scotoma and finally by adherence of all scotomas leaving small islands of central and temporal vision. (Kanski 2007)

Comparing the visual fields between PACG and POAG, the damage is more diffuse in the angle closure type while there is no difference in the structural damage uniformity in both types when measured by OCT NFL thickness. (Boland, Zhang et al. 2008)

Anterior chamber angle.

- Gonioscopy is an important diagnostic tool to pick up early changes in the anterior chamber (AC) of PACG and should be considered as a routine part of the eye examination (Vijaya, George et al. 2008). It may be either diagnostic for any abnormalities in the angle and estimation of its width, or therapeutic by visualisation of the angle during laser trabeculoplasty or goniotomy procedure (Kanski 2007).
- Ultrasound BioMicroscopy (UBM) is a high frequency B scan to assess the configuration of the angle and analyse the mechanism of angle closure dynamically. (Pavlin, Easterbrook et al. 1993) It is helpful in extreme narrow angles, where it is so difficult to clarify the iris insertion position by gonioscopy even with indentation, also preferred in dark room provocative testing. (Elaine K. Woo, Pavlin et al. 1999)

Intraocular pressure. Intraocular pressure is measured using a Goldmann applanation tonometer. It measures the pressure by the amount of force applied to flatten the cornea. If the patient is bed ridden or anaesthetized we can use Perkin applanation tonometer, a hand-held tonometer.

Optic disc changes. Disc changes are assessed by optical coherence tomography (OCT) showing multiple cross sections of the retina using high-resolution quality. (Kanski 2007)

Management of Primary Angle-Closure Glaucoma

The main goal for treatment is to prevent further damage to the optic nerve head thus saving vision. To date, the only method used to achieve this target is to maintain the IOP within the normal range. It is essential to monitor the progress of the disease by baseline evaluation, and the follow-up visits.

Laser Peripheral Iridotomy

Laser peripheral irodotomy is the cornerstone of managing PACG due to pupil block, and, if treatment is indicated, is generally recommended in all forms of angle-closure to eliminate any element of pupil block. Laser peripheral irodotomy allows aqueous to flow directly from the posterior to the anterior chamber circumventing the pupil block to aqueous flow, and allowing the peripheral iris to move away from the trabecular meshwork. However, this approach will not be effective in the presence of peripheral anterior synechiae, or non-pupil block mechanisms, or in the presence of a very large lens due to cataract.

Medication

Ocular hypotensive therapy is routinely used in concert with laser peripheral irodotomy to achieve reduction of IOP when it remains high despite laser peripheral irodotomy. Medications such as prostaglandin analogues, carbonic anhydrase inhibitors, α- agonists and β- antagonists, have been shown to prevent the progressive damage of the optic disc and visual field loss in cases with chronic PACG by lowering the IOP. (Sharmini, Yin et al. 2009)

Laser Peripheral iridoplasty

Laser peripheral iridoplasty acts by pulling the iris root away from the angle through immediate focal iris stromal contraction leading to widening of the irido-corneal angle. It can be used alone, or combined with medical treatments in managing acute PACG. Both strategies have a similar result of lowering the IOP by greater than 75% within an hour after the iridoplasty in cases of acute PACG. (Lam, Lai et al. 1998; Tham, Lai et al. 1999)

Trabeculectomy

If the IOP cannot be controlled medically or following laser treatment then trabeculectomy is an effective method to control IOP in both acute and chronic PACG. Unfortunately the failure rate of the surgery in PACG is higher than that of POAG. (Aung, Tow et al. 2000) The eyes should be monitored frequently afterwards to ensure that the IOP remains within normal range. (Tarongoy, Ho et al. 2009)

Phacoemulsification

Removal of the lens, either as a clear lens extraction or cataract extraction will relieve appositional iriodotrabecular contact and is a possible surgical option. The prevalence of PACG decreases with an increase in the rate of cataract surgery. The

surgery widens the anterior chamber and irido-corneal angle as the artificial intraocular lens inserted is much narrower than the natural crystalline lens, thus reducing the incidence of acute attack of PACG. (Keenan, Salmon et al. 2009)

Genetics considerations in angle-closure glaucoma

At the beginning of this study, the genetic contribution to PACG was largely unknown. Pathogenesis of PACG has a multi-factorial inheritance (Lowe 1972) where there is interaction between multiple genes along with environmental factors, and not following Mendelian patterns except in the extreme case of nanophthalmos.

Family history and ethnicity highlight the genetic predisposition of the disease. PACG is more common in Asian and Eskimo populations than Caucasians, and first degree relatives of patients with PACG show higher probability of developing narrow angles. (Wang, Wu et al. 2002; Amerasinghe, Zhang et al. 2011) Most studies have looked for genetic associations with PACG by analysing a number of candidate genes in cohorts of unrelated cases. Genes were chosen for their previous association with other glaucoma subtypes or their association with one of the PACG risk factors such as hyperopia or short axial length.

Unlike PACG, primary open angle glaucoma has been much more extensively studied. Up to 20 different loci have been identified for this complex disease, but only a few have been replicated in further studies. (Fan, Wang et al. 2006) Of these loci, the relevant genes have been identified in only a few cases; *Myocilin,* at 1q24 (Fingert, Heon et al. 1999) *Optineurin* at 10p13 (Sarfarazi, Child et al. 1998; Alward,

Kwon et al. 2003; Craig, Hewitt et al. 2006) *WD repeat-containing protein 36* at 5q22.1. (Monemi, Spaeth et al. 2005; Hewitt, Dimasi et al. 2006) More recently, genome-wide association studies have identified; *SIX homeobox 1/ SIX homeobox 6* (*SIX1/SIX6*) at 14q23.1 (Ramdas, van Koolwijk et al. 2010; Wiggs, Yaspan et al. 2012) *Caveolin 1/ Caveolin 2* at 7q31.1 *(CAV1/CAV2)* (Thorleifsson, Walters et al. 2010; Wiggs, Kang et al. 2011) *Transmembrane and coiled-coil domains 1 (TMCO1)* at 1q22-q25, and *CDKN2B antisense RNA 1* (*CDKN2B-AS1)* at 9p21.3. (Burdon, Macgregor et al. 2011; Sharma, Burdon et al. 2012)

Because glaucoma consists of many subtypes of diseases with overlapping phenotypic similarities, researchers have studied forms of glaucoma grouped according to specific clinical features. For example age of onset (such as in juvenile and congenital forms of glaucoma), or clinical presentation (such as secondary glaucomas associated with pigment dispersion or exfoliation syndrome). Identifying *Myocilin* as a glaucoma-causing gene and its role accounting for up to 4% of POAG was the end result of multiple cumulative experimental approaches. The mutations within the *Myocilin* gene were discovered in a large autosomal dominant family pedigree affected with juvenile open-angle glaucoma. (Stone, Fingert et al. 1997) Then myocilin protein had been detected in the trabecular meshwork by cellular studies. (Polansky, Fauss et al. 1997) Subsequent studies have reported that approximately 3–5% of primary open-angle glaucoma cases worldwide are attributable to mutations in the *Myocilin* gene. (Wiggs, Allingham et al. 1998; Fingert, Heon et al. 1999) Recently a mouse model of *Myocilin* glaucoma has been developed to investigate the role of this gene in the development of POAG. (Shepard,

Jacobson et al. 2007; Paper, Kroeber et al. 2008) By combining all these results, we have a better understanding of *Myocilin* function and its role in POAG pathogenesis.

The same strategy needs to be conducted for PACG, so the first target is to identify the causative gene(s) for PACG. Until mid-2012 there was no genome-wide association study (GWAS) published for PACG. The complex nature of the disease, the late age of onset, and the lower prevalence of PACG in our population has made the search for causative genes difficult in comparison to POAG. Recently, the first genome wide association study for PACG was conducted in a large group of patients with PACG from Asian ethnic groups identifying three new susceptibility loci; rs11024102 in *PLEKHA7;* rs3753841 in *COL11A1*, and rs1015213 located between *PCMTD1* and *ST18.* (Wilkins, Gasteiger et al. 1999)

Unlike PACG, nanophthalmos has been linked to several specific genes and loci. For autosomal dominant nanophthalmos, studies have reported linkage to chromosome 11p (Othman, Sullivan et al. 1998) 2q11-q14 (Li, Wang et al. 2008) and 17p12-q12. (Hu, Yu et al. 2011) To date additional families showing linkage to these regions have not been reported and the causative genes in these families has not been identified. For autosomal recessive nanophthalmos, two major genes have been reported *Membrane frizzled-related protein* (*MFRP)* (Sundin, Leppert et al. 2005) and *Protease serine 56* (*PRSS56*). (Gal, Rau et al. 2011; Orr, Dube et al. 2011) Mutations in the *MFRP* gene have been shown to cause autosomal recessive nanophthalmos, both isolated (Sundin, Leppert et al. 2005) or in conjunction with retinitis pigmentosa and other retinal features. (Ayala-Ramirez, Graue-Wiechers et

al. 2006; Zenteno, Buentello-Volante et al. 2009; Mukhopadhyay, Sergouniotis et al. 2010) *MFRP* is a frizzled related protein likely involved in the Wnt signalling pathway, important in ocular development. (Sundin, Leppert et al. 2005) The gene is expressed in retina during the later stages of embryonic development and patients homozygous for *MFRP* mutations do not appear to undergo the normal process of axial growth to correct refraction and obtain emmetropia. (Sundin, Dharmaraj et al. 2008) *PRSS56* is a serine peptidase of the chymotrypsin family, and has been reported following linkage analysis and fine mapping in nanophthalmos families from Tunisia and the Faroe Islands. (Gal, Rau et al. 2011) *PRSS56* is highly expressed in retinal ganglion cells and may also be involved in the remodelling of the eye during early post-natal development to establish emmetropia. (Gal, Rau et al. 2011)

The importance of identifying the genetic cause behind these two eye conditions is to reduce blindness from this severe condition, and to improve our understanding about the development of the disease. This can offer better methods for improving the diagnosis and the treatment. Identifying the genetic risk can help us to screen the high risk individuals on a regular basis and provide early management of any complications that rise from this condition. We hypothesised that due to the high rate of angle-closure glaucoma in individuals with nanophthalmos, identified causative genes for this condition would also be attractive candidates for PACG.

In this thesis, I set out to achieve a better understanding of genetic contributions to ACG, with the following specific aims:

1. To identify the genetic risk factors in the development of PACG and attempting to replicate previously associated candidate genes in two different populations (Australian Caucasian and Nepalese cohorts) recruited as part of this PhD project.

2. To investigate genetic causation in families with nanophthalmos and, to seek association of nanophthalmos genes with PACG disease.

Chapter 2

MATERIALS AND METHODS

2.1 Nanophthalmos

Participant recruitment

Twelve families with at least one affected member participated in this study (**Figure 2.1**). Nanophthalmos was defined as: bilateral symmetrical small eyes, with axial length <20 mm, hyperopic refractive error >+7.00 dioptres, shallow anterior chamber, thick lenses and thick sclera.

This study adhered to the tenets of the declaration of Helsinki and approval was given by the Southern Adelaide Clinical Human Research Ethics Committee. Written informed consent was obtained from all participants.

The participants were referred to the Australian New Zealand Registry of Advanced Glaucoma (ANZRAG) by their treating specialist. (Souzeau, Goldberg et al. 2011) All families were from Australia except for Families 9, 10 and 11 which were from New Caledonia. Genomic DNA was extracted from either peripheral whole blood using QiaAmp DNA blood Maxi Kit (Qiagen, Doncaster, Victoria, Australia) or from saliva using Oragene® saliva DNA collection kits (DNA Genotek, Ottawa, Canada) according to manufacturer's protocols.

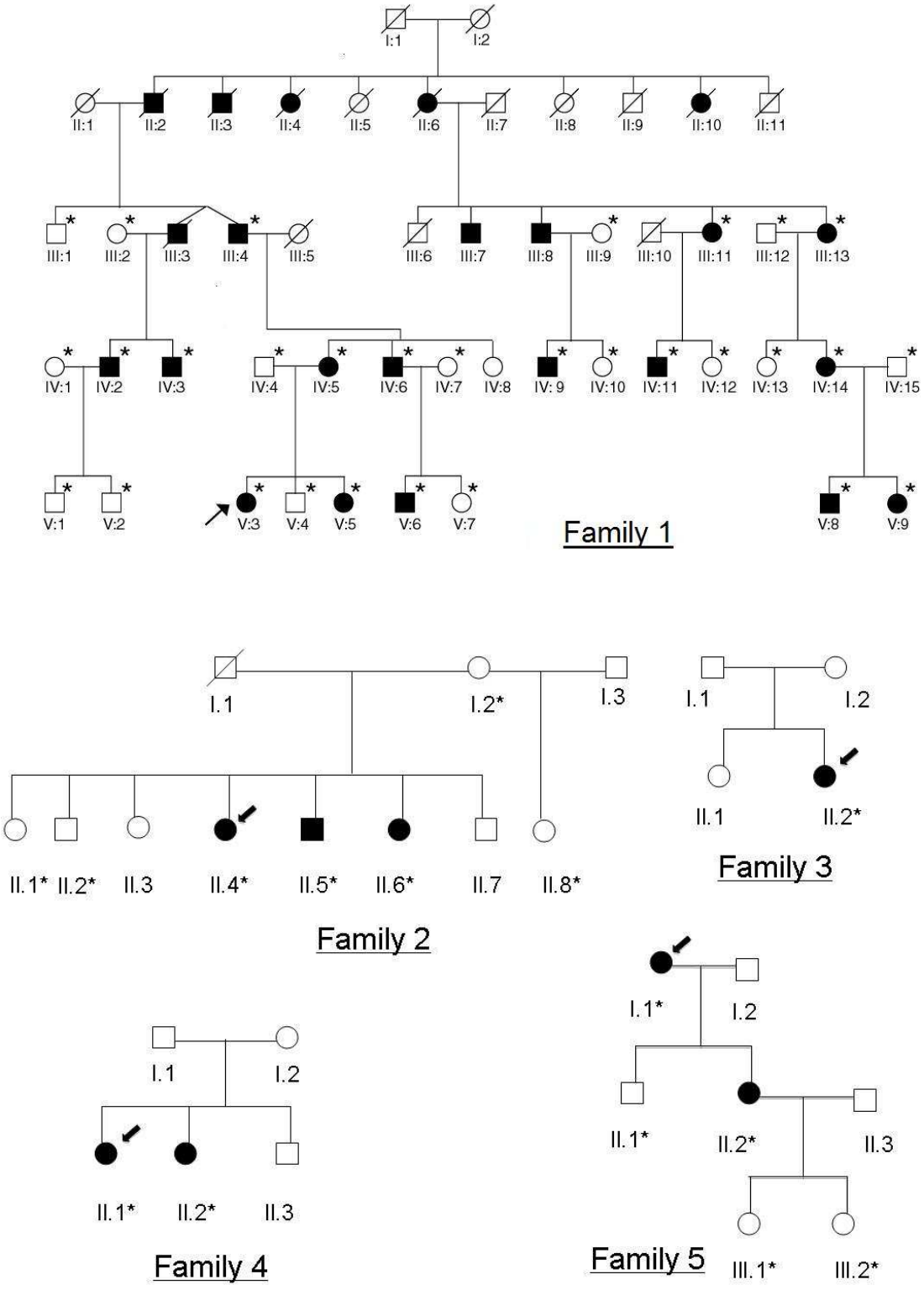

Figure 2.1. Pedigrees of nanophthalmos families. (See next page for legend)

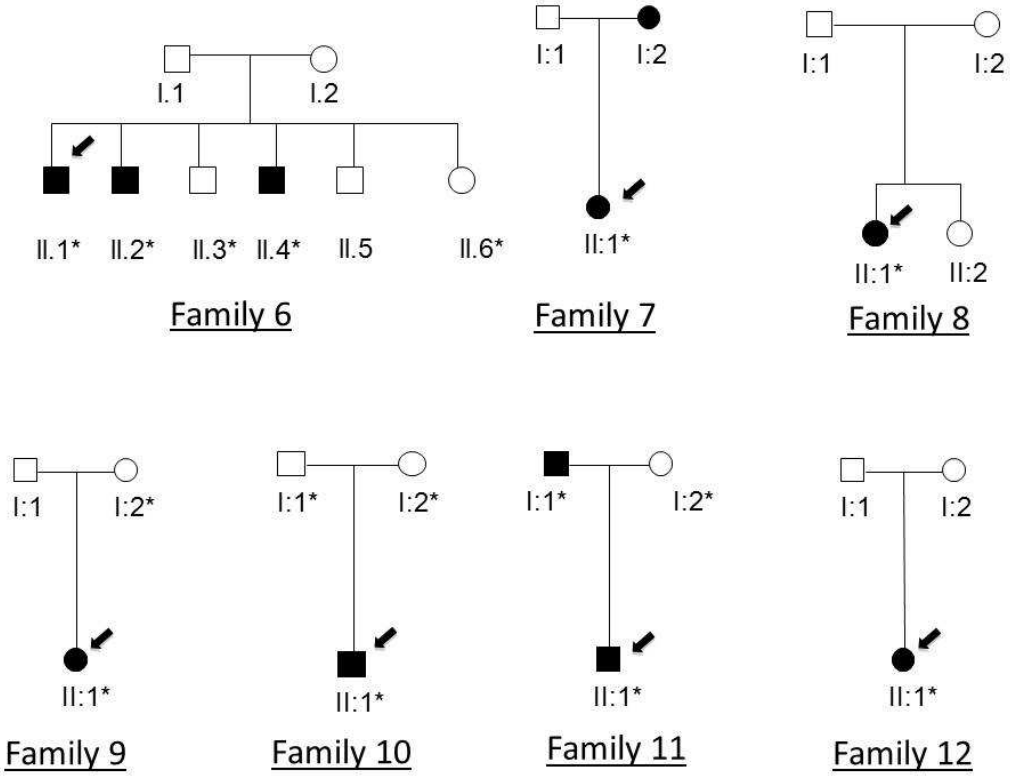

Figure 2.1. Pedigrees of nanophthalmos families. Square symbols indicate male, round symbols female, diagonal line deceased, dark symbols are individual with nanophthalmos, unfilled symbol unaffected individuals, the arrow points to the proband, and (*) indicates DNA collected.

Direct DNA sequencing

Primers were designed to amplify exons and flanking intron sequence (http://frodo.wi.mit.edu/) for *MFRP* (**Appendix 1**) and *TMEM98* (**Appendix 2**). Primers for sequencing *PRSS56* have been published previously. (Orr, Dube et al. 2011) All primers were synthesised by Geneworks Pty Ltd.

Exons were amplified by polymerase chain reaction (PCR) using HotStar Plus Taq® DNA Polymerase (Qiagen). All PCR reactions followed the same protocol with a 15 min for enzyme activation at 95°C, followed by 30 cycles of (denaturation at 95°C of 30 sec, annealing at 60°C for 30 sec, and elongation at 72°C for 30 sec extension), and followed by a final elongation step of 72 °C for 5 min. PCR product was visualised on 1% agarose gel stained with Gel Red™ (Biotium) and purified for sequencing using 0.5µl Exonuclease l (20U/µl) and 2.0µl Shrimp Alkaline Phosphatase (SAP) (1U/µl) for each sample, incubated at 37°C for 60 minutes then inactivated by heating to 80°C for 20 minutes. (Bell 2008) Sequencing of the PCR products was performed using BigDye Terminators (Applied Biosystems, Foster City, CA) and electrophoresed on an ABI 3100 DNA sequencer (Applied Biosystems). Chromatograms were compared to each other and the reference sequence using Sequencher® Software 5.0 (GeneCodes Corporation, Ann Arbor, MI).

Identified variants were checked for novelty by comparison to dbSNP (http://www.ncbi.nlm.nih.gov/snp) and the exome variant server (NHLBI GO Exome Sequencing Project, Seattle, WA) (http://evs.gs.washington.edu/EVS/) [date accessed; November 2012].

The potential functional significance of non-synonymous variants were analysed using PolyPhen2 (Adzhubei, Schmidt et al. 2010) SIFT (Ng and Henikoff 2001) and Mutation Taster (Schwarz, Rodelsperger et al. 2010) programmes. PolyPhen-2 (Polymorphism Phenotyping v2) is a tool which predicts possible impact of an amino acid substitution on the structure and function of a human protein using straightforward physical and comparative considerations. The variant is either classified, as benign, possibly damaging, or probably damaging. (Adzhubei, Schmidt et al. 2010) SIFT prediction is based on the degree of conservation of amino acid residues in sequence alignments derived from closely related sequences, collected through PSI-BLAST. The amino acid substitution is predicted damaging is the score is <= 0.05, and tolerated if the score is > 0.05. (Ng and Henikoff 2001) Mutation Taster integrates information from different biomedical databases. Depending on the nature of alteration, Mutation Taster chooses between different prediction models: 'silent/polymorphism' for synonymous or intronic alterations, or 'disease-causing' for alterations affecting a single amino acid, or alteration causing complex changes in the amino acid sequence. (Schwarz, Rodelsperger et al. 2010)

2.2 Primary Angle-Closure Glaucoma

Recruitment of Participants

The cohorts in this study were recruited from two different populations (Australia and Nepal). This study was conducted in accordance with the Declaration of Helsinki and its subsequent revisions. Written informed consent was obtained from each individual.

The Australian cohort consisted of participants recruited from ophthalmology clinics in Australia and New Zealand. Most patients from the Flinders eye clinic and Royal Adelaide Hospital eye clinic were recruited by the candidate, Dr. Mona S Awadalla. Patients from other Australian States and New Zealand were recruited through the Australian and New Zealand Registry of Advanced Glaucoma (ANZRAG). (Souzeau, Goldberg et al. 2011) Approval was obtained from the Southern Adelaide Clinical Human Research Ethics Committee. All participants share the same ethnicity: Caucasian, of European descent. The "Normal South Australian" control group (NSA) was ascertained from aged care facilities in Adelaide, South Australia and from members of the Flinders Medical Centre volunteer service.

The Nepalese cohort was recruited from the Nepal Glaucoma Eye Clinic, Tilganga Institute of Ophthalmology, Kathmandu, Nepal by Dr. Suman S Thapa. The recruitment was based on a population-based cross-sectional study. Citizens above the age 40 years and resident in the defined sample area were included in the study. (Thapa, Paudyal et al. 2012) The aim for Dr. Thapa's study was to estimate the prevalence of POAG and PACG among Nepalese citizens in this area. Ethics

approval was obtained from the Institutional Review Committee of the Tilganga Institute of Ophthalmology (TIO). The control group was chosen specifically to be matched for age, gender and ethnic group to the Nepalese cases. (Thapa, Rana et al. 2011)

All participants from both cohorts underwent a detailed questionnaire containing information regarding sex, age, ethnicity, age at diagnosis of PACG, family history of glaucoma, and previous glaucoma surgery or laser trabeculoplasty. They also had a complete eye examination including; slit lamp examination of the anterior chamber, gonioscopy, best corrected visual acuity, measurement of IOP, fundus examination with special attention to optic disc parameters, and visual field assessment. Objective refraction was carried out using a streak retinoscope (Beta 200, Heine, Germany), which was followed by a subjective refraction. (Thapa, Rana et al. 2011)

Inclusion Criteria

Cases were classified into three categories following the ISGEO classification into primary angle-closure suspect (PACS), primary angle-closure (PAC), and primary angle-closure glaucoma (PACG). (Foster, Buhrmann et al. 2002) Controls were required to have no PACG, and no family history of any type of glaucoma. Participants with pseudophakia or secondary angle-closure glaucoma caused by events such as uveitis, trauma or lens subluxation were excluded.

As recruitment was part of this PhD project, the number of available participants varies between chapters reflecting the number of participants recruited up to the time of each analysis. The earlier studies used 100 cases and 216 controls in the Australian cohort and 100 cases and 200 controls in the Nepalese cohort for the GWAS (Chapter 5). 106 cases and 288 controls in the Australian cohort and 106 cases and 204 controls in the Nepalese cohort were used to investigate candidate genes *Membrane frizzled-related protein (MFRP), Matrix metalloproteinase-9 (MMP-9), Hepatocyte growth factor (HGF), Calcitonin receptor-like (CALCRL),* and *Methyltetrahydrase folate reductase (MTHFR*) (Chapter 6). The number of Australian cases increased to 200 when testing candidate genes *Protease serine 56 (PRSS56), Cytochrome P450 (CYP1B1), Endothelial nitric oxide synthase (eNOS),* and *Neurotrophin 4 (NTF4*). The number of cases in the Australian cohort was further increased to 310 and 288 controls, and in the Nepalese cohort the cases reached the number of 160 cases and 324 controls with the inclusion of primary angle-closure suspects in the analysis of *TMEM98* with PACG, and in the replication studies of our GWAS, and the recently published GWAS.

SNP selection and genotyping for candidate gene studies

Candidate genes were selected based on recent findings in the literature relevant to PACG. Here we used known common variants in the human genome reported by HapMap to select tag SNPs to look for association with PACG.

Tag SNPs relevant to the gene were selected on the basis of linkage disequilibrium patterns observed in the Caucasian samples from HapMap (CEU: CEPH, and Utah

residents with ancestry from northern and western Europe) for the Australian cohort. For the Nepalese cohort SNPs were selected from the HapMap Han Chinese in Beijing, China (CHB) sample as the most closely related population available at the time of the study. We consider the choice of tag SNPs appropriate, as allele frequencies and linkage disequilibrium structure were similar between the Nepalese and CHB HapMap datasets for the chosen tag SNPs.

SNPs were selected using the tagger program implemented in Haploview 4.2 (http://www.broadinstitute.org/mpg/haploview). Pairwise tagging was used and tag SNPs must have an r^2>0.8 with SNPs displaying a minor allele frequency of >5% in the target population.

Peripheral whole blood samples were obtained from all participants. Genomic DNA was extracted using the QiaAmp Blood Midi (Nepalese samples) or Maxi (Australian samples) Kit (Qiagen, Doncaster, Victoria, Australia). Genotyping was conducted using the iPLEX Gold chemistry (Sequenom Inc, San Diego, California) on an Autoflex mass spectrometer (Sequenom Inc, San Diego, California) at the Australia Genome Research Facility (AGRF), Brisbane.

Statistical analyses

Baseline characteristics of cases and controls were compared using a t-test for continuous variables and chi-square test for discrete traits. SNPs were assessed for compliance with Hardy-Weinberg equilibrium using a chi-square test. Linkage Disequilibrium between markers was calculated using Haploview 4.2 All association

analyses were conducted using PLINK (v1.06). (Purcell, Neale et al. 2007) Genetic association was assessed under an allelic model with respect to the minor allele. Bonferroni correction was applied to each p-value according to the number of SNPs typed from that gene. Further combined analysis was conducted with the Cochran-Mantel-Haenszel 2x2xK test (cmh) performed to minimize the population stratification. As the genetic matching between cases and controls was not perfect, we subjected the association tests to adjustments for sex and age using logistic regression in PLINK.

Haplotype analyses from our data were conducted in PLINK based on the observed linkage disequilibrium blocks, as visualised in Haploview using the "solid spine" definition. (Barrett, Fry et al. 2005) Haplotype block is defined as sets of consecutive SNPs between which there is little or no evidence of historical recombination. (Gabriel, Schaffner et al. 2002) Haplotype tests were adjusted with a simple Bonferroni test for the number of observed haplotypes in the block examined with frequency >1%.

Power calculations for this study were performed using the Genetic Power Calculator (Purcell, Cherny et al. 2003) for each cohort utilising population specific PACG prevalence, minor allele frequencies, and relative risk.

More detailed methods specific to individual studies are provided separately in each chapter.

Chapter 3

GENETIC VARIATIONS OF *MFRP* AND *PRSS56* IN FAMILIES WITH NANOPHTHALMOS

Introduction

Membrane frizzled-related protein (*MFRP*, OMIM 606227) was the first gene to be identified for isolated autosomal recessive nanophthalmos, using genome-wide linkage followed by exome and genomic sequencing to detect mutations. It is located on chromosome 11q23.3 (genetic locus NNO2; OMIM 609549). (Sundin, Leppert et al. 2005) *MFRP* has also been found to be associated with syndromic forms of microphthalmia with retinal degeneration. (Ayala-Ramirez, Graue-Wiechers et al. 2006; Crespi, Buil et al. 2008) One of the MFRP protein domains is the cysteine-rich domain that binds to wingless type protein (Wnt), which is involved in ocular development. (Katoh 2001) *MFRP* is expressed in the retinal pigment epithelium and ciliary body. It has been suggested that its function is restricted to ocular development (Sundin, Dharmaraj et al. 2008) and lack of *MFRP* function during childhood appears to lead to disruption of the emmetropization process and development of refractive error in patients with nanophthalmos. (Mandal, Vasireddy et al. 2006)

In 2009, genome-wide linkage analysis was conducted on six consanguineous Tunisian families with autosomal recessive posterior microphthalmia, and a genetic locus was identified on chromosome 2q37.1. (Hmani-Aifa, Ben Salem et al. 2009) Further sequencing analyses were conducted in these families to identify the

causative gene, and two novel mutations have been identified in the *Protease Serine 56* (*PRSS56*) gene, with additional support for causation coming from a mouse model. (Nair, Hmani-Aifa et al. 2011) Additional segregating variants were identified in families with nanophthalmos (Orr, Dube et al. 2011) and families with posterior microphthalmia in independent studies. (Gal, Rau et al. 2011) Thus, *PRSS56* has also been clearly implicated in autosomal recessive nanophthalmos.

Aim

We aimed to identify novel segregating variants in *MFRP* and *PRSS65* in families with nanophthalmos.

Methods

Coding regions and exon/intron boundaries of the *MFRP* and *PRSS56* genes were screened by direct sequencing in the probands of the eleven families. The large Family 1 was excluded as earlier linkage analysis (see chapter 4) had eliminated these loci in this family. Details of recruitment and direct sequencing methods have been described previously in **Section2.1**. PCR primers of *MFRP* are in **Appendix 1**, and primers for *PRSS56* have been published previously. (Orr, Dube et al. 2011)

For sequencing of the PCR products, chromatograms were compared to each other and the reference sequence (NM_031433 for *MFRP*, and NM_001195129.1 for *PRSS56*) using Sequencher® Software 5.0 (GeneCodes Corporation, Ann Arbor, MI).

Results

We ascertained eleven families with non-syndromic forms of nanophthalmos; 30 members were recruited, of whom 18 were affected. Families 5, 7, and 11 showed autosomal dominant inheritance and the remainder segregate in an apparent autosomal recessive mode. Most families are of Caucasian origin except 10 and 11, which are Polynesian and Melanesian from New Caledonia, respectively.

All patients presented with high hyperopia with mean refraction of +8.4 dioptres (standard deviation (SD) 4 dioptres) in association with short axial length with a mean of 18.8mm (SD 1.2 mm).

Variants in *MFRP*

Two novel heterozygous *MFRP* variants were identified in the proband of Family 3 (II:2). The first is a predicted splice site variant at position c.1124+1G>T, p.R375fsX91, altering the first base of intron 9 (**Figure 3.1.a**). This is predicted to disrupt the donor splice site resulting in the inclusion of intronic sequence in at least some portion of exon 9 in the processed mRNA. The second variant is a missense variant at position c.1709C>T (p.Ala570Val) in exon 12 **(Figure 3.1.b**). These variants are not present in dbSNP v.135 or in the exome variant server. No further DNA samples were available from Family 3, so segregation of this variant with disease could not be assessed (**Figure 3.1.c**).

Polyphen2, SIFT and Mutation Taster were used to predict the functional significance of the allele replacement for the *MFRP* missense variant found in the proband of Family 3. PolyPhen2 predicted the variant to be benign with total score of

0.192 (specificity 0.73, sensitivity 0.88) under the HumVar algorithm. SIFT score also found the variant to be tolerated with score of 0.36. Mutation Taster predicted the variant to be a harmless polymorphism. All variants identified in *MFRP* in the probands are presented in **Appendix 3.a.**

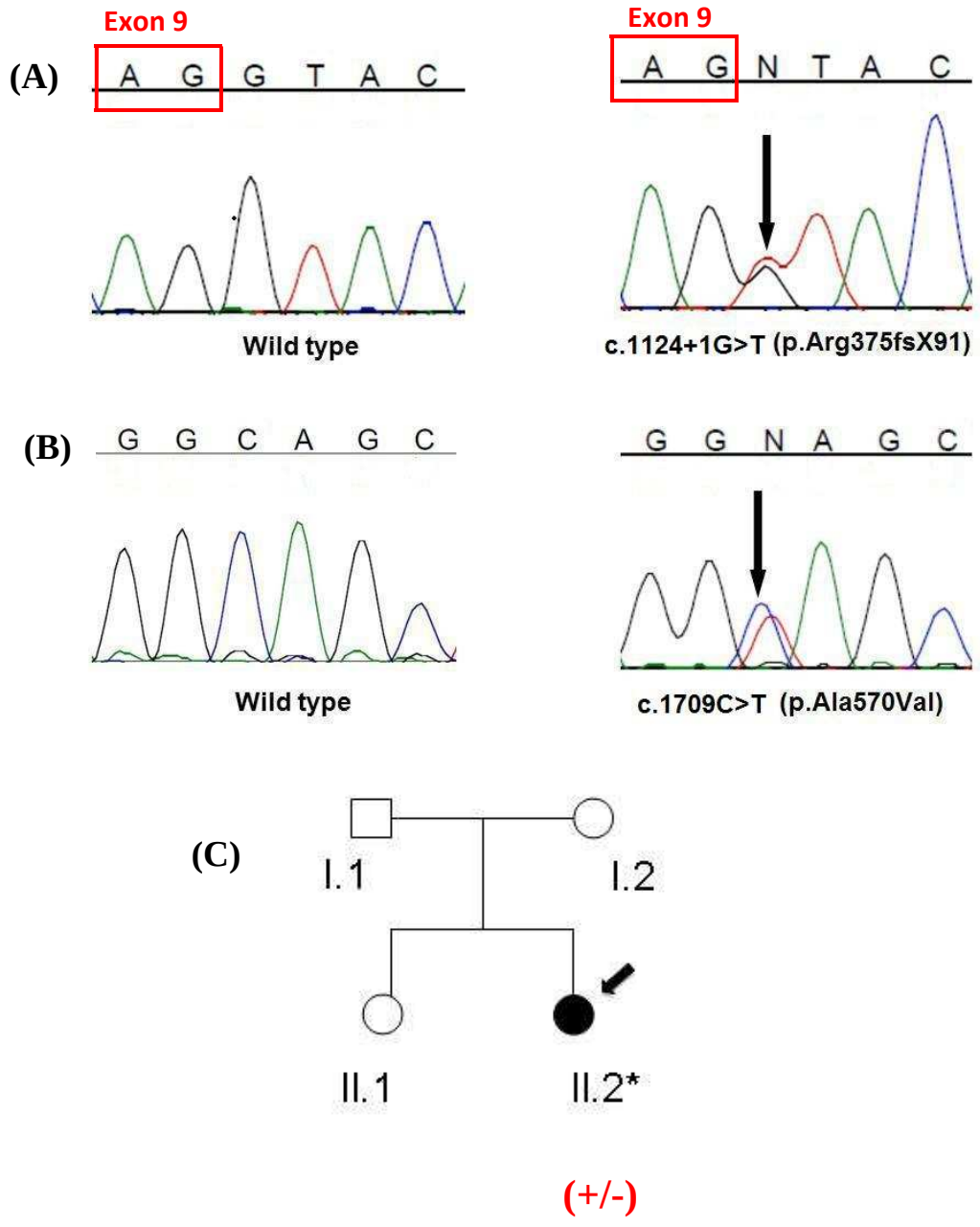

Figure 3.1. Novel variants in *MFRP* in the proband ll:2 of Family 3. (See next page for legend)

Figure 3.1. Novel variants in *MFRP* in the proband ll:2 of Family 3. The arrow points to the variant in sequence chromatograms in the patient sample. (A) Splice variant at the first base of intron 9 (c.1124+1G>T). End of exon 9 is indicated by red rectangular. (B) Missense variant at exon 12 (c.1709C>T). The panels also show the wild type of the corresponding regions in controls. (C) Pedigrees of nanophthalmos Family 3. Square symbols indicate male, round symbols female, diagonal line deceased, dark symbols are individual with nanophthalmos, unfilled symbol unaffected individuals, (+/-) indicates the heterozygous variant.

Variants in *PRSS56*

Two novel variants were identified in *PRSS56* in two unrelated families.

In Family 2, a frameshift variant was detected in the proband (II:4), c.1066delC in exon 9, resulting in the predicted inclusion of 147 amino acids followed by premature stop codon (p.Pro355fsX147) (**Figure 3.2.a**). This variant was observed in a heterozygous state in all affected family members (II:5, and II:6) (**Figure 3.2.b**). No other variants segregated in this family and thus the second variant leading to the assumed recessive phenotype is as yet unknown.

In the autosomal dominant Family 5, one novel heterozygous frameshift variant was detected in exon 13 in *PRSS56* gene (**Figure 3.3.a**), c.1573delG at the protein level p.Cys536fsX54 of the proband (I:1). The variant was not found in the other affected individual (II.2) and thus does not segregate with nanophthalmos (**Figure 3.3.b**). It was also not detected in the unaffected participants. No potentially pathogenic variants were found in remaining families. The list of variants identified in the probands is presented in **Appendix 3.b**. Polyphen-2 and SIFT programmes do not detect the pathogenicity of DNA sequence alteration in frameshift variants. No internal Ensembl transcript ID was found for *PRSS56* using Mutation Taster as in December 2012.

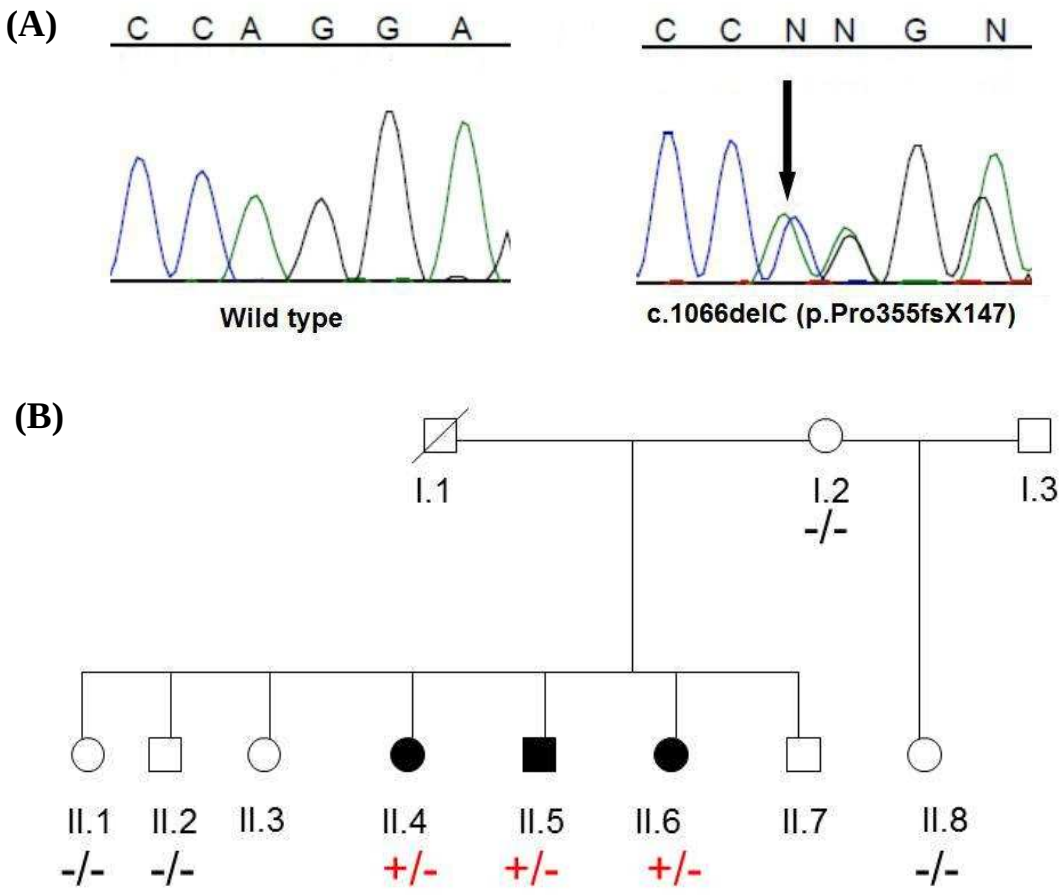

Figure 3.2. Novel variant in *PRSS56* in Family 2. (A) The arrow points to the frameshift variant at exon 9 (c.1066delC) in the sequence chromatogram in patient ll:4. The panels show the wild type of the corresponding regions in controls. DNA sequences are shown on the top of the figure. (B) Pedigrees of nanophthalmos Family 2. Square symbols indicate male, round symbols female, diagonal line deceased, dark symbols are individual with nanophthalmos, unfilled symbol unaffected individuals, (+/-) indicates the presence of the frameshift heterozygous variant and (-/-) presents the wild type.

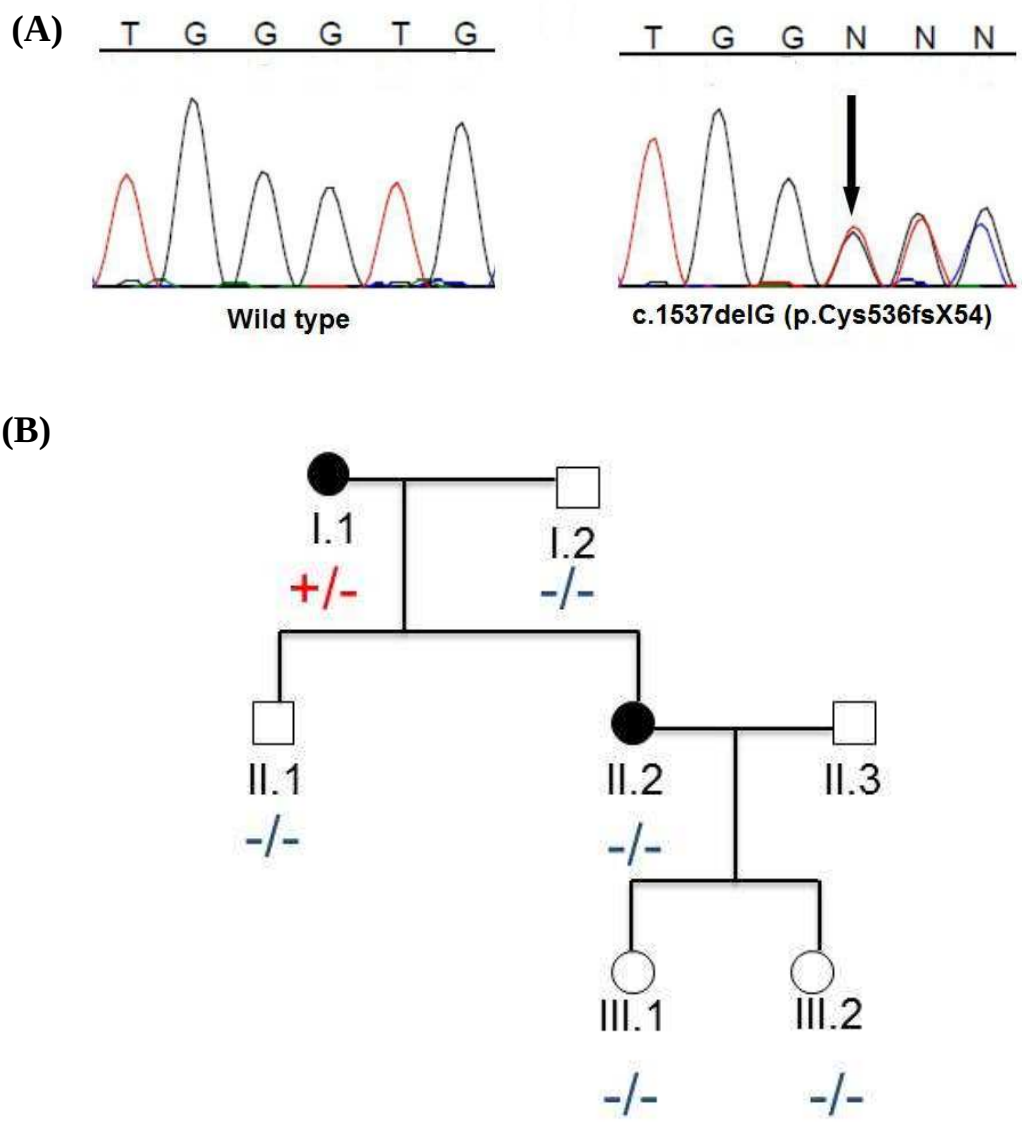

Figure 3.3. Novel variant in *PRSS56* in the proband of Family 5. (See next page for legend)

Figure 3.3. Novel variant in *PRSS56* in the proband of Family 5. (A) The arrow points to frameshift variant at exon 13 (c.1573delG) in the sequence chromatogram in patient l:1 of Family 5. The panels show the wild type of the corresponding regions in controls. DNA sequences are shown on the top of the figure. (B) Pedigrees of nanophthalmos Family 5. Square symbols indicate male, round symbols female, diagonal line deceased, dark symbols are individual with nanophthalmos, unfilled symbol unaffected individuals, (+/-) indicates the frameshift heterozygous variant and (-/-) presents the wild type.

Discussion

We identified novel variants in two genes previously shown to cause autosomal recessive nanophthalmos (*PRSS56* and *MFRP)* in three of our nanophthalmos families (families 2, 3, and 5). We identified two heterozygous variants in individual II:2 of Family 3 in *MFRP*. The c.1709C>T **(**p.Ala570Val) variant was predicted unlikely to be pathogenic. However, bioinformatics predictions may not be completely accurate, for example the specificity of the prediction by PolyPhen2 was 0.73 and the sensitivity was 0.88 for this variant. It is reported that PolyPhen-2 achieves true positive prediction rates of 92% on the HumDiv dataset and 73% on the HumVar dataset (Adzhubei, Schmidt et al. 2010),.,thus certain percentage of misclassification can occur with such predictions. Given that this is a novel variant identified in a patient with a disease caused by this gene, there is a high likelihood that this variant has some functional effect. The presence of a splice variant of the first base at intron 9 in *MFRP* gene is expected to be a functional change in this patient and it is plausible that in the context of this likely null allele that the milder p.Ala570Val substitution has some detectable functional consequence. Additional family members were not available and thus segregation of these variants could not be assessed.

PRSS56 is broadly expressed in the human eye especially in the retina and the sclera, suggesting it is essential to eye development. (Gal, Rau et al. 2011) Alteration of *PRSS56* in a mouse model revealed a phenotype similar to nanophthalmos in humans. (Nair, Hmani-Aifa et al. 2011) The genetic alteration in the mouse model was a T to A transversion in the splice donor site of exon 11, which results in

retention of intron 11 in the mutant transcript leading to small insertion followed by premature stop codon. The mouse carrying the mutant allele displayed significant decrease in the axial length and equatorial diameter compared to wild type, while the lens diameter remained similar to wild type animals. The mouse also had a narrow anterior chamber, and developed angle-closure glaucoma. (Nair, Hmani-Aifa et al. 2011) Identification of a novel variant in one of our families further confirms the association of *PRSS56* with recessive nanophthalmos in the Australian population.

In Family 2, we found a segregating heterozygous frameshift variant caused by a 1bp deletion (c.1066delC) resulting in p.Pro355fsX147, in the affected participants II:4, II:5, and II:6. Interestingly, in the same location Gal and colleagues (Gal, Rau et al. 2011) found a segregating homozygous variant in a Tunisian family consisting of healthy consanguineous parents and 11 children, five of them having an autosomal recessive posterior microphthalmia (POM). The variant is 1 bp duplication (c.1066dupC) leading to inclusion of 152 amino acid followed by premature stop codon (p.Pro356fsX152). The investigators also compared the phenotypes of nanophthalmos and posterior microphthalmia and concluded both phenotypes were very similar and the difference was only in the corneal diameter (micro-cornea in the patients with nanophthalmos and normal cornea in patients with posterior microphthalmia) and thus these two conditions are likely to represent a continuum of phenotypes.

As the inheritance of nanophthalmos in Family 2 appears to be recessive, it would be expected that a second variant should be present in all affected individuals. The sequencing strategy may have been unable to detect the second variant, potentially

due to deletions in a primer binding site or regulatory mutations outside the screened exons. Alternatively, a second gene may contribute to the phenotype in this family. In addition, we do not have DNA or clinical information from the father (I:1) and thus his contribution to this disease is unknown and although unlikely given the family's knowledge of his eyesight, dominant inheritance cannot be definitively excluded.

The frameshift variants observed in *MFRP* and *PRSS56* are both likely to be pathogenic through introducing nonsense sequence and a premature stop codon. The mRNAs containing these premature stop codons are likely to be degraded through nonsense-mediated decay resulting in a loss of function.

Although previous reports have shown *MFRP* and *PRSS56* associated nanophthalmos to be limited to autosomal recessive inheritance, we looked for variants in nanophthalmos families with autosomal dominant inheritance. Other genes, for example *Crystallin, alpha A* (*CRYAA*) in congenital cataract, have been reported to contribute to both dominant and recessive inheritance. (Litt, Kramer et al. 1998; Khan, Aldahmesh et al. 2007) Our study concludes that *MFRP* and *PRSS56* do not account for autosomal dominant nanophthalmos in these families.

In conclusion we identified variants in *MFRP* and *PRSS56* in two out of ten families with autosomal recessive nanophthalmos. These findings show *MFRP* and *PRSS56* account for a minority of cases in the studied Caucasian population. Further investigation is required to identify other nanophthalmos genes.

Chapter 4

A MUTATION IN *TMEM98* IN A LARGE CAUCASIAN KINDRED WITH AUTOSOMAL DOMINANT NANOPHTHALMOS, AND ITS ASSOCIATION WITH PACG

Introduction

In contrast to recessive nanophthalmos, multiple studies have reported different loci for dominant nanophthalmos; however, no additional families in these linkage regions have been reported and the causative gene in these families has not been identified. The first locus identified was linked to chromosome 11p in a family from the United States of America. (Othman, Sullivan et al. 1998) Subsequently, loci have been described on 2q11-q14 in a Chinese family (Li, Wang et al. 2008) and 17p12-q12 also in a Chinese pedigree. (Hu, Yu et al. 2011)

Hyperopia and Angle-closure glaucoma are the main complications in patients with nanophthalmos. Identifying the causative gene in autosomal dominant nanophthalmos will help in the future to identify high-risk individuals at an earlier age and provide regular eye screening. This will allow early detection and management of angle-closure glaucoma and prevent blindness, which has been a common outcome in these families.

Aim

1. To identify the causative gene for autosomal dominant nanophthalmos in a large family of European ancestry.
2. To test the identified novel gene in additional families with nanophthalmos.
3. To investigate the association of the novel candidate gene in unrelated individuals with PACG and hyperopia.

Methods

Recruitment

Family 1 (**Figure 2.1**) was identified following presentation of the proband at Flinders Medical Centre, Adelaide, Australia for evaluation and treatment related to angle-closure glaucoma. Following full ophthalmic evaluation of the proband, V:3, by A/Prof Jamie E Craig, the primary diagnosis of isolated nanophthalmos was made. The family history of this patient was obtained and the extended family traced over five generations. Thirty family members were recruited into the study, 15 of whom were diagnosed with nanophthalmos. An additional seven family members were reported to have the same phenotype, but were not available for study. The proband and her immediate family reside in Australia; but the majority of her extended family lives in the United Kingdom (UK).

The proband (V:3) received full ophthalmic examination which included refraction, IOP measurement (via Goldmann tonometry), central corneal thickness measurement (via Pachymetry), slit lamp biomicroscopy, A-scan ultrasonography to determine axial length, and optic disc tomography. Angle-closure glaucoma status was assessed

in all participants, but it was not a part of the criteria used to determine affection status. The rest of the family members were classified with nanophthalmos if they had an axial length <20.00 mm and/or refractive error >+7.00 dioptres, in line with other published work on autosomal dominant nanophthalmos. (Othman, Sullivan et al. 1998)

Genome-wide linkage study

All available family members were genotyped on Xba 10K SNP arrays (Affymetrix, Santa Clara, CA, USA) at the Australian Genome Research Facility (Melbourne, Australia). Data were provided in the form of linkage format files and analyses were conducted in MERLIN by Dr Kathryn P Burdon and Kate Laurie. (Abecasis, Cherny et al. 2002) Due to computational limitations on the number of members of a pedigree, initial genome-wide linkage analysis was conducted using individuals from the proband's branch of the family (descendants of II:1 and II:2), excluding IV:1, V:1, V:2 and V:7 under a fully penetrant dominant model. To confirm the findings, different individuals were excluded and the analysis repeated.

Analysis was then repeated in the remaining branch of the family (descendants of II:6 and II:7). Results were compared and only a single region on chromosome 17 showed linkage in both halves of the family. SNPs surrounding the linked region on chromosome 17 were extracted from the dataset and files were formatted with MEGA2 (Mukhopadhyay, Almasy et al. 2005) for linkage analysis on the entire pedigree in SimWalk2. (Sobel and Lange 1996) A highly penetrant dominant model was used to calculate Location scores (equivalent to multi-point LOD scores) and

location scores vs. chromosome location were plotted. Haplotypes were reconstructed in MERLIN (Abecasis, Cherny et al. 2002) on sub-sections of the pedigree with overlapping individuals included in each run to facilitate combining the data into the whole pedigree.

Exome sequencing

Sequencing was performed in five individuals selected to represent both main branches of the family; four affected (IV:5, IV:2, V:9, and IV:9) and one unaffected member (IV:4) were chosen. Enrichment for the exome was performed with the TruSeq Exome Enrichment Kit (Illumina Inc. San Diego, CA, USA) and enriched DNA was sequenced on HiSeq 2000 (Illumina Inc) by the Australian Genome Research Facility (AGRF). Sequence alignment to hg19 was conducted with Illumina CASAVA v1.8.1 and aligner module ELAND v2. Realignment and variant calls were made with Illumina Exome Script and variants annotated by ANNOVAR. All bioinformatics was conducted by the sequencing service provider.

Data were provided from the service provider as a list of variants for each sample compared to the human reference. The lists were filtered according to the following criteria:

1. Present in the linkage region.
2. Not present in dbSNP135, or the exome variant server.
3. Segregated in all five sequenced individuals.
4. Missense, stop or splice variant.

Segregation in the remainder of the family was assessed by Sanger sequencing as described in **Section 2.1** using primers for *TMEM98* exon 8-1 (**Appendix 2**). Chromatograms were compared to each other and the reference sequence (NM_001033504.1) using Sequencher® Software (GeneCodes Corporation, Ann Arbor, MI).

The presence of the novel missense variant was tested in 285 independent unaffected controls using a restriction fragment length polymorphism. The NSA cohort was ascertained from aged residential care facilities in Adelaide, South Australia. The mutation introduces a cut site for *Bsu36I* (New England BioLabs Inc.). PCR was performed using the same primers used for sequencing above. 10 µl of PCR product was digested with 2 units *Bsu36I* enzyme and 0.2ul BSA in NEBuffer 3 and incubated at 37°C for 2 hours. The digest products were visualized on 1.4% agarose gel stained with Gel Red (Biotium^{TM}).

Test on additional nanophthalmos families

Direct sequencing was done on the rest of nanophthalmos families to identify novel variants in *TMEM98*. Recruitment, DNA extraction and sequencing of the probands are described in **Section 2.1**. Functional significance of the allele replacement in *TMEM98* was analysed using PolyPhen-2, SIFT and Mutation Taster programmes, using Ensembl protein ID ENSP00000261713.

Expression analysis

Ocular tissues including sclera, iris, retina, ciliary body, optic nerve, optic nerve head and corneal endothelium were from post-mortem human eyes, and obtained through the Eye Bank of South Australia according to guidelines of the Southern Adelaide Clinical Human Research Ethics Committee. Total RNA was extracted from tissues using RNeasy® micro kit (QIAGEN) protocol for human tissue. Primers were designed through NCBI/ Primer-Blast (http://www.ncbi.nlm.nih.gov/tools/primer-blast/index.cgi?).

Isoform 1 (NM_015544) forward primer (5'-3') GCACCTGCCATCCTCTTCCCCA and reverse primer (5'-3') GCAGTCGTCCGTGCGTCCAG. Isoform 2 (NM_001033504) forward primer (5'-3') GGGAGCCACAGCCTGAGCTTT and reverse primer (5'-3') AGGAGCAGGGCAGTCGTCCG. First strand cDNA was synthesized using the SuperScript III reverse transcriptase (Invitrogen^{TM}). PCR was conducted with the following conditions; 95°C for 15 min, (95°c for 30s, 62°C for 30s, 72°C for 30s) x30 cycles for retina, optic nerve, ciliary body, iris, and lens and x32 cycles for sclera, then 72°c for 5 min. PCR product was visualised on 1.4% agarose gel stained with Gel Red (Biotium^{TM}) and purified for sequencing using exonuclease l (20U/µl) – USB® Shrimp Alkaline Phosphatase (SAP) (1U/µl), incubated at 37^{o}C for 60 minutes then inactivate by heating to 80^{o}C for 20 minutes.

Association of *TMEM98* with PACG and hyperopia

Finally we tested *TMEM98* for association of common sequence variation in independent cases with PACG and hyperopia as both conditions are complications of nanophthalmos. In PACG, we used tag SNP methodology on both Australian and

Nepalese cohorts as described in **Section 2.2**. The analysis was done in mid-2012, so we had 310 cases and 288 controls in the Australian cohort, and 160 cases and 324 controls in the Nepalese cohort. Seven tag SNPs were selected. The numbers of tag SNPs chosen for both cohorts are presented in **Table 4.1**.

For hyperopia, we selected participants with refraction > +6.00 dioptres and axial length of more than 20.00 mm. There were total of 20 participants in total from two different cohorts; six NSA controls, and 14 PACG cases. The gene was assessed for coding variants using direct sequencing methodology as described in **Section 2.1** to screen coding exons and intron/exon boundaries.

Table 4.1. Tag SNPs and its base position selected for each cohort in *TMEM98* gene.

SNP	bp Position	Australia	Nepal
rs12952271	31255616	-	Y
rs3025293	31259984	-	Y
rs28923	31261649	Y	Y
rs29014	31261974	Y	-
rs28921	31265745	Y	Y
rs28920	31265855	Y	Y
rs11851	31268429	Y	-

“Y” indicates that the tag SNP was selected to represent variation in the specified cohort, “-” tag SNP was not selected for that cohort, “Chr” chromosome.

Results

Family 1 presented with an autosomal dominant nanophthalmos. Fifteen family members were classified as affected and their details are given in **Table 4.2**. The affected members presented with abnormally thick sclera, mean refraction and axial length of +11.8±2.5 dioptres and 17.6±0.6 mm, respectively. Best corrected visual acuity in these patients ranged from no perception of light to 6/6 and visual acuity did not necessarily correlate between the two eyes of each patient. Angle-closure glaucoma was detected in six of the 16 patients, including the proband (V:3). Individual IV:2 demonstrated elevated IOP but without signs of glaucoma at the time of recruitment. Representative images of the ocular phenotype showing the proband (V.3), sister (V.5), and her mother (IV.5) are shown, with shallow anterior chamber depth and narrow irido-corneal angle in both slit-lamp and Pentacam images **Figure 4.1**.

Table 4.2. Clinical characteristics of the affected family members.

ID	Age	BCVA		Refraction (D)		Axial length (mm)		IOP (mmHg)		ACG
	(years)	RE	LE	RE	LE	RE	LE	RE	LE	
III:4	91	n/a	n/a	+11.5	n/a	n/a	n/a	n/a	n/a	n/a
III:10	78	6/24	6/30	+15.00	+15.00	18.12	17.92	13	14	No
III:13	86	HM	CF	+9.50	n/a	18.02	n/a	16	17	ACG
III:15	84	n/a	n/a	+7.00	+9.50	17.43	17.31	n/a	n/a	ACG
IV:2	64	6/6	6/9	+11.00	+11.00	17	n/a	24	24	No
IV:3	49	6/9	6/12	+13.75	+12.87	n/a	n/a	18	18	n/a
IV:5	61	6/48	6/12	+14.00	+15.00	17.1	17.14	33	26	ACG
IV:7	63	n/a	n/a	+11.87	+12.37	n/a	n/a	18	19	No
IV:14	52	n/a	n/a	+9.00	+10.00	n/a	n/a	n/a	n/a	n/a
IV:16	49	n/a	n/a	+12.50	+12.00	n/a	n/a	n/a	n/a	n/a
IV:21	52	6/9	6/36	+14.25	+14.50	n/a	n/a	n/a	n/a	ACG
V:3	34	6/60	6/6	+9.75	+10.50	18.46	18.34	42	41	Yes
V:5	26	6/12	6/15	+15.50	+15.00	17.02	16.9	19	18	No
V:7	30	6/6	6/6	+13.25	+13.75	n/a	n/a	n/a	n/a	n/a
V:14	24	6/12	NLP	+7.50	n/a	18.42	n/a	40	n/a	ACG
V:15	26	n/a	n/a	+8.25	+8.50	n/a	n/a	11	11	No

RE=right eye, LE=left eye, BCVA=best corrected visual acuity, D=dioptres, IOP=highest recorded intraocular pressure, ACG=angle-closure glaucoma, N/A=data unavailable, HM=hand movement CF=count fingers, NLP=no perception of light

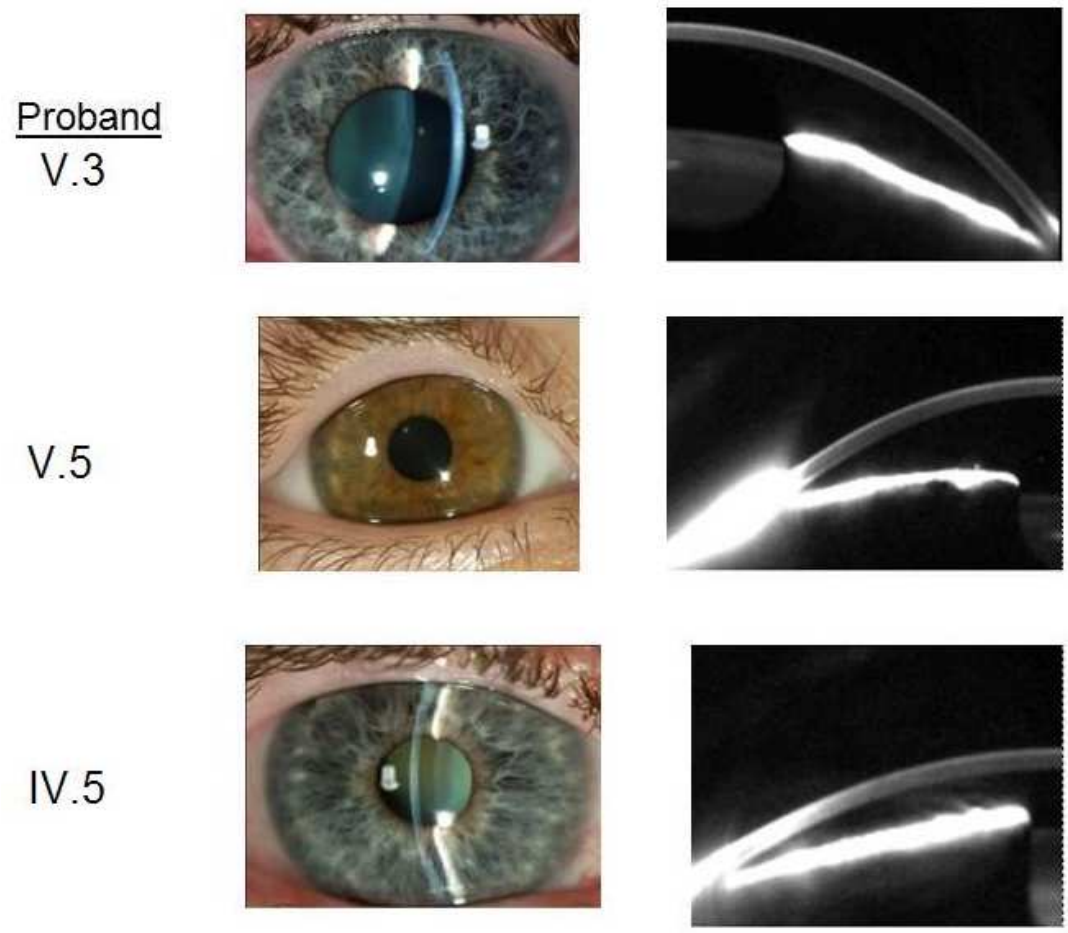

Figure 4.1. Clinical photos of the affected members in the Australian branch of Family 1. External eye appearance of patients with nanophthalmos presented in participants V.3, V.5, and IV.5. Corresponding Pentacam photos of the affected individuals show narrow irido-corneal angle and shallow anterior chamber depth in the affected eyes.

Linkage analysis in the branch of the pedigree descended from II:1 and II:2 is shown in **Figure 4.2.a**. Linkage was excluded to previously reported nanophthalmos regions on chromosomes 11p, 11q, 2q; however, linkage was detected in the first branch of the family on chromosome 17 between SNP markers rs2323659 and rs967293 with a maximum LOD score of 2.67. The region was defined by recombination events in individuals III:3 (untyped) and IV:7. The remaining branch of the family similarly showed linkage to this region on chromosome 17; however, no recombinants were observed that would further refine the linkage region. The linked region is ~16.9Mb in physical distance between 15.3Mb and 32.7Mb, and located at 17p12-q12, encompassing the centromere of chromosome 17. Multipoint linkage analysis of this region in the entire family using SimWalk2 gave a location score of 4.1 **(Figure 4.2.b**).

The 5' boundary marker rs2323659 is located on the short arm of the chromosome. The next informative marker, rs1589464 is separated from the boundary marker by approximately 10Mb, including the centromere. At the other end of the linked region, the recombination event in individual IV:16 occurred between rs952540 and rs967293. These markers are separated by ~370kb and this region contains no annotated coding exons. Thus further fine mapping at this end of the linked region is unwarranted. The linkage region contains 383 transcripts annotated in the UCSC genome browser, from 250 genes.

Figure 4.2. Genome-wide linkage plot of Family 1. (See next page for legend)

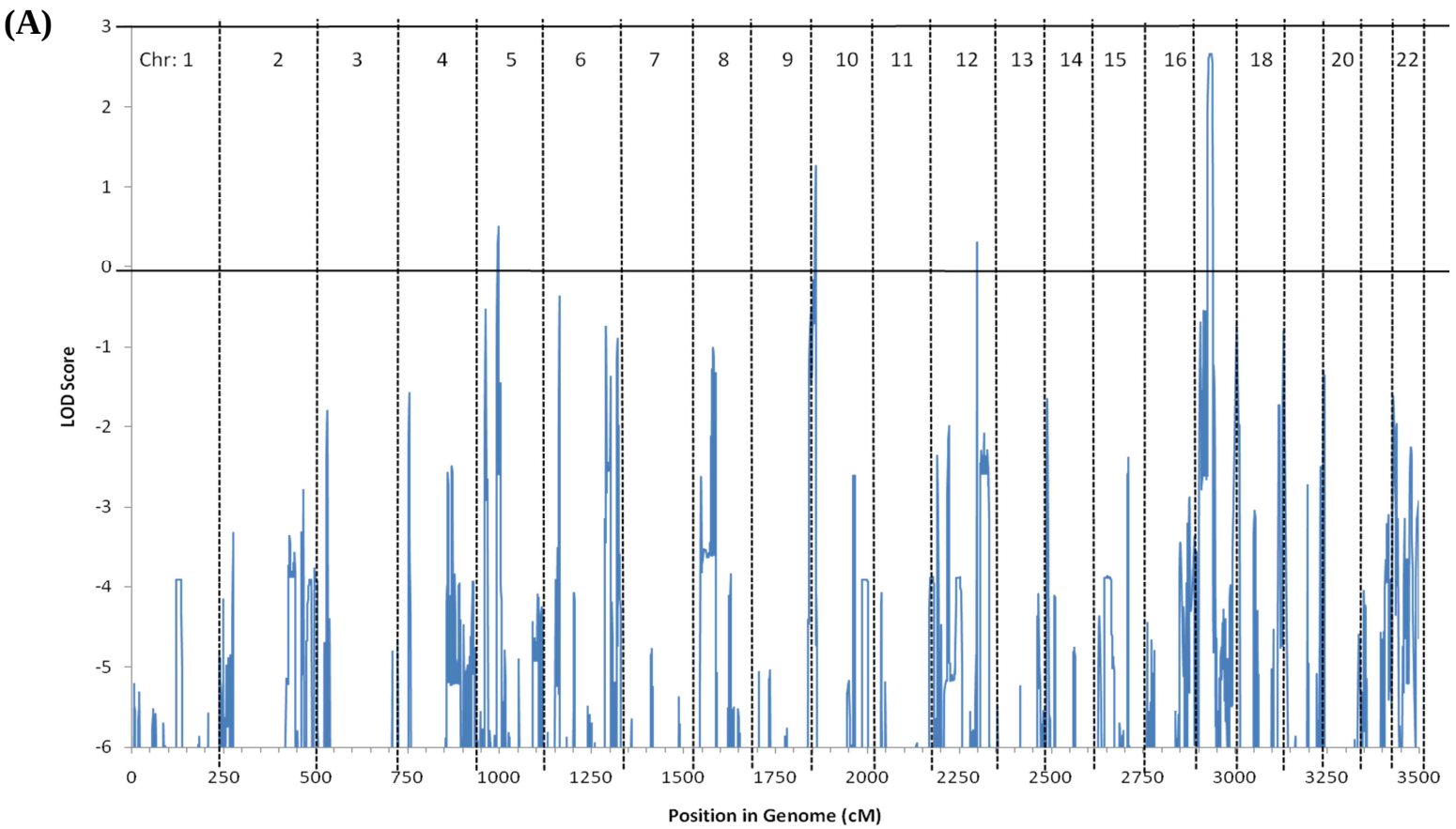

Figure 4.2. Continue

(B)

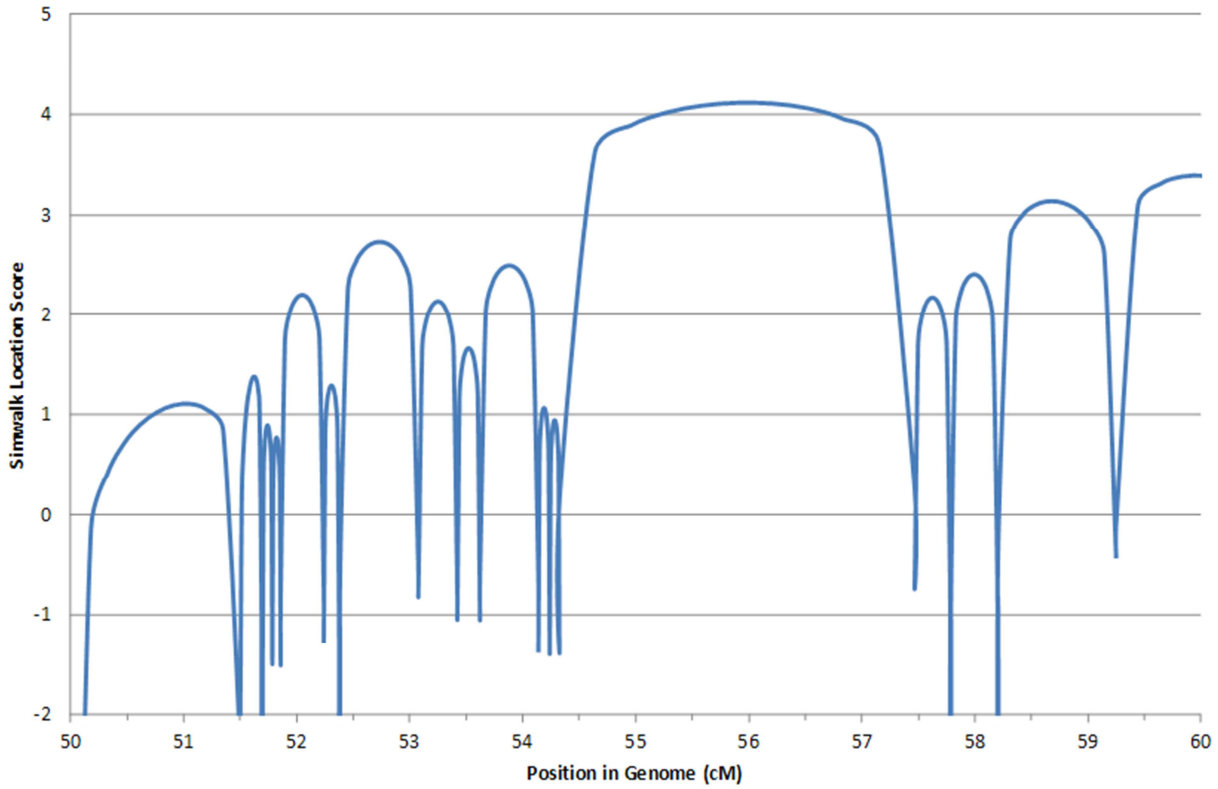

Figure 4.2. Genome-wide linkage plot of Family 1 A) Linkage plot showing LOD scores across the whole genome for the Australian branch of the family (descendants of II:1 and II:2). A suggestive peak was identified on chromosome 17. B) Linkage plot showing multi-point LOD scores (Location scores) for the linked region of chromosome 17 (between 50 and 60 cM) in the entire family. A maximum LOD score of 4.11 was noted at marker rs952581.

Three novel variants meeting the stringent filtering criteria outlined in the methods were identified in genes within the linkage region by whole exome sequencing. Two of these were later reported in dbSNP database (dbSNP135), leaving only one novel variant, located in exon 8 of the *TMEM98* (*Transmembrane protein 98*) gene, segregating in the 5 individuals (4 affected, 1 unaffected) sequenced. It is a substitution at position c.577G>C (NM_015544.2) leading to changing of the coding protein alanine to proline at p.Ala193Pro (**Figure 4.3**). Segregation with nanopthalmos was confirmed in the remainder of the family (**Figure 4.4**). The variant is neither present in db SNP v.135 nor in the Exome Variant Server (as at November 2012). It was not observed in 285 unaffected unrelated Caucasian controls using RFLP methodology. The mutation resulted in bands of 180 and 420 basepairs following digestion with Bsu36I and the undigested wild type product was 600bp (**Figure 4.5**).

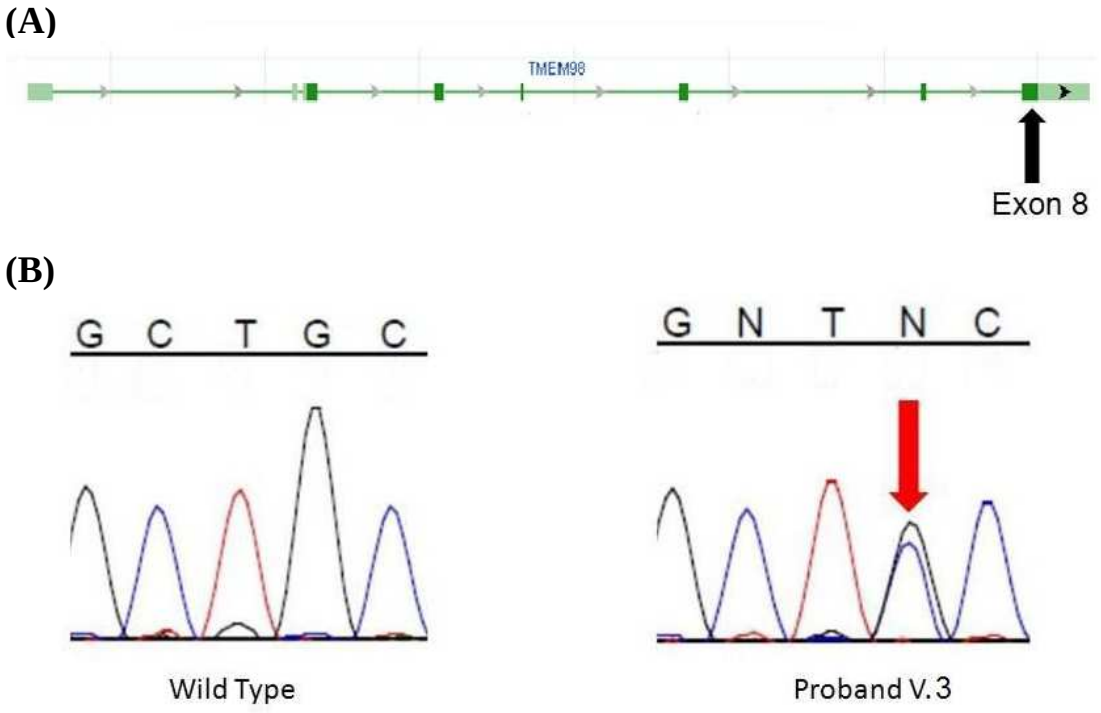

Figure 4.3. Mutation located in exon 8 of *TMEM98* gene. (A) Ideogram of *TMEM98* and the black arrow points to exon 8. (B) Mutation analysis showing sequence chromatograms for the novel mutation in *TMEM98* in the proband V.4 of Family 1. Red arrow points to the mutation c.577G>C (p.Ala193Pro) in the proband. The panels also show the wild type band observed in controls.

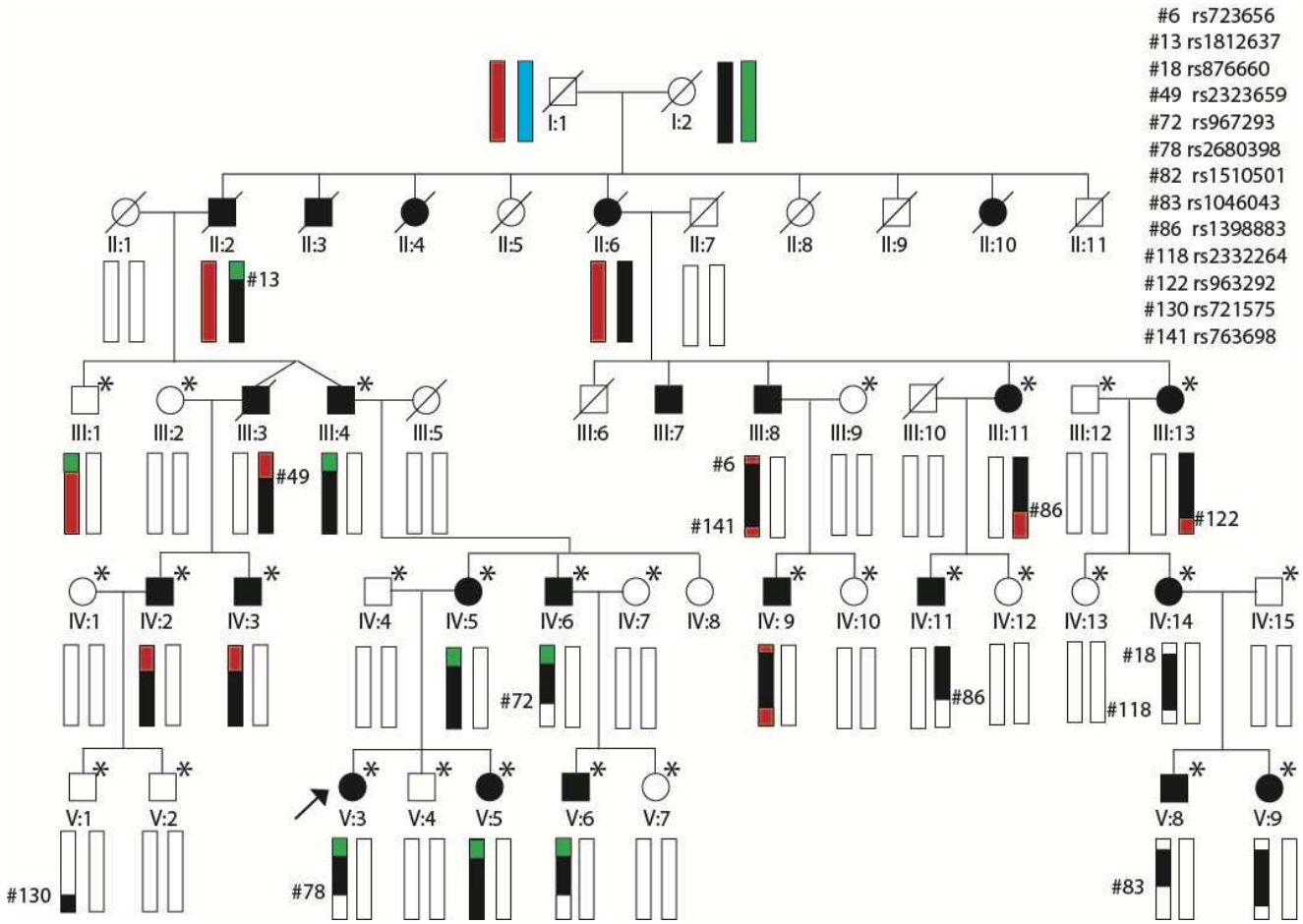

Figure 4.4. Family 1 displaying autosomal dominant nanophthalmos. (See next page for legend)

Figure 4.4. Family 1 displaying autosomal dominant nanophthalmos. Square symbols indicate males, circles indicate females, and diagonal line indicates deceased individuals. Blackened symbol indicates affected individual. The proband is indicated by an arrow. Individuals marked with * had DNA available and were included in the linkage study. Haplotypes at the linked region of chromosome 17 are shown and the segregating haplotype is coloured black. The markers at the boundaries of recombination events are indicated.

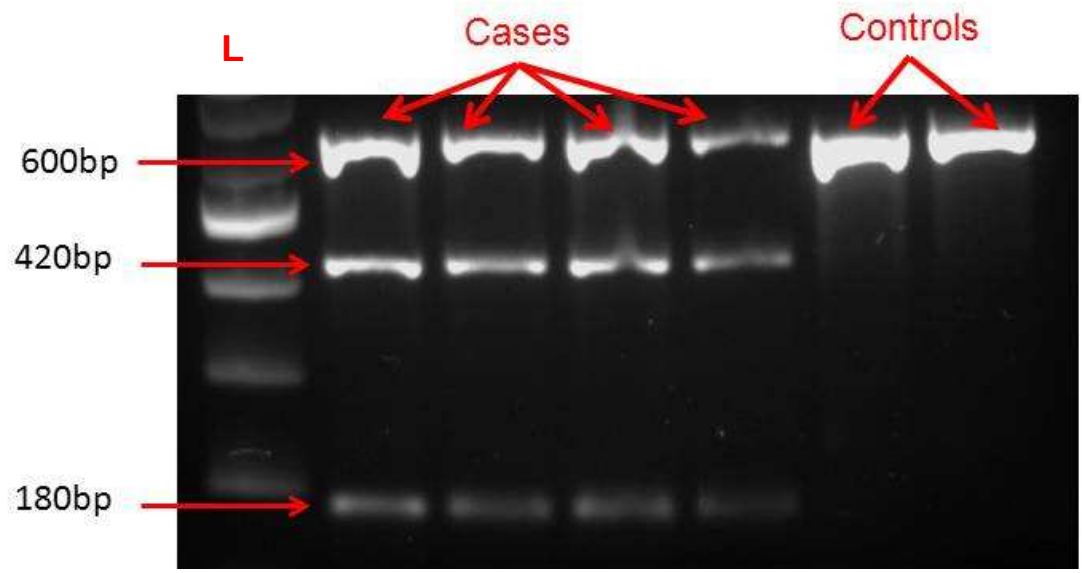

Figure 4.5. Representative result of restriction enzyme digestion for c.677G>C (*TMEM98*) on 1.4% agarose gel. The PCR products containing c.677G>C were digested by restriction enzyme Bsu36I. Fragments containing the C allele at site c.677G>C was cleaved. Lane (L) shows 100 bp ladder. Cases show genotype G/C (600 bp, 420 bp, and 180 bp), controls show wild type genotype G/G (600 bp).

Functional prediction

Polyphen-2 predicts this mutation to be possibly damaging with a score of ~60% (sensitivity 81% and specificity of 83%) under the HumVar algorithm which is the most relevant for Mendelian disorders. SIFT predicts the mutation to be damaging with a score of 0.05. Mutation Master found the variant to be disease-causing.

Expression Analysis

There are two annotated transcripts for *TMEM98*: isoform 2 differs in the 5' UTR compared to isoform 1, however both variants encode the same protein. The expression of both transcripts of *TMEM98* in ocular tissues was assessed by RT-PCR. Isoform 1 revealed a product of 544bp (expected 576bp), and isoform 2 showed a product of 534bp (expected 562) by sequencing of cDNA. Both isoforms were found to be expressed in all ocular tissues assessed including corneal endothelium, iris, sclera, optic nerve, optic nerve head, and retina. RT-PCR results for isoforms 1 and 2 are presented in **Figure 4.6**.

Analysis in independent families with nanophthalmos

Independent families with non-syndromic forms of nanophthalmos (**Section 2.1**) were sequenced to detect variants in *TMEM98*. No novel variants were detected in independent families with nanophthalmos. All variants identified in *TMEM98* in the probands are presented in **Appendix 4.**

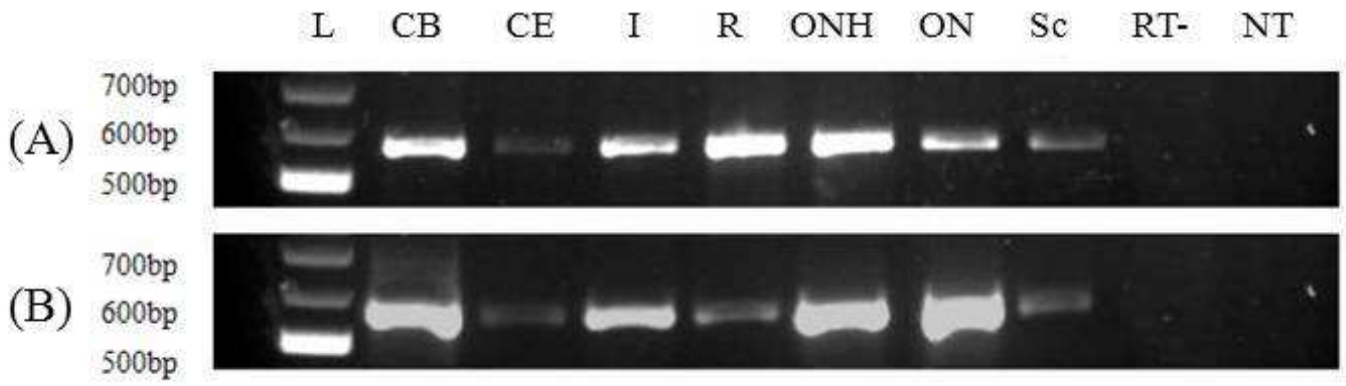

Figure 4.6. Expression analysis of *TMEM98* in human ocular tissues. (A) Isoform 1 (B) Isoform 2. RT-PCR products were observed in ciliary body (CB), iris (I), sclera (Sc), corneal endothelium (CE), optic nerve head (ONH), optic nerve (ON), and retina (R). RT negative (RT-) and a no template (NT) samples were used as a negative control to rule out contamination of the RT-PCR reaction mix. 100bp ladder is indicated by (L).

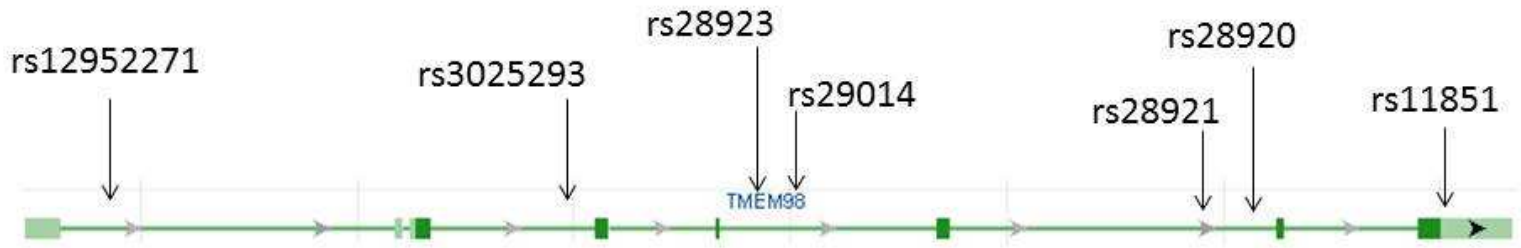

Figure 4.7. *TMEM98* gene ideogram depicting the location of all tag SNPs genotyped. Exons are indicated by solid boxes and joined by introns indicated by lines. Figure adapted from NCBI website (http://www.ncbi.nlm.nih.gov/gene).

TMEM98 association with PACG and hyperopia

Angle-closure glaucoma and hyperopia are the main complications in patients with nanophthalmos. First we tested whether common variations in *TMEM98* gene are associated with PACG. All selected tag SNPs are located in introns, except for rs11851 located in the 3' untranslated region. The physical location of the tag SNPs are presented in **Figure 4.7**.

In the Australian cohort, SNP rs3025293 (A allele) showed nominal association with PACG with p-value of 0.041 (OR 0.6, 95% CI 0.3-0.9), and rs11851 (C allele) with p-value of 0.045 (OR 1.7, 95% CI 0.9-2.9). The combined analysis showed rs3025293, and rs29014 showed nominal associations with p-value of 0.015 and 0.021, respectively. None of the above SNPs survived correction for multiple testing (Bonferroni correction for the seven SNPs is 0.05/7= 0.007 (**Table 4.3**). No association was found in the Nepalese cohort.

The power of this study at α=0.05 was assessed. The prevalence of PACG is similar in both Australian (0.4%) (Day, Baio et al. 2012) and Nepalese cohorts (0.43%). (Thapa, Paudyal et al. 2012) Assuming complete linkage disequilibrium between the disease-causing variant and the marker, we have a power of 85% in the Australian cohort and 76% in the Nepalese cohort to detect a genotypic relative risk of 1.1 with a risk allele frequency of 0.3 under an additive model.

In the haplotype results, the global p-value reached significance in the Australian cohort (p-value= 0.021) but not in the Nepalese (p-value= 0.584). The variants

formed one linkage disequilibrium block (**Figure 4.8**). Two rare haplotypes showed borderline association in the Australian cohort. The first haplotype, GGTGCTC which was associated with increased risk of PACG, contains the risk alleles (rs3025293 G allele, rs11851 C allele) of the two borderline significant SNPs (p-value 0.045, OR 1.7, 95% CI 0.9-2.9). The GATGCTT haplotype has a protective effect and it contains the protective alleles (rs3025293 A allele, rs11851 T allele) of the two borderline SNPs (p-value of 0.045, OR 0.6, 95% CI 0.3-1.0), and the GGTGCCT haplotype with p-value 0.047 (OR 0.4, 95% CI 0.2-0.9) (**Table 4.4**).

No associations were observed in the Nepalese cohort.

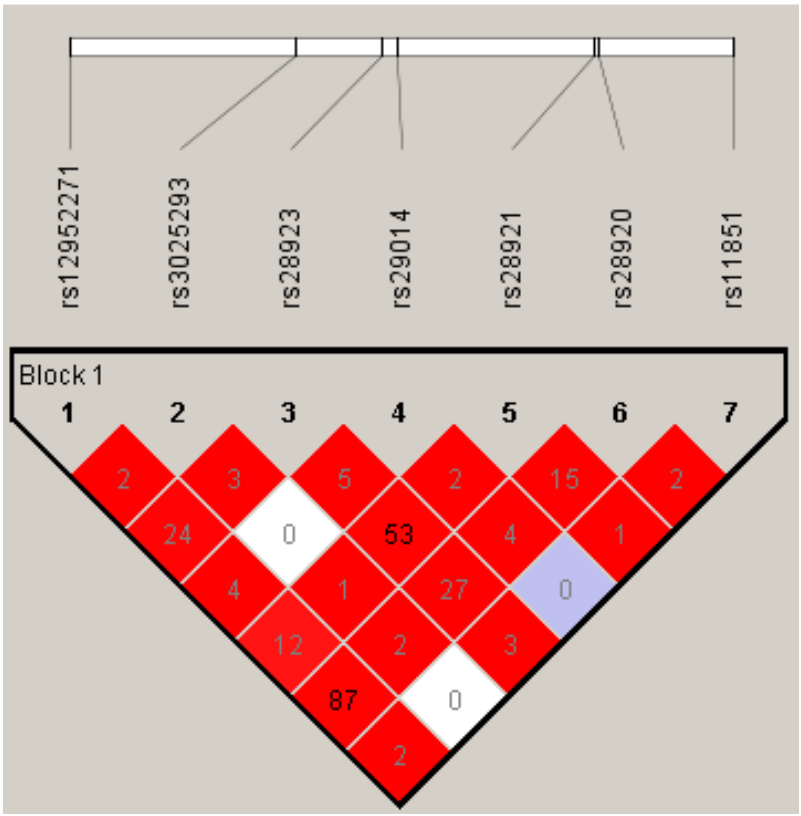

Figure 4.8. LD plot of tag SNPs in *TMEM98* haplotype. Linkage disequilibrium plot generated in Haploview shows the haplotype block structure in the Australian population using the solid spine definition. The number in the box represents the r^2 value.

Table 4.3. Minor Allele frequencies of the tag SNPs in *TMEM98* gene in both Australian and Nepalese cohort unadjusted p-value for association under the allelic model with odds ratio (95% CI). Bold p-value indicates significance after Bonferroni correction for 7 SNPs (0.007). Table shows the unadjusted p-value, and combined p-value using Cochran-Mantel-Haenszel 2x2xK test.

SNP	N#	Minor allele	Australian			Nepalese			Combined p-value
			MAF	p-value	OR (95%CI)	MAF	p-value	OR (95%CI)	
rs12952271	1	A	0.31	0.354	1.1 (0.9-1.4)	0.27	0.800	1.0 (0.8-1.4)	0.164
rs3025293	2	A	0.04	0.041	0.6 (0.3-0.9)	0.07	0.478	0.8 (0.5-1.4)	0.015
rs28923	3	C	0.38	0.330	1.1 (0.9-1.4)	0.49	0.753	0.9 (0.7-1.2)	0.418
rs29014	4	C	0.09	0.703	1.1 (0.7-1.6)	0.05	0.052	2.0 (0.9-4.2)	0.021
rs28921	5	G	0.23	0.910	0.9 (0.8-1.3)	0.44	0.690	1.0 (0.8-1.4)	0.109
rs28920	6	C	0.32	0.921	1.0 (0.8-1.3)	0.3	0.616	1.1 (0.8-1.4)	0.415
rs11851	7	C	0.06	0.045	1.7 (0.9-2.9)	0.03	0.510	0.8 (0.3-1.7)	0.097

p*= p-value adjusted for sex and age. OR (95% CI) = odds ratio (95% confidence interval). Chr= chromosome. MAF= minor allele frequency

Table 4.4. Haplotype association between variants across *TMEM98* gene and primary angle-closure glaucoma in Australian and Nepalese cohorts. The significantly associated haplotypes are highlighted in bold. The order of SNPs in haplotype follows the numbering of SNPs in Table 4.3.

Haplotype 1 2 3 4 5 6 7	**Australian**				**Nepal**			
	Cases	**Controls**	**p-value**	**OR (95% CI)**	**Case**	**Control**	**p-value**	**OR (95% CI)**
A G T G C C T	0.31	0.29	0.397	1.1 (0.9-1.4)	0.25	0.24	0.666	1.1 (0.8-1.5)
G **G** T G C T **C**	0.06	0.04	**0.045**	1.7 (0.9-2.9)	0.03	0.04	0.483	0.7 (0.3-1.7)
G G T G C T T	0.11	0.14	0.053	0.7 (0.4-1.0)	0.05	0.06	0.503	0.8 (0.4-1.5)
G G C G C T T	0.14	0.12	0.171	1.2 (0.8-1.7)	0.07	0.09	0.336	0.8 (0.4-1.4)
G **A** T G C T **T**	0.04	0.06	**0.045**	0.6 (0.3-1.0)	0.07	0.08	0.600	0.9 (0.5-1.5)
G G C G G T T	0.24	0.24	0.996	0.9 (0.7-1.3)	0.43	0.42	0.804	0.9 (0.7-1.4)
G G T C C T T	0.09	0.08	0.691	0.9 (0.6-1.5)	0.05	0.02	0.058	1.9 (0.9-4.2)
G G T G C C T	0.02	0.04	**0.047**	0.4 (0.2-0.9)	0.06	0.05	0.828	1.0 (0.5-1.9)
	global p-value **0.021**				global p-value 0.584			

OR= odds ratio, 95% CI= 95% confidence interval.

For unrelated hyperopia cases, we sequenced 20 individuals who presented with refraction of > +6.00 dioptres (**Table 4.5**). The mean refraction of these participants was +7.10 dioptres (SD 2.4). The sequencing results reported 12 common variants and no novel variants in these patients (**Table 4.6**).

Table 4.5. Spherical equivalent of participants with hyperopia to test for association with *TMEM98*. Participants were recruited to have refraction of more than +6.00 dioptres.

Participant ID	Refraction (Dioptres)		Angle-closure glaucoma status
	Left eye	Right eye	
ACG066	+13.00	n/a	Present
ACG072	+7.50	+5.50	Present
ACG093	n/a	+7.37	Present
ACG116	+7.75	+8.50	Present
ACG121	+6.00	+7.25	Present
ACG147	+6.25	n/a	Present
ACG150	+7.25	+6.50	Present
ACG193	-3.12	+6.37	Present
ACG154	+12.50	+9.50	Present
ACG247	+4.00	+6.75	Present
ACG292	+7.50	+7.0	Present
ACG301	+8.00	+8.00	Present
ACG314	+6.75	+6.50	Present
ACG332	+5.50	+7.75	Present
NSA262	+6.50	+5.00	Absent
NSA180	+6.50	+6.25	Absent
NSA040	+6.00	+6.75	Absent
NSA079	+5.50	+7.00	Absent
NSA231	+3.75	+7.50	Absent
NSA107	+0.75	+15.00	Absent

Table 4.6. Single nucleotide polymorphisms identified by sequencing *TMEM98* gene in 20 cases with hyperopia. The table shows the alleles, location in the gene, the minor allele frequencies (MAF) in cases with hyperopia and MAF obtained from NCBI website (http://www.ncbi.nlm.nih.gov/snp).

SNP	Alleles	Location	MAF (NCBI)	Protein	MAF (Hyperopia cases)
rs9911256	A/G	exon	0.06	n/a	0.10
rs11558976	A/G	exon	0.04	n/a	0.07
rs148593533	A/G	exon	0.01	p.Leu37Leu	0.05
rs72817027	C/G	intron	0.03	n/a	0.05
rs29019	T/C	exon	0.06	p.Asp65Asp	0.05
rs29016	A/G	intron	0.06	n/a	0.05
rs11080195	C/A	3' UTR	0.04	n/a	0.05
rs28259	T/C	3' UTR	0.05	n/a	0.05
rs28258	T/A	3' UTR	0.09	n/a	0.10
rs28919	T/C	3' UTR	0.34	n/a	0.23
rs9772	T/C	3' UTR	0.29	n/a	0.15
rs11851	G/A	3' UTR	0.09	n/a	0.10

Discussion

In this chapter we described a large pedigree of Caucasian background with autosomal dominant nanophthalmos and localized the gene to a 16.9 Mb region on chromosome 17p11.2-q12 between 15.3Mb and 32.7Mb. Diagnosis of nanophthalmos in this Caucasian family was based on an axial length less than 20mm and/or refractive error greater than +7.00 dioptres.

When sequencing the whole exome to identify the causative gene, a single novel segregating missense variant was identified in the linkage interval meeting our filtering criteria, located in *TMEM98*. The p.Ala193Pro variant is predicted to be damaging and, given the lack of other segregating putatively functional variants, is likely to be the causative mutation in this family. Absence of the missense mutation in 285 normal controls and in the exome variant server strengthens the hypothesis that this gene is the cause of nanophthalmos in this family. However no pathogenic variants were identified in additional families with nanophthalmos, which indicates that other genetic loci for this disorder are yet to be identified and replication of this finding in an independent family is yet to occur.

TMEM98 is found to be expressed in eye tissues affected by the disorder such as the sclera and also the tissues of irido corneal angle including ciliary body and iris, which are involved in the pathogenesis of angle-closure glaucoma. To my knowledge, very little is known about the function of *TMEM98* in general and even less in the eye and no clear functional domains have been identified. The level of TMEM98 antibody staining was reported in most normal tissues, as well as in 88% of cancers (http://www.proteinatlas.org/ENSG00000006042).

A similar linkage region has been previously reported in a Chinese family with nanophthalmos, specifically from 14.1Mb to 33.0 Mb. (Hu, Yu et al. 2011) Thus the region reported in our study is entirely encompassed by the previously reported region in the Chinese family. The overall phenotype appears similar to that described in the linked Chinese family (Yu, Hu et al. 2009) although the Caucasian family has on average slightly worse refraction (mean of +11.80 D compared to +8.00 D) and correspondingly slightly shorter axial length (mean of 17.6 mm compared to 19.2 mm). Rates of glaucoma are similar between the two families. It is possible that the causative gene is different between the two families, but it is highly likely that they are both caused by the same gene within the smaller region defined by the Caucasian family, given that the phenotype is quite similar between the two families.

The trend of association with PACG in the Australian and combined analysis suggests that this gene may play a role in the course of developing narrow angles in the population. It is expressed in ciliary body and iris, which are important in the pathogenesis of angle-closure glaucoma. We have a power of 80% to detect SNPs with MAF of 0.31. However the associated SNPs are rare and a replication in a larger cohort is essential to detect an effect. Identifying the functional role of this gene in the eye will also help uncover the involvement of *TMEM98* in the development of angle-closure glaucoma.

In conclusion, this is the first study to report mutations in *TMEM98*, to identify a novel gene to be linked to autosomal dominant type of nanophthalmos, and to show a possible association with angle-closure glaucoma.

Chapter 5

GENOME-WIDE ASSOCIATION STUDY TO IDENTIFY GENETIC SUSCEPTIBILITY LOCI FOR PRIMARY ANGLE-CLOSURE GLAUCOMA

Introduction

A genome-wide association study (GWAS) is a method employed to find genes associated with a disease or trait. No hypothesis is required about what genes will be included. It screens the whole genome without bias to candidate genes of known function. A GWAS investigates the association of genetic markers with the disease phenotype, and positive genetic markers at any region will be further analysed regardless of the gene function. GWAS has been widely used to identify various loci associated with other complex eye diseases such as age-related macular degeneration (Klein, Zeiss et al. 2005; Rivera, Fisher et al. 2005; Edwards, Fridley et al. 2008) keratoconus (Burdon, Macgregor et al. 2011) open angle glaucoma (Burdon, Macgregor et al. 2011) and pseudoexfoliation disease. (Thorleifsson, Magnusson et al. 2007; Craig, Hewitt et al. 2009; Krumbiegel, Pasutto et al. 2011)

In this chapter we conducted a GWAS in our PACG cohorts using a novel blood pooling methodology, whereby the whole blood is pooled before the DNA extraction stage and pooled samples are genotyped. This reduces the cost and the time of the study and has been previously validated in eye diseases with known genes of large effect size. (Craig, Hewitt et al. 2009)

Aim

PACG is a complex disease, with the causative genes yet to be identified. Thus, in order to further understanding of the genetics of PACG, a GWAS was conducted using cohorts from Australia and Nepal to detect novel susceptibility loci.

Methods

Sample Selection

This part of the study was conducted earlier in the PhD (2010). The Australian cohort included 100 cases and 216 controls, and in the Nepalese cohort included 100 cases and 200 controls. Further details about the cohort are presented in **Section 2.2**.

Blood pool methodology

The Australian and Nepalese blood samples used in constructing the pool were stored in a cold room at 4°C in EDTA blood collection tubes. The pooling procedure has been described previously. (Craig, Hewitt et al. 2009) In brief, each sample was first lysed with QIAGEN protease® then an equal volume of 200µl blood of each case sample from one cohort were pooled together and the same was done for control samples, forming at the end a single blood sample for each case and control cohort. The DNA was extracted from each of the pooled blood tubes using QIAamp DNA blood maxi kit following the manufacture's protocol. Each pool was prepared in duplicate. The concentration of DNA samples was estimated using the Smartspec Plus spectrophotometer (Bio-Rad, Sydney, Australia).

Genotyping methodology

Blood pool genotyping was carried by the department of Genetics and Population Health at the Queensland Institute of Medical Research (QIMR). DNA from each pool was hybridized to multiple 1M Illumina arrays. Each array slide has the capacity to genotype two independent samples and was allocated to receive a case and a control pool. All analyses of array data and the statistics were designed and conducted by Dr Stuart Macgregor. Bead-level intensity data were analysed and SNPs with beadscore values ≤50 were excluded. Copy number variants and SNPs from the sex chromosomes were not analysed. To allow pooling analysis an option in the Illumina software was used to make raw two colour (green/red) beadscores available as output from array scans. (Macgregor, Zhao et al. 2008) Beadscores required calibration because green beadscores tended to be larger than red beadscores. Illumina 1M arrays had 20 stripes per array, each with 50,000 SNPs. Within each stripe, half of the SNPs were from the Illumina ‘‘TOP’’ strand (A/C and A/G SNPs) and half were from the Illumina ‘‘BOTTOM’’ strand (T/C and T/G SNPs). The pooling allele frequency (PAF) was computed as the corrected red intensity divided by the total (corrected red plus green) intensity. Normalization was performed within stripe, separately for each strand by rescaling the red beadscore to make the mean PAF value = 0.5 (for all SNPs on that stripe/strand). A very small number of SNPs had <5 PAF estimates available and were dropped. (Craig, Hewitt et al. 2009)

SNPs were removed from the analysis if they had a minor allele frequency <2% in the HapMap reference samples. SNPs were also removed from the analysis if they

had a -log10(P) quality control value >6. With these criteria, the pooling method has shown to be a reliable technique to find genetic susceptibility loci for complex diseases when compared to individual genotyping. (Pearson, Huentelman et al. 2007; Macgregor, Zhao et al. 2008; Bosse, Bacot et al. 2009) This pooling methodology has an important limitation in the lack of individual genotype data and thus we are unable to adjust for covariates in the analysis. In addition, due to error in the allele frequency estimation the power of pooling-based GWAS studies will decrease compared to individual level genotyping. In the Australian cohort 851,989 SNPs were retained after standard quality control, while in the Nepalese control we had 860,265 SNPs.

SNP selection and individual genotyping

The top 10,000 SNPs showing significant differences between case and control frequencies in each cohort of PACG were supplied by Dr Macgregor for data mining. A SNP was given priority for individual validation if it has a p-value of less than $1x10^{-07}$ in either the Australian or Nepalese cohort, or $p<1x10^{-08}$ in the meta-analysis of both cohorts. These prioritised SNPs were assigned to a multiplex for individual validation and replication. The ability for a SNP to be included in a multiplex is dependent on the base change of the SNP and the flanking sequence.

Individual genotyping for validation used the same samples as in the blood pool. For replication analyses additional samples subsequently recruited into each cohort were used. The top ranked SNPs were genotyped for validation and replication using the iPLEX Gold chemistry (Sequenom Inc., San Diego, California) on an Autoflex mass

spectrometer (Sequenom Inc., San Diego, California) at the Australia Genome Research Facility (AGRF), Brisbane. SNP associations were considered as validated if they reached p-value of $<5x10^{-08}$ in the allelic model of the univariate analyses in the original pooled cohort, and replicated if the significant SNP had p-value of less than 0.05 in additional independent participants recruited. All analyses of individual genotyping were conducted in PLINK (v1.06).

Results

GWAS in the Australian cohort

The Australian cohort consisted of 100 cases (24 Acute PACG, 45 chronic PACG, and 31 PACS) and 216 controls. The GWAS results of the Australian cohort did not show striking genome-wide significant hits, as indicated in **Figure 5.1.** The level of genome-wide significance is $p<5x10^{-08}$.

The top variant, rs10505841 on chromosome 12, had a p-value of $4.6x10^{-8}$; however, it failed quality control checks. Several SNPs were however of potential interest as they showed a trend towards association, which requires individual genotyping for validation and replication; rs7612146 (*SEC22A*) on chromosome 3 with p-value of $1.44x10^{-07}$, rs332540 (*LOC133789*) on chromosome 5 with p-value of $1.65x10^{-07}$ and rs10066520 (located between *JAKMIP2-SPINK1)* on chromosome 5 with p-value of $2.19x10^{-07}$ (**Table 5.1**).

Table 5.1. Top ranked SNPs from the Australian cohort.

Gene Symbol	Chr	SNP ID	bp position	p-value	Relation to the gene
SEC22A	3	rs7612146	120312970	1.44 x10^{-07}	intron
LOC133789	5	rs332540	85984431	1.65 x10^{-07}	exon
JAKMIP2	5	rs10066520	142314627	2.19 x10^{-07}	within 5kp

bp=base position, chr=chromosome

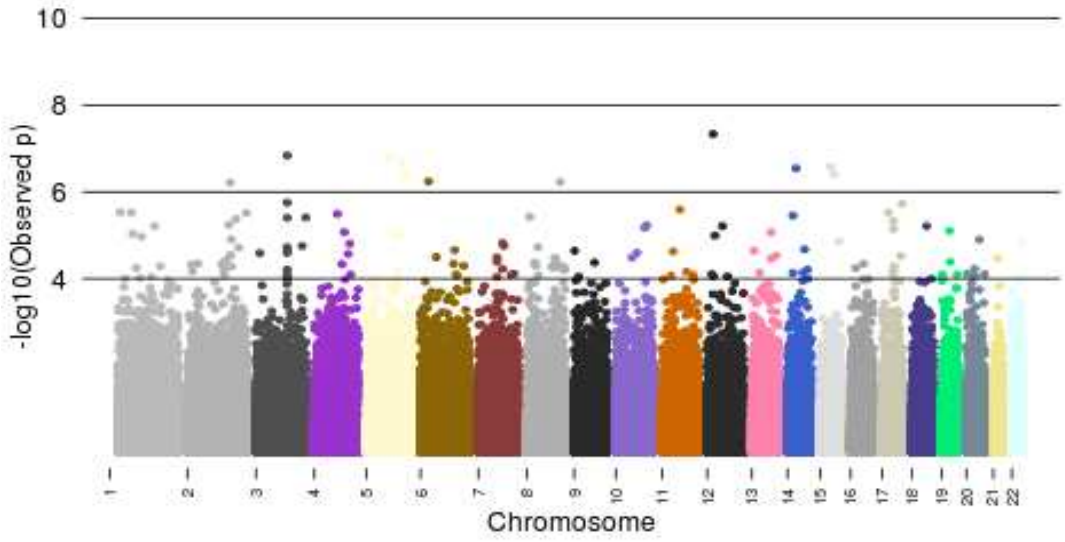

Figure 5.1. Manhattan Plot showing the GWAS results from the Australian cohort. Each dot represents a SNP with its –log p value. Each column represents a chromosome.

GWAS in the Nepalese cohort

The Nepalese cohort consisted of 100 cases (50 acute PACG, 50 chronic PACG, and no PACS) and 200 controls matched for age, gender and ethnic group. In the GWAS on Nepalese samples, five SNPs had significant association p-values of $<5x10^{-08}$ as presented in **Figure 5.2**; rs6917933 (*DDX43* gene) on chromosome 6 with p-value of $2.77x10^{-15}$, rs10037437 (*LOC285577*) on chromosome 5 with p-value of $2.68x10^{-12}$, rs3735351 (*PARP12*) on chromosome 7 with p-value of $2.28x10^{-10}$, rs4146792 (*FAM198A*) on chromosome 3 with p-value of $6.02x10^{-10}$, and rs9895456 (*ASIC2*) on chromosome 17 with p-value of 3.44×10^{-09} (**Table 5.2**). Further validation and replication is required to detect whether these strong results are false positive or not.

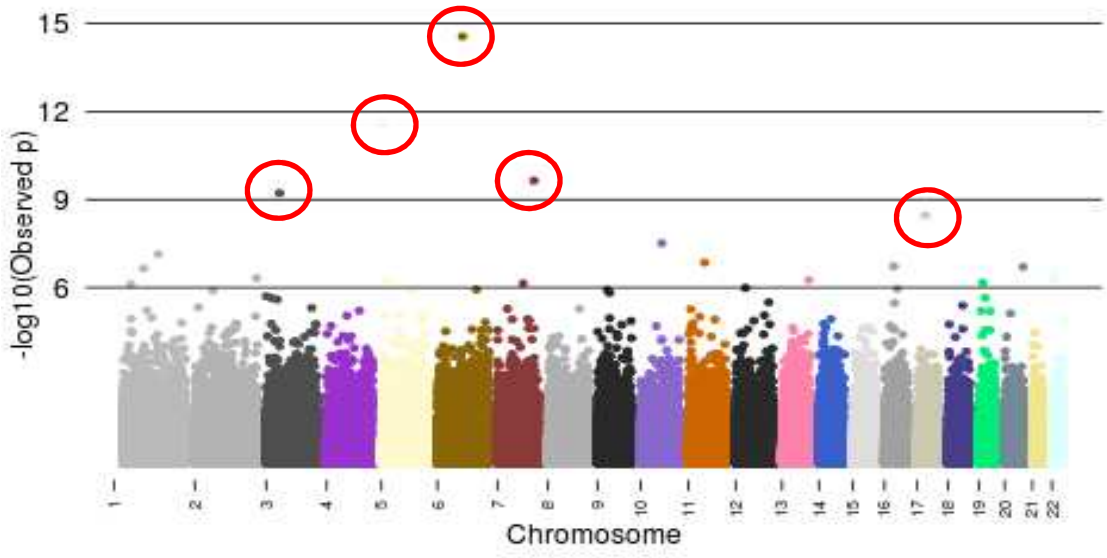

Figure 5.2. Manhattan plot of the top ranked SNPs from GWAS results on Nepalese cohort with PACG. Circled SNPs reached genome wide significance ($p<5x10^{-08}$).

Table 5.2. Top Ranked SNPs of the Nepalese cohort.

Gene Symbol	Chr	SNP	bp position	p-value	Relation to the gene
DDX43	6	rs6917933	71302766	2.77E-15	5'UTR
LOC285577	5	rs10037437	3309754	2.68E-12	within 80kb
PARP12	7	rs3735351	134018561	2.28E-10	intron
FAM198A	3	rs4146792	43081068	6.02E-10	intron
ASIC2	17	rs9895456	27667387	3.44E-09	intron
S100A7	1	rs12132927	124794940	7.25E-08	intron
GLYAT	11	rs948559	54803184	1.42E-07	within 20kb
HAR1A	20	rs6011613	58449973	1.99E-07	intron
CDH18	5	rs2972819	19490583	6.05E-07	intron
SPC24	19	rs8111157	10835294	6.89E-07	intron
PDIK1L	1	rs2783711	24682916	7.71E-07	within 9kb

Validation and replication in the Australian cohort

Validation analysis was conducted using the 100 cases and 216 controls included in the Australian pools. SNP were considered validated if they reached a p-value of $5x10^{-08}$ in the individually typed samples from the pools (**Table 5.3**).

An independent cohort of patients subsequently recruited was used for replication. This consisted of 210 cases and 72 controls in the Australian cohort. 28 of these cases were identified with acute PACG, 113 cases with chronic PACG, and 69 cases with PACS.

None of the SNPs in the Australian cohort reached the level of significance for validation, but one SNP rs10066520 (located between *JAKMIP2-SPINK1*) on

chromosome 5 showed any level of association in the replication with p-value 0.028 (OR 0.4, 95%CI 0.2-0.9). No associations were found when analysing the combined validation and replication cohorts.

Validation and replication in the Nepalese cohort

Validation analysis was conducted on the 100 cases and 200 controls from the Nepalese pools. In the replication cohort, 60 cases and 118 controls were included in the study; all 60 cases were identified as PACS (**Table 5.4**).

SNP rs10037437 was unable to be genotyped due to an inability to design a Sequenom assay for this SNP. It is in strong LD with rs10039361 in the HapMap CHB reference sample (r^2=1), and thus this SNP was typed as a proxy. Four SNPs showed a trend towards significance in the validation results however none reach level of genome-wide significance (>$5x10^{-08}$); rs6917933 (p-value 0.005), rs10039361 with p-value 0.007 (OR 2.3, 95%CI 1.2-4.4), rs3735351 with p-value 0.004 (OR 0.1, 95%CI 0.01-0.7), rs4146792 with p-value 0.003 (OR 0.2, 95%CI 0.1-0.7), and rs9895456 with p-value 0.017 (OR 0.3, 95%CI 0.1-0.9).

The odds ratio was not calculated for rs6917933 (*DDX43* gene) as the minor allele was not present in cases of the validation cohort. None of the above SNPs reached the required level of significance nor did they show association in the independent Nepalese cohort. No genome-wide significant signals were detected when analysing the combined validation and replication cohorts.

Table 5.3. The table shows p-value of the top ranked SNPs in the Australian cohort from the pooled GWAS data, validation, replication and combined analysis from the individual genotyping data.

SNP	GWAS	Validation		Replication		Combined	
	p-value	**p-value**	**OR (95% CI)**	**p-value**	**OR (95% CI)**	**p-value**	**OR (95% CI)**
rs7612146	$1.44x10^{-07}$	0.393	0.8 (0.5-1.3)	0.715	0.8 (0.2-2.8)	0.544	0.9 (0.7-1.3)
rs332540	$1.65x10^{-07}$	0.405	1.2 (0.7-2.1)	0.885	1.1 (0.3-5.0)	0.387	1.2 (0.8-1.7)
rs10066520	$2.19x10^{-07}$	0.944	1.0 (0.7-1.4)	0.028	0.4 (0.2-0.9)	0.495	1.1 (0.9-1.4)

OR= odds ratio, CI=confidence interval, Bold p-value indicated significance. p-value of $<5x10^{-08}$ in validation is considered GWAS significant. p-value of <0.05 is required in replication to reach level of significance.

Table 5.4. The table shows p-value for validation and replication of the top ranked SNPs in the Nepalese cohort

SNP	DNA Pool	Validation		Replication		Combined	
	p-value	p-value	OR(95% CI)	p-value	OR(95% CI)	p-value	OR(95% CI)
rs6917933	2.77E-15	0.005	-	0.550	1.4 (0.5-4.0)	0.114	0.5 (0.2-1.2)
rs10039361	-	0.007	2.3 (1.2-4.4)	0.221	1.9 (0.7-5.4)	0.119	1.2 (0.9-1.6)
rs3735351	2.28E-10	0.004	0.1 (0.01-0.7)	0.170	2.8 (0.6-12.6)	0.074	0.4 (0.2-1.1)
rs4146792	6.02E-10	0.003	0.2 (0.1-0.7)	0.370	0.7 (0.4-1.4)	0.007	0.5 (0.3-0.8)
rs9895456	3.44E-09	0.017	0.3 (0.1-0.9)	0.925	1.0 (0.4-2.7)	0.067	0.5 (0.3-1.1)
rs12132927	7.25E-08	0.765	1.1 (0.7-1.5)	1.000	1.0 (0.6-1.7)	0.800	1.0 (0.8-1.4)
rs948559	1.42E-07	0.964	0.3 (0.1-0.9)	0.914	1.0 (0.4-2.7)	0.972	1.0 (0.8-1.3)
rs6011613	1.99E-07	0.595	0.9 (0.6-1.4)	0.026	0.5 (0.3-0.9)	0.063	0.7 (0.5-1.0)
rs2972819	6.05E-07	0.575	0.8 (0.5-1.6)	0.640	0.8 (0.3-2.0)	0.478	0.8 (0.5-1.4)
rs8111157	6.89E-07	0.787	0.9 (0.6-1.4)	0.918	0.9 (0.6-1.6)	0.776	1.0 (0.7-1.3)
rs2783711	7.71E-07	0.432	1.6 (0.5-5.3)	0.050	2.5 (1.0-6.2)	0.052	2.0 (1.0-4.2)

p-value of $<5x10^{-08}$ in validation is considered GWAS significant. p-value of <0.05 is required in replication to reach level of significance. OR= odds ratio, CI=confidence interval.

Discussion

Much research has been conducted to investigate the underlying genetic causes of PACG for a better understanding of this disease. Here we attempted to conduct a GWAS study to identify the susceptibly gene candidates for this disease.

This GWAS was the first to be done for PACG at the time it was performed. Genetic markers that showed significant association with the disease were not validated through individual genotyping in the Australian cohort. In the Nepalese cohort only five SNPs showed a p-value of <0.003 in validation but failed to reach level required for significance.

Several limitations of this study are apparent. The inability to follow up a number of SNPs that were significant in the blood pool due to failed assay design on the Sequenom platform is a limitation, and different technologies may be needed in future studies to genotype these SNPs. Also the blood-pooling design can lead to pooling error and possible imprecision in allele frequency estimation. It is also of note that all associations detected in the blood pooling were significantly reduced on individual typing; this can be from inflation of their result in the pool. Other significant SNPs may have not been detected in the pooling due to a false reduction in associations. Suboptimal power in both cohorts was another limitation. The limitation in the Nepalese cohort is we don't have the proper reference population, and HapMap CHB population was used as the most closely related population available at the time of the study, as allele frequencies and linkage disequilibrium structure were similar between the Nepalese and CHB HapMap datasets as explained

previously in **Section 2.2.** The potential explanation for the lack of significance in the Nepalese replication cohort, in addition to the small number, is that all 60 cases were identified having PACS, whereas all cases included in the blood pool presented with PACG.

In conclusion, this GWAS was not able to identify significant associations with PACG in either cohort. It is accepted that additional GWAS on a much larger cohorts will be essential to detect an effect. The aim of this chapter was to determine if a susceptibility locus of large effect size such as *Lysyl oxidase-like 1* (*LOXL1)* for pseudoexfoliation syndrome (Thorleifsson, Magnusson et al. 2007) and *Complement factor H (CFH)* for age-related macular degeneration (Klein, Zeiss et al. 2005) existed for angle-closure glaucoma. The next three chapters investigate the association of previously reported candidate genes with PACG in our cohorts, and in addition to testing the association of nanophthalmos-associated genes (*MFRP*, and *PRSS56*) with PACG.

Chapter 6

CANDIDATE GENE STUDY FOR IDENTIFYING GENETIC RISK FACTORS FOR PRIMARY ANGLE-CLOSURE GLAUCOMA

Introduction

Hepatocyte Growth Factor (*HGF* OMIM: 142409) plays an important role in stimulating the growth and migration of various ocular tissues including cornea, iris, retinal pigment epithelium, lens epithelium and trabecular meshwork. (Li, Weng et al. 1996; Weng, Liang et al. 1997; He, He et al. 1998; Wordinger, Clark et al. 1998) It affects the emmetropization process of the eye. Various investigators have revealed that the concentration of *HGF* in the aqueous humor was significantly higher in glaucomatous eyes than in cataract eyes used as a control group, with no difference between open angle and angle-closure glaucoma. (Hu, Han et al. 2001; Veerappan, Pertile et al. 2010)

The increase in the *HGF* concentration in aqueous humor of glaucomatous eyes possibly reflects the functional effects of *HGF* on enhancement of aqueous flow and an attempt to repair trabecular injury, rather than directly causing glaucoma. (Hu and Ritch 2001)

No previous study has looked for association of *HGF* with PACG, but other studies found association with myopia (near-sightedness) (Han, Yap et al. 2006; Yanovitch, Li et al. 2009) and keratoconus (an eye condition that affects growth and refraction

of the eye). (Burdon, Macgregor et al. 2011) Two intronic SNPs rs12536657 and rs5745718 within the *HGF* gene have been reported to be significantly associated with hyperopia (severe farsightedness) in a Caucasian cohort. (Veerappan, Pertile et al. 2010) Furthermore SNP rs12536657 in the same study was also shown to be associated with myopia. The authors hypothesised that what seems to be refraction in different directions (hyperopia and myopia) with the same allele of the SNP could result from the influence of neighbouring SNPs, gene–gene interactions, or gene–environmental influences. Since both PACG and hyperopia share the same feature of a relatively short axial length (Sihota, Lakshmaiah et al. 2000), we hypothesized the association of this gene with PACG.

Matrix Metalloproteinase-9 (*MMP-9* OMIM: 120361) is one of a tightly regulated family of zinc-dependent enzymes, and is important in remodelling of the extra-cellular matrix (ECM). (Wong, Sethi et al. 2002) The MMP9 protein plays an important role in extracellular matrix remodelling by cleaving denatured collagen and type IV collagen in the basement membrane. Unlike *HGF, MMP-9* has been previously investigated for association with PACG. An association was identified via candidate genes studies between SNP rs17576 in the *MMP-9* gene and PACG in 78 Taiwanese patients. (Wang, Chiang et al. 2006) The researchers postulated that the gene activity may have been down regulated in PACG patients, leading to reduction of *MMP-9* activity in ECM remodelling during ocular development and thus shorter axial length. SNP rs17576 is located in exon 6 of the *MMP-9* gene, where the mutation leads to the substitution of positively charged amino-acid (arginine) by an uncharged amino acid (glutamine) at residue 279. (Natividad, Cooke et al. 2006)

This non-synonymous substitution is situated in the coding sequence of a highly conserved gelatinase-specific fibronectin type II domain (FN2). (Allan, Docherty et al. 1995) The FN2 domain is one of three types of the internal repeats that combine to form larger domains within fibronectin (a plasma protein that binds various cell surface compounds such as collagen, fibrin, heparin, DNA and actin). This domain is responsible for the collagen affinity of *MMP-9*. (Banyai and Patthy 1991) Neither a study involving 217 Singaporean (Aung, Yong et al. 2008) nor one including 211 Southern Chinese patients (Cong, Guo et al. 2009) replicated this association. However, the latter reported an association between another SNP rs2250889 in the *MMP-9* gene with PACG. SNP rs2250889 is also a missense mutation located in exon 10, in the second COOH-terminal hemopexin-like domain of *MMP-9*. It leads to a substantial change from proline (a cyclic, nonpolar amino acid) to arginine (a positively charged residue). (Cong, Guo et al. 2009) The precise impact of these mutations on protein function is currently unknown, but it has been suggested that it could lead to partial loss of function in ECM remodelling during eye growth and development. (Wang, Chiang et al. 2006)

Methyl-tetrahydrofolate Reductase (*MTHFR* OMIM: 607093) encodes for the methylene tetrahydrofolate reductase (MTHFR) enzyme, which is responsible for the conversion of homocysteine to methionine. (Yamada, Chen et al. 2001) Michael and colleagues (Michael, Qamar et al. 2008; Micheal, Qamar et al. 2009) identified two non-synonymous SNPs associated with PACG in the Pakistani population c.677C>T (rs1801133) and c.1298A>C (rs1801131 The c.677C>T is a missense mutation leading to the substitution of valine for alanine at position 222 of the MTHFR

enzyme, causing the synthesis of a thermolabile enzyme. A further SNP, c.1298A>C, which is located within the COOH terminal regulatory domain of the *MTHFR*, results in substitution of glutamate to alanine residue. Apparently the c.1298A>C mutation alone does not significantly affect homocysteine levels, but requires the combination of the c.677C>T mutation to have an effect. (Ghazouani, Abboud et al. 2009) Both mutations are associated with a reduction in MTHFR enzyme activity (Van Der Put, Gabreels et al. 1998), which leads to an increase in circulating homocysteine levels. (Weisberg, Jacques et al. 2001) High homocysteine levels may predispose to neuronal cell death (Lipton, Kim et al. 1997) and extracellular matrix (ECM) remodelling. (Tyagi 1998)

Membrane Frizzled-Related Protein (MFRP OMIM: 606227) is known for its association with autosomal recessive nanophthalmos in multiple studies, and we reported it to be the cause of recessive nanophthalmos in Family 3 in this thesis (**Chapter 3**). As nanophthalmos patients often develop severe angle-closure glaucoma due to the crowding of the anterior chamber from the relatively large-sized lens, *MFRP* has been studied in relation to PACG in 63 Taiwanese patients (Wang, Lin et al. 2008) and 108 Chinese patients (Aung, Lim et al. 2008) by direct sequencing, but no variants have been detected. We tested the common variations within this gene with PACG.

Calcitonin Receptor-like Receptor (*CALCRL* OMIM: 114190) is a G protein-coupled receptor transported to the cell membrane from the endoplasmic reticulum by receptor activity-modifying protein 2 (RAMP2), where it is glycosylated and

becomes a receptor for adrenomedulin (AM). (McLatchie, Fraser et al. 1998) AM is expressed in the irido-ciliary body where it has a relaxant effect on the iris sphincter. Topical administration of an AM antagonist has a strong effect on IOP through specific AM receptors, implying that AM is a candidate for an IOP modulator. (Taniguchi, Kawase et al. 1999) Overexpression of this gene causes pupillary sphincter muscle relaxation, closure of the anterior chamber angle with obstruction of the aqueous outflow and elevation of the IOP. (Yousufzai, Ali et al. 1999) Cao and colleagues (Cao, Liu et al. 2009) identified a possible association between the intronic SNP rs1157699 in *CALCRL* and acute PACG in Chinese individuals.

Aim

This chapter will focus on a candidate gene study that was undertaken with the aim of replicating previously reported genetic associations of PACG in our cohorts from Australia and Nepal. The hypothesis was that common polymorphisms within the selected genes contribute to PACG risk.

Methods

This study was conducted in 2010. At that time the Australian cohort consisted of 106 cases and 288 controls while the Nepalese cohort contained 106 cases and 204 controls. In this chapter we tested the association of five genes (*HGF, MMP-9, MTHFR, MFRP,* and *CALCRL*) with PACG. SNPs selection and analyses followed the same protocol as presented in **section 2.2.** The numbers of tag SNPs chosen in

each gene for both cohorts are presented in **Table 6.1.**

Previously reported SNPs for association with PACG were included in the selection of tag SNPs; rs12536657, and rs5745718 in *HGF* (Veerappan, Pertile et al. 2010) rs17576 in *MMP-9* (Wang, Chiang et al. 2006) rs1801133 in *MTHFR* (Micheal, Qamar et al. 2009) rs36015759 and rs35885438 in *MFRP*. (Wang, Lin et al. 2008)

Table 6.1. Tag SNPs, chromosome and base position in each gene included in this chapter. "Y" indicates that the tag SNP was selected to represent variation in the specified cohort, "-" tag SNP was not selected for that cohort, "*" SNPs included for direct comparison to previous studies, "Chr" chromosome.

Chr	Gene	SNP	bp Position	Australia	Nepal
7	*HGF*	rs5745752	75939418	Y	Y
		rs5745718 *	75939418	Y	Y
		rs5745692	81358266	Y	Y
		rs5745616	76002095	Y	Y
		rs3735520	76004677	Y	Y
		rs2286194	75959471	Y	Y
		rs17501080	76007434	Y	Y
		rs17155414	75966501	Y	Y
		rs12707453	75973166	Y	Y
		rs12540393	75967934	Y	-
		rs12536657 *	75954170	Y	Y
		rs17427817	75968182	-	Y
20	*MMP-9*	rs17577	41384546	Y	Y
		rs3787268	41383166	Y	Y
		rs3918254	41381826	Y	Y
		rs17576 *	41381660	-	-
		rs3918249	41379559	-	Y

Table 6.1. Continue

Chr	Gene	SNP	bp Position	Australia	Nepal
1	*MTHFR*	rs9651118	11017270	Y	Y
		rs1801133 *	11856378	Y	Y
		rs2066470	11018113	Y	-
		rs7538516	10991768	Y	-
		rs4845881	10982979	Y	-
		rs12121543	11009747	Y	-
		rs6541003	11010943	-	Y
		rs4846040	10992134	-	Y
11	*MFRP*	rs2510143	115156930	Y	Y
		rs3814759	115158279	Y	-
		rs948414	115155497	Y	Y
		rs10790289	115155864	Y	Y
		rs948413	115155470	Y	Y
		rs883245	115158010	Y	-
		rs11217241	115154002	-	Y
		rs12421909	115156600	-	Y
		rs36015759 *	115156978	-	Y
		rs35885438 *	115155745	-	Y
2	*CALCRL*	rs840617	180089856	Y	Y
		rs6759535	180097633	Y	Y
		rs3771073	180145781	Y	Y
		rs7591567	180164026	Y	Y
		rs3821183	180115725	Y	Y
		rs10931283	180071262	-	Y
		rs13411274	180095532	-	Y
		rs9288141	180119187	-	Y

Results

In total, 705 individuals (310 Nepalese and 395 Australians) were included in this study. **Table 6.2** displays characteristics and clinical data of cases and controls for each cohort. Age and gender differences between cases and controls were evident in the Australian cohort but not the Nepalese. Spherical equivalent was not statistically different between Nepalese cases and controls ($p=0.16$), while Australian cases were more hyperopic than controls ($p<0.001$). No SNP deviated from Hardy-Weinberg equilibrium in either cohort ($p<0.05$), and thus all SNPs were subsequently included in the association study. The overall genotyping call rate was >98%.

Power calculations were conducted assuming complete linkage between the disease-causing variant and marker SNP, and a prevalence of PACG in the Caucasian population of 0.4%. (Day, Baio et al. 2012) Our Australian subset had 86% power to detect a significant genetic association for PACG at the $\alpha=0.05$ level for a genotypic relative risk of 1.3, and a risk allele frequency of 0.4 under an additive model. The prevalence of PACG in the Nepalese population is 0.43%. (Thapa, Paudyal et al. 2012) In our Nepalese cohort, under an additive model we had 82% power to detect a genetic variant with same effect size and allele frequency as that outlined for our Australian cohort.

Table 6.2. Characteristics of the Nepalese and Australian cohorts.

Variables	Australian			Nepalese		
	Case	**Control**	**P-value**	**Case**	**Control**	**P-value**
Number	107	288	-	106	204	-
Sex (% female)	67%	53%	0.01	76%	75%	0.85
Mean age in years (SD)	76 (8.2)	69 (11.2)	<0.001	57.3(12.30)	60.3(13.7)	0.07
Mean SE in dioptres (SD)	0.9 (2.2)	0.1 (0.4)	<0.001	-0.30 (1.64)	0.1 (0.3)	0.16

SD= standard deviation; SE= spherical equivalent

Hepatocyte growth factor

In *HGF*, all 12 tag SNPs were located in the introns, with the physical location presented in **Figure 6.1**. Bonferroni correction for the 12 SNPs was 0.05/12= 0.0042.

In the Nepalese cohort, four SNPs reached statistical significance for association with PACG; rs5745718, A allele, (p=0.002, OR 2.2, 95%CI 1.3-3.5), rs12536657, A allele, (p=0.002, OR 2.1, 95%CI 1.3-3.3), rs12540393, C allele, (p=0.001, OR 2.2, 95%CI 1.4-3.5) and rs17427817, C allele, (p=0.001, OR 2.2, 95%CI 1.4-3.5). After using multivariate analyses controlling for sex and age via logistic regression, three SNPs remained significantly associated with PACG rs5745718 (p=0.003), rs12540393 (p=0.001) and rs17427817 (p=0.001) (**Table 6.3**). The analysis was also adjusted for refraction, as *HGF* is reported to be associated with different types of refractive error diseases (myopia and hyperopia), and all four SNPs remained significant. No associations were found in the Australian cohort or in the combined analysis.

Haplotypic associations with PACG were investigated in the Nepalese cohort. Two haplotype blocks were identified under the "solid spine" block definition, as displayed in **Figure 6.2**. Block 1 was defined by all SNPs between rs5745752 and rs5745616 and block 2 as SNPs rs3735520 to rs17501080. In block 1 the frequency of the GAATGCCAG haplotype was significantly greater in cases (18%) than in controls (9%) with p-value of 0.001 (OR 2.0, 95%CI 1.3-3.3) and remained significant after Bonferroni correction for the 6 haplotypes observed (p=0.006). Additionally, in block 2 the frequency of the CCA haplotype was found to be higher

in cases 15% than controls 8% with p-value of 0.017 (OR 1.8, 95%CI 1.1-2.9), but this difference did not remain statistically significant following Bonferroni correction (p=0.068) (**Table 6.4**).

In the Australian cohort, a rare haplotype ACGTGTGAA in block 1 showed nominal association with p-value of 0.026 (OR 0.4, 95%CI 0.1-1.1); however, it did not pass Bonferroni correction for the nine haplotypes observed (corrected p=0.234). This haplotype appears to be protective in the Australian cohort as the frequency is higher in controls 7% than in cases 3%. This haplotype is rare and not associated in the Nepalese cohort (p=0.288, OR 1.3, 95%CI 0.7-2.1).

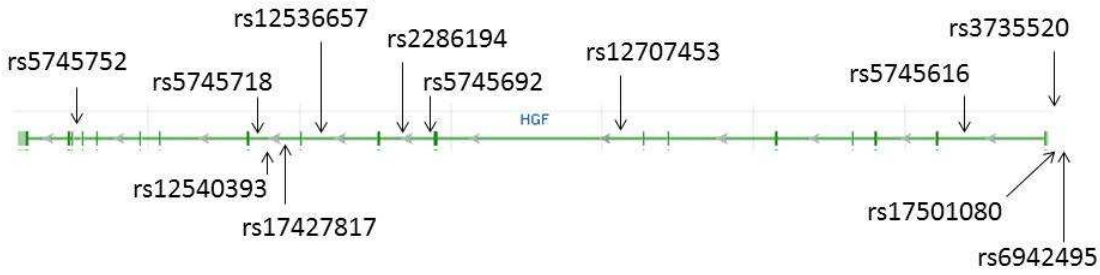

Figure 6.1. *HGF* gene ideogram depicting the location of all tag SNPs genotyped. Exons are indicated by solid boxes and joined by introns indicated by lines. Figure adapted from NCBI website (http://www.ncbi.nlm.nih.gov/gene)

Table 6.3. Allelic association results for *HGF* gene in both Australian and Nepalese cohorts. p-values of less than 0.05 are highlighted in bold. Table shows the unadjusted p-value, adjusted p-value for sex and age, and combined p-value using Cochran-Mantel-Haenszel 2x2xK test

N#	SNP	Minor Allele	Australian				Nepalese				Combined p-value
			MAF	p-value	OR	p*	MAF	p-value	OR	p*	
1	rs5745752	A	0.28	0.827	1.0 (0.7-1.4)	0.810	0.36	0.754	0.9 (0.7-1.3)	0.694	0.707
2	rs5745718	A	0.21	0.365	1.2 (0.8-1.7)	0.310	0.18	**0.002**	**2.2 (1.3-3.5)**	**0.003**	0.261
3	rs12536657	A	0.21	0.543	1.1 (0.7-1.6)	0.395	0.19	**0.002**	**2.1 (1.3-3.3)**	**0.009**	0.174
4	rs2286194	A	0.18	0.555	1.1 (0.7-1.7)	0.574	0.17	0.485	0.9 (0.6-1.3)	0.453	0.942
5	rs5745692	C	0.06	0.110	1.8 (0.8-3.8)	0.313	0.01	0.133	0.2 (0.03-1.9)	0.992	0.532
6	rs12540393	C	0.23	0.386	1.2 (0.8-1.7)	0.326	0.21	**0.001**	**2.2 (1.4-3.5)**	**0.001**	0.167
7	rs17427817	C	0.23	0.386	1.2 (0.8-1.7)	0.328	0.21	**0.001**	**2.2 (1.4-3.5)**	**0.001**	0.167
8	rs12707453	G	0.16	0.876	1.0 (0.6-1.6)	0.773	0.23	0.752	0.9 (0.6-1.4)	0.787	0.893
9	rs5745616	A	0.23	0.946	1.0 (0.6-1.4)	0.604	0.35	0.545	1.1 (0.8-1.6)	0.474	0.689
10	rs3735520	T	0.41	0.942	1.0 (0.7-1.4)	0.923	0.38	0.247	0.8 (0.6-1.1)	0.139	0.384
11	rs6942495	C	0.45	0.911	1.0 (0.7-1.3)	0.756	0.48	0.752	0.9 (0.7-1.3)	0.880	0.886
12	rs17501080	C	0.13	0.431	1.2 (0.7-1.9)	0.618	0.12	0.575	1.2 (0.7-2.0)	0.862	0.816

OR= Odds Ratio; 95%CI= 95% confidence interval; *p-value adjusted for sex and age; MAF= minor allele frequency.

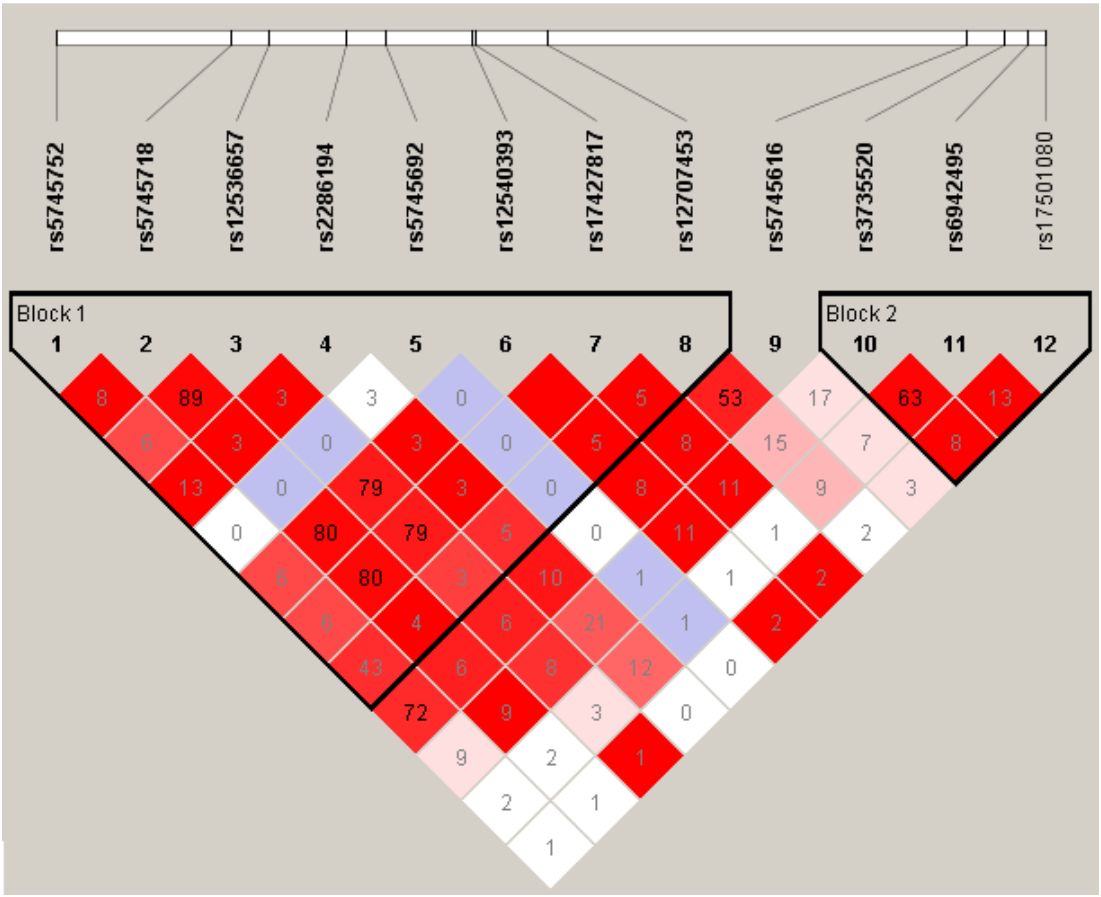

Figure 6.2. LD plot of tag SNPs in *HGF* haplotype. Linkage disequilibrium plot generated in Haploview shows the haplotype block structure using the solid spine definition in the Nepalese cohort. The number in the box represents the r^2 value.

Table 6.4. Common haplotypes in *HGF* (>1% frequency) observed, and their association with PACG. Bold values are considered significant at the p<0.05 level. The order of SNPs in haplotypes follows the order in Table 6.3.

Block	Haplotype	Australian				Nepalese			
	1 2 3 4 5 6 7 8 9	Case	Control	OR (95%CI)	P-value	Case	Control	OR (95%CI)	P-value
1	A C G T G T G G A	0.14	0.13	1.1 (0.7-2.0)	0.555	0.22	0.24	0.9 (0.6-1.5)	0.877
	G A A T G C C A G	0.21	0.23	2.0 (1.2-3.2)	0.632	0.18	0.09	2.0 (1.3-3.3)	**0.001**
	G C G A G T G A G	0.19	0.17	1.1 (0.7-1.9)	0.575	0.18	0.19	0.9 (0.6-1.4)	0.594
	G C G T G T G A G	0.34	0.32	1.1 (0.7-1.7)	0.629	0.27	0.36	0.7 (0.5-1.0)	0.084
	A C G T G T G A G	-	-	-	-	0.01	0.03	0.3 (0.1-1.2)	0.074
	A C G T G T G A A	0.03	0.07	0.4 (0.1-1.1)	**0.026**	0.12	0.09	1.3 (0.7-2.1)	0.288
	A C G T G T G G G	0.02	0.02	0.9 (0.2-3.1)	0.790	-	-	-	-
	A C G T G C C A G	0.02	0.03	0.8 (0.3-2.5)	0.618	-	-	-	-
	A C G T C T G A A	0.05	0.03	1.7 (0.8-3.9)	0.167	-	-	-	-
2	C G C	0.13	0.15	1.1 (0.7-1.9)	0.500	0.11	0.12	1.1 (0.6-1.9)	0.513
	C G A	0.42	0.39	1.2 (0.7-2.0)	0.482	0.35	0.38	0.9 (0.6-1.2)	0.424
	T C A	0.41	0.41	1.1 (0.7-1.9)	0.984	0.37	0.42	0.8 (0.6-1.2)	0.249
	C C A	0.05	0.05	1.0 (0.4-2.3)	0.696	0.15	0.08	1.8 (1.1-2.9)	**0.017**
		global p-value 0.450				global p-value 0.180			

OR= odds ratio, 95% CI= 95% confidence interval.

Matrix Metalloproteinase-9

In *MMP-9*, most tag SNPs were located in the introns, except for rs17576 and rs2274756 with the physical location presented in **Figure 6.3**. Bonferroni correction for the 5 SNPs was 0.05/5= 0.01.

In the Australian cohort two *MMP-9* SNPs, rs3918249 (C allele) and rs17576 (G allele), were significantly associated under an allelic model with p-values of 0.006 (OR1.6, 95%CI 1.1-2.2) for both SNPs. SNPs rs2274756, A allele, (p-value 0.017, OR 1.7, 95%CI 1.1-2.6) showed nominal significance that did not survive correction for multiple testing (**Table 6.5**). Multivariate analyses were conducted to control for age and gender. The first two SNPs remained significant with p=0.010 for both. No associations were found in the Nepalese cohort. The combined analysis showed only one SNP rs2274756 to pass the Bonferroni correction (p-value of 0.008).

Analysis of the linkage disequilibrium structure between the five tag SNPs showed one haplotype block (**Figure 6.4**). A positive haplotypic association, with a global p-value of 0.014 was found in the Australian cohort. The tag SNPs formed three haplotypes in this population. The commonest haplotype, TGACG, had a significantly higher frequency in controls (69%) than in PACG cases (59%), p=0.006 (OR 0.6, 95%CI 0.5-0.9). This remained significant after Bonferroni correction for the three haplotypes observed (p=0.018). The CGGCG haplotype was more frequent in PACG cases 17% than in controls 11% (p-value 0.035, OR 1.6, 95%CI 1.0-2.5), but did not remain significant following multiple testing correction (corrected p=0.105) (**Table 6.6**).

Table 6.5. Allelic association results for *MMP-9* gene in both Australian and Nepalese cohorts. p-values of less than 0.05 are highlighted in bold. Table shows the unadjusted p-value, adjusted p-value for sex and age, and combined p-value using Cochran-Mantel-Haenszel 2x2xK test

N#	SNP	Minor Allele	Australian				Nepalese				Combined p-value
			MAF	p-value	OR	p*	MAF	p-value	OR	p*	
1	rs3918249	C	0.41	**0.006**	1.6 (1.1-2.2)	**0.010**	0.37	0.55	0.9 (0.6-1.3)	0.573	**0.018**
2	rs17576	G	0.41	**0.006**	1.6 (1.1-2.2)	**0.010**	0.37	0.59	0.9 (0.6-1.3)	0.615	**0.021**
3	rs3918254	T	0.00	0.476	2.7 (0.1-43)	0.082	0.14	0.63	0.9 (0.5-1.4)	0.737	0.717
4	rs3787268	A	0.23	0.235	1.3 (0.8-1.8)	0.064	0.23	0.83	0.9 (0.6-1.4)	0.790	0.494
5	rs2274756	A	0.17	**0.017**	1.7 (1.1-2.6)	0.245	0.26	0.14	1.3 (0.9-1.9)	0.152	**0.008**

OR= Odds Ratio; 95%CI= 95% confidence interval; p*= p-value adjusted for sex and age; MAF= minor allele frequency.

Table 6.6. Haplotype frequencies of *MMP-9* gene in patients with PACG and unaffected controls. P<0.05 level is considered statistically significant. The order of SNPs in haplotype follows the order in Table 6.5.

Haplotype 1 2 3 4 5	**Australian**				**Nepalese**			
	Cases	**Controls**	**OR (95% CI)**	**p-value**	**Cases**	**Controls**	**OR (95% CI)**	**p-value**
C G G C G	0.17	0.11	1.6 (1.0-2.5)	**0.035**	0.26	0.21	1.3 (0.9-1.9)	0.154
T G A C G	0.59	0.69	0.6 (0.5-0.9)	**0.006**	0.37	0.39	0.7 (0.5-1.2)	0.636
C G G C A	0.23	0.19	1.3 (0.8-1.8)	0.217	0.23	0.24	0.7 (0.4-1.2)	0.744
C G G T G	-	-	-	-	0.14	0.16	0.7 (0.4-1.3)	0.654
	global p-value **0.014**				global p-value 0.686			

OR= odds ratio, 95% CI= 95% confidence interval

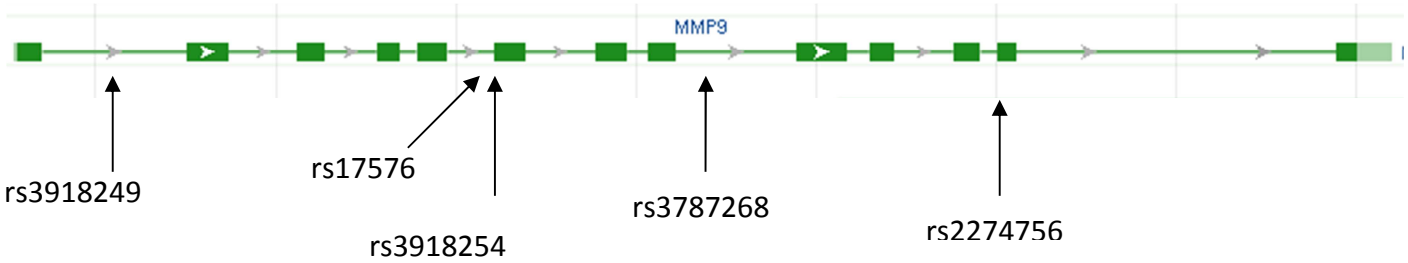

Figure 6.3. *MMP-9* gene ideogram depicting the location of all tag SNPs genotyped. Exons are indicated by solid boxes and joined by introns indicated by lines. Figure adapted from NCBI website (http://www.ncbi.nlm.nih.gov/gene)

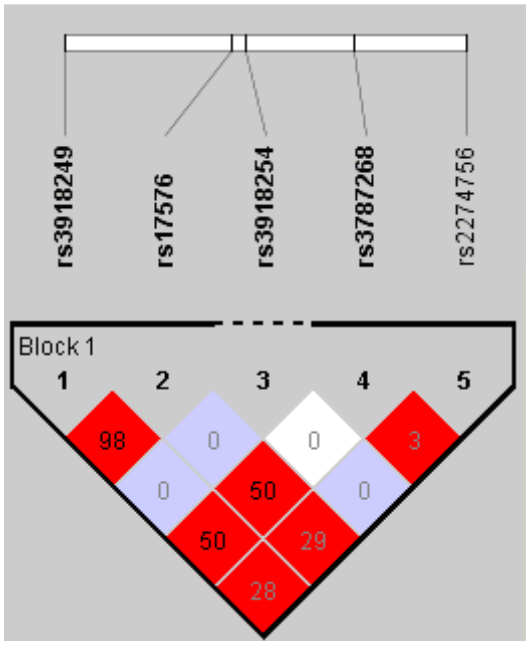

Figure 6.4. LD plot of tag SNPs in *MMP-9* haplotype. Linkage disequilibrium plot generated in Haploview shows the haplotype block structure using the solid spine definition in the Australian cohort. The number in the box represents the r^2 value.

Methyl tetrahydrofolate reductase

In *MTHFR*, most SNPs were located in introns except rs2274976, rs1801133, and rs2066470 which were located in exons. The physical location is presented in **Figure 6.5.**

No association was detected in *MTHFR* with PACG in either allelic (**Table 6.7**) or haplotypic (**Table 6.8**) results in either Australian or Nepalese cohorts.

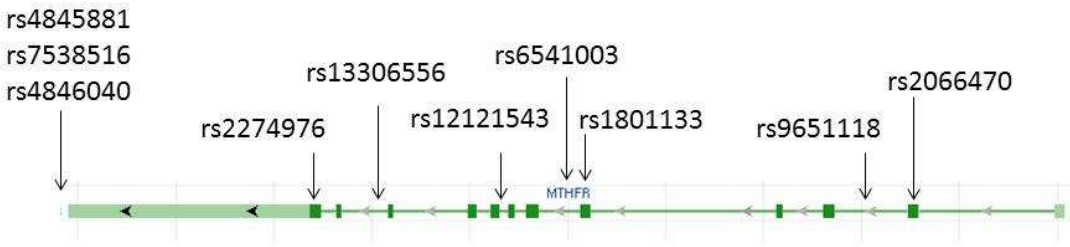

Figure 6.5. *MTHFR* gene ideogram depicting the location of all tag SNPs genotyped. Exons are indicated by solid boxes and joined by introns indicated by lines. Figure adapted from NCBI website (http://www.ncbi.nlm.nih.gov/gene)

Table 6.7. Allelic association results for *MTHFR* gene in both Australian and Nepalese cohorts. p-values of less than 0.05 are highlighted in bold. Table shows the unadjusted p-value, adjusted p-value for sex and age, and combined p-value using Cochran-Mantel-Haenszel 2x2xK test

N#	SNP	Minor Allele	Australian				Nepalese				Combined p-value
			MAF	p-value	OR	p*	MAF	p-value	OR	p*	
1	rs4845881	G	0.32	0.224	1.2 (0.8-1.7)	0.135	0.36	0.593	1.1 (0.8-1.6)	0.658	0.608
2	rs7538516	C	0.33	0.356	1.2 (0.8-1.6)	0.216	0.34	0.192	1.3 (0.9-1.8)	0.254	0.894
3	rs4846040	C	0.28	0.318	1.2 (0.8-1.7)	0.333	0.28	0.110	1.4 (0.9-2.0)	0.121	0.763
4	rs2274976	A	0.05	0.313	1.4 (0.7-2.9)	0.209	0.09	0.580	0.8 (0.5-1.5)	0.554	0.277
5	rs13306556	A	0.12	0.952	1.0 (0.6-1.6)	0.413	0.11	0.416	0.8 (0.5-1.4)	0.386	0.596
6	rs12121543	A	0.27	0.986	1.0 (0.7-1.4)	0.776	0.29	0.087	1.4 (1.0-2.0)	0.118	0.252
7	rs6541003	G	0.42	0.619	1.1 (0.7-1.5)	0.291	0.37	0.296	1.2 (0.8-1.7)	0.353	0.743
8	rs1801133	T	0.30	0.753	1.0 (0.7-1.4)	0.998	0.22	0.151	0.7 (0.5-1.1)	0.160	0.235
8	rs9651118	C	0.24	0.596	1.1 (0.7-1.6)	0.371	0.35	0.982	1.0 (0.7-1.4)	0.886	0.710
10	rs2066470	T	0.12	0.983	1.0 (0.6-1.6)	0.474	0.09	0.672	1.1 (0.6-2.1)	0.848	0.780

OR= Odds Ratio; 95%CI= 95% confidence interval; p*= p-value adjusted for sex and age; MAF= minor allele frequency.

Table 6.8. Haplotype frequencies of *MTHFR* in PACG patients and controls. The order of SNPs in haplotype follows the same order in Table 6.7

Haplotype 1 2 3 4 5 6 7 8 9 10	Australian				Nepalese			
	Cases	Controls	OR(95% CI)	p-value	Cases	Controls	OR(95% CI)	p-value
A T G G G C A T T C	0.31	0.32	0.8 (0.5-1.4)	0.582	0.22	0.28	0.7 (0.5-1.1)	0.175
A T G G G C A C C C	0.24	0.21	1.1 (0.6-1.8)	0.419	0.34	0.33	1.3 (0.8-2.0)	0.727
A T G G G C A C T C	0.03	0.03	1.1 (0.4-3.0)	0.614	0.06	0.05	1.4 (0.6-3.2)	0.790
G T G A A A G C T T	0.03	0.04	0.7 (0.2-2.0)	0.612	0.03	0.02	2.3 (0.7-7.6)	0.333
G C C G G A G C T C	0.14	0.16	0.8 (0.5-1.5)	0.529	0.20	0.15	1.8 (1.1-3.1)	0.068
G C C G G C G C T C	0.13	0.15	0.8 (0.5-1.3)	0.414	0.07	0.09	1.1 (0.5-2.2)	0.645
G C G A A A G C T T	0.02	0.03	0.7 (0.2-2.4)	0.546	0.03	0.04	1.2 (0.5-2.8)	0.941
A T G G A A G C T T	0.05	0.03	1.7 (0.7-4.1)	0.194	-	-	-	-
	global p-value 0.830				global p-value 0.333			

95% CI= 95% confidence interval. OR= odds ratio.

Membrane Frizzled-type Protein

In *MFRP*, most tag SNPs were located in introns, except for rs35885438, rs2510143 and rs36015759 which were located in exons, and rs883245 which was located in the 5' untranslated region. The physical location presented in **Figure 6.6**.

Three SNPs from the *MFRP* gene were nominally associated with PACG: rs948414 T allele, (p=0.025, OR 1.5, 95%CI 1.0-2.0) and rs36015759 A allele, (p=0.021, OR 1.6, 95%CI 1.0-2.5) in the Australian Caucasian population. In the Nepalese cohort, SNP rs10790289 C allele was associated (p=0.037, OR 1.4, 95%CI 1.0-2.0); however, none of them showed association when the results were adjusted for sex and age (p-values of 0.185, 0.075 and 0.063, respectively). In the combined analysis, SNPs that were associated in the Australian cohort rs948414 and rs36015759 showed association in the combined analysis with p-values of 0.047 and 0.029, respectively. Interestingly, two other SNPs rs948413 and rs2510143 showed significance with p-value of 0.029, and 0.034, respectively; however, these two latter SNPs were not associated in either cohort individually (**Table 6.9**). None of the SNPs survived Bonferroni correction (0.05/11= 0.004). No significant associations were found in the haplotype results in either cohort (**Table 6.10**).

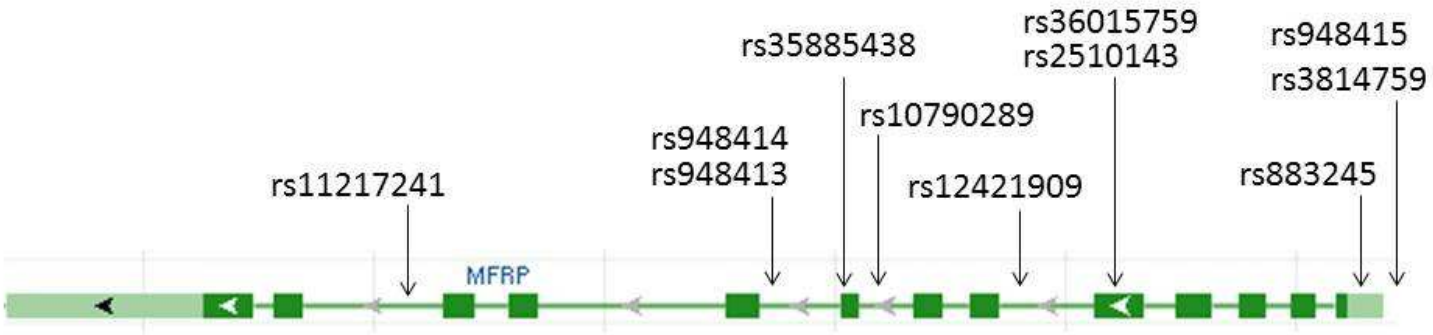

Figure 6.6. *MFRP* gene ideogram depicting the location of all tag SNPs genotyped. Exons are indicated by solid boxes and joined by introns indicated by lines. Figure adapted from NCBI website (http://www.ncbi.nlm.nih.gov/gene)

Table 6.9. Allelic association results for *MFRP* gene in both Australian and Nepalese cohorts. p-values of less than 0.05 are highlighted in bold. Table shows the unadjusted p-value, adjusted p-value for sex and age, and combined p-value using Cochran-Mantel-Haenszel 2x2xK test.

N#	SNP	Minor Allele	Australian				Nepalese				Combined p-value
			MAF	p-value	OR	p*	MAF	p-value	OR	p*	
1	rs11217241	T	0.06	0.880	1.0 (0.5-2.1)	0.315	0.41	0.312	0.8 (0.6-1.2)	0.354	0.332
2	rs948413	A	0.37	0.078	1.3 (0.9-1.8)	0.242	0.42	0.184	0.8 (0.5-1.1)	0.235	**0.029**
3	rs948414	T	0.32	**0.025**	1.5 (1.0-2.0)	0.185	0.37	0.593	0.9 (0.6-1.3)	0.567	**0.047**
4	rs35885438	T	0.04	0.917	1.0 (0.4-2.2)	0.747	0.15	0.516	1.2 (0.7-1.9)	0.449	0.543
5	rs10790289	C	0.45	0.555	1.1 (0.8-1.5)	0.759	0.53	**0.037**	1.4 (1.0-2.0)	0.063	0.063
6	rs12421909	T	0.08	0.214	1.5 (0.8-2.6)	0.053	0.30	0.960	1.0 (0.7-1.4)	0.987	0.567
7	rs2510143	A	0.05	0.243	1.6 (0.7-3.3)	0.054	0.14	0.078	1.6 (0.9-2.7)	0.080	**0.034**
8	rs36015759	A	0.15	**0.021**	1.6 (1.0-2.5)	0.075	0.21	0.439	0.9 (0.6-1.3)	0.403	**0.029**
9	rs883245	C	0.43	0.105	1.3 (0.9-1.7)	0.463	0.37	0.234	1.2 (0.9-1.8)	0.285	0.691
10	rs948415	G	0.38	0.291	1.2 (0.8-1.6)	0.435	0.36	0.314	1.2 (0.8-1.7)	0.376	0.922
11	rs3814759	G	0.38	0.331	1.2 (0.8-1.6)	0.457	0.36	0.314	1.2 (0.8-1.7)	0.372	0.973

OR= Odds Ratio; 95%CI= 95% confidence interval; p*= p-value adjusted for sex and age; MAF= minor allele frequency.

Table 6.10. Haplotypic association of *MFRP* tag SNPs in PACG patients and controls. The order of SNPs follows the order in Table 6.9.

Haplotype 1 2 3 4 5 6 7 8 9 10 11	Australian				Nepalese			
	Cases	Controls	OR (95% CI)	P-value	Cases	Controls	OR (95% CI)	P-value
T G C C C C G G T A A	-	-	-	-	0.05	0.04	1.4 (0.4-4.9)	0.541
C G C C T C G G T A A	0.29	0.22	1.4 (0.8-2.3)	0.085	0.10	0.07	1.3 (0.6-3.0)	0.243
T A T C C T G G T A A	-	-	-	-	0.04	0.06	0.5 (0.1-1.5)	0.296
C A T C C C G G T A A	0.12	0.15	0.7 (0.3-1.3)	0.215	0.07	0.10	0.5 (0.2-1.3)	0.139
C G C C C C G G T A A	0.10	0.06	1.6 (0.7-3.6)	0.093	0.06	0.07	0.7 (0.2-1.9)	0.674
T G C C T T G G T A A	-	-	-	-	0.03	0.04	0.8 (0.2-3.3)	0.680
C G C C T T G G T A A	-	-	-	-	0.02	0.05	0.2 (0.1-1.2)	0.074
T G C C T C G G T A A	-	-	-	-	0.02	0.03	0.8 (0.3-2.0)	0.889
T G C T C T G G T A A	-	-	-	-	0.04	0.02	1.5 (0.4-5.6)	0.453

Figure 6.10. Continue

Haplotype	Australian				Nepalese			
1 2 3 4 5 6 7 8 9 10 11	**Cases**	**Controls**	**OR (95% CI)**	**P-value**	**Cases**	**Controls**	**OR (95% CI)**	**P-value**
C A T C C C G G C G G	0.07	0.08	0.9 (0.4-1.9)	0.852	0.03	0.05	0.3 (0.1-1.4)	0.176
T G C T C C G G T A A	-	-	-	-	0.01	0.02	0.2 (0.1-1.6)	0.128
C A T C C C G A C G G	-	-	-	-	0.04	0.03	1.1 (0.3-3.6)	0.504
C G C C T C G A C G G	0.07	0.10	0.6 (0.2-1.3)	0.160	0.04	0.03	1.1 (0.3-3.5)	0.483
C G C C T C G G C A A	0.03	0.05	0.6 (0.2-2.0)	0.323	-	-	-	-
C G C C T C G G C G G	0.04	0.02	2.3 (0.7-7.3)	0.086	-	-	-	-
C A T C T C G G T A A	0.02	0.03	0.3 (0.1-1.9)	0.229	-	-	-	-
C A T C T C G A C G G	0.03	0.03	0.9 (0.2-3.6)	0.630	-	-	-	-
	global p-value 0.069				global p-value 0.326			

OR= Odds Ratio; 95%CI= 95% confidence interval.

Calcitonin-like receptor inhibitor

In *CALCRL*, all nine tag SNPs were located in the introns, with the physical location presented in **Figure 6.7**. In the single SNP association analysis, no significant allelic associations were detected in either cohort (**Table 6.11**). However, in the Australian cohort the global haplotype p-value for association at the *CALCRL* gene was suggestive (**Figure 6.8**), but not significant (p=0.063). One of the six haplotypes in the *CALCRL* gene (AATACAGAT) was significantly associated with PACG in the Australian cohort, with a p-value of 0.004 (OR 0.1, 95% CI 0.02-0.7). The association remained significant following Bonferroni correction for the six observed haplotypes (corrected p=0.024) (**Table 6.12**). This rare haplotype was more frequent in controls than cases (4% vs 1%, respectively).

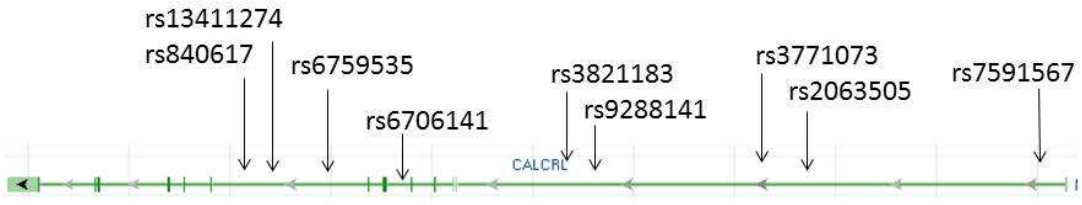

Figure 6.7. *CALCRL* gene ideogram depicting the location of all tag SNPs genotyped. Exons are indicated by solid boxes and joined by introns indicated by lines. Figure adapted from NCBI website (http://www.ncbi.nlm.nih.gov/gene)

Table 6.11. Allelic association results for *CALCRL* gene in both Australian and Nepalese cohorts. p-values of less than 0.05 are highlighted in bold. Table shows the unadjusted p-value, adjusted p-value for sex and age, and combined p-value using Cochran-Mantel-Haenszel 2x2xK test

N#	SNP	Minor Allele	Australian				Nepalese				Combined p-value
			MAF	p-value	OR	p*	MAF	p-value	OR	p*	
1	rs840617	A	0.13	0.122	1.42 (0.9-2.2)	0.795	0.27	0.263	1.2 (0.8-1.8)	0.326	0.831
2	rs13411274	C	0.35	0.368	1.16 (0.8-1.6)	0.916	0.17	0.090	0.7 (0.4-1.1)	0.072	0.706
3	rs6759535	T	0.43	0.581	1.09 (0.7-1.5)	0.447	0.32	0.703	0.9 (0.7-1.3)	0.635	0.506
4	rs6706141	G	0.36	0.451	1.13 (0.8-1.5)	0.843	0.30	0.834	1.0 (0.7-1.5)	0.707	0.485
5	rs3821183	T	0.16	0.683	1.09 (0.7-1.6)	0.485	0.26	0.680	0.9 (0.6-1.3)	0.693	0.563
6	rs9288141	G	0.06	0.699	1.14 (0.5-2.2)	0.467	0.12	0.387	1.3 (0.7-2.2)	0.485	0.358
7	rs3771073	C	0.43	0.731	1.05 (0.7-1.4)	0.819	0.24	0.342	0.8 (0.6-1.2)	0.332	0.724
8	rs2063505	G	0.37	0.665	1.07 (0.7-1.4)	0.792	0.29	0.931	1.0 (0.7-1.5)	0.855	0.703
9	rs7591567	C	0.33	0.530	1.11 (0.7-1.5)	0.884	0.15	0.226	0.8 (0.5-1.2)	0.202	0.809

OR= Odds Ratio; 95%CI= 95% confidence interval; p*= p-value adjusted for sex and age; MAF= minor allele frequency.

Table 6.12. Haplotype association between variants across *CALCRL* gene and primary angle-closure glaucoma in Australian and Nepalese cohorts. The significantly associated haplotype is highlighted in bold. The order of SNPs in haplotype follow the order Table 6.11.

Haplotype	**Australian**				**Nepalese**			
1 2 3 4 5 6 7 8 9	**Case**	**Control**	**OR (95% CI)**	**p-value**	**Case**	**Control**	**OR (95% CI)**	**p-value**
T A C G C A G G T	0.38	0.33	1.1 (0.7-1.5)	0.665	0.31	0.27	1.3 (0.7-2.1)	0.534
T A C A T A G A T	0.16	0.16	0.8 (0.5-1.2)	0.634	0.27	0.25	1.2 (0.6-2.0)	0.926
T C T A C A C A C	0.35	0.31	0.9 (0.6-1.4)	0.656	0.15	0.17	0.9 (0.4-1.6)	0.168
A A C A C G G A T	0.03	0.02	1.1 (0.3-3.1)	0.665	0.08	0.09	1.6 (0.8-3.1)	0.163
A A T A C A C A T	0.07	0.08	0.7 (0.3-1.3)	0.381	0.08	0.07	1.4 (0.6-3.1)	0.629
A A T A C A G A T	0.01	0.04	0.1 (0.02-0.7)	**0.004**	0.08	0.07	1.1 (0.5-2.1)	0.762
	global p-value 0.063				global p-value 0.465			

OR= odds ratio, 95% CI= 95% confidence interval.

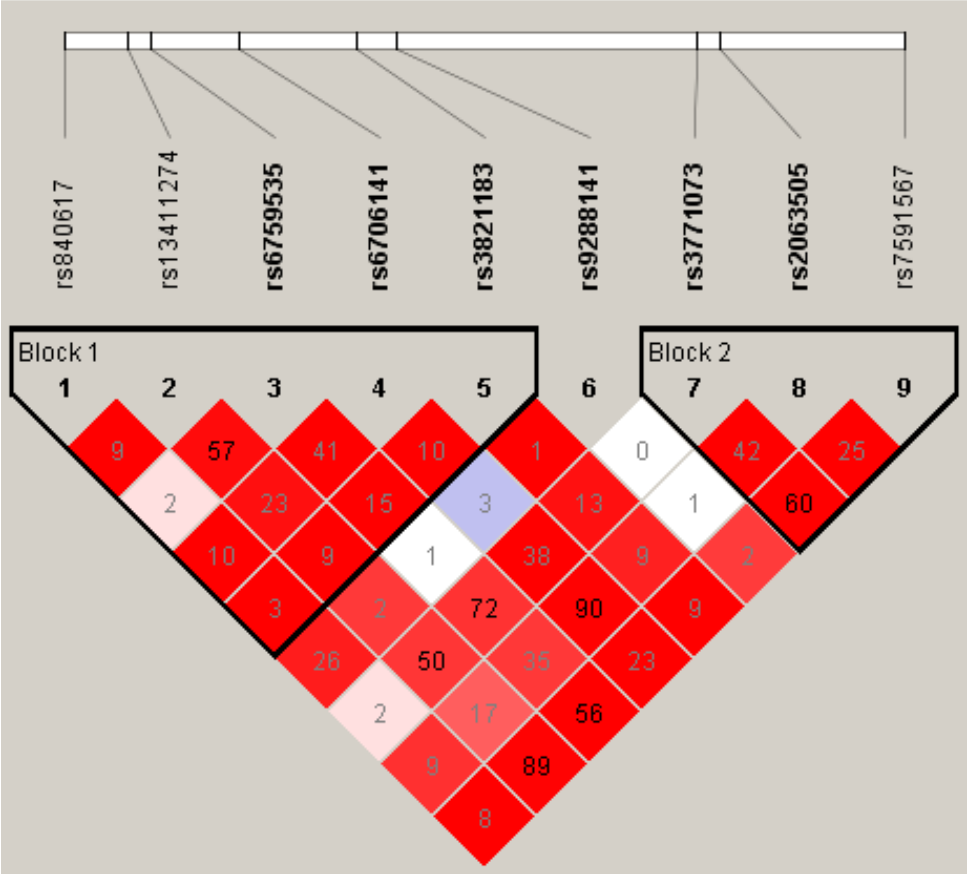

Figure 6.8. LD plot of tag SNPs in *CALCRL* haplotype. Linkage disequilibrium plot generated in Haploview shows the haplotype block structure using the solid spine definition in the Australian cohort. The number in the box represents the r^2 value.

Discussion

In this chapter we investigated the association of five different candidate genes with the disease. The genes were chosen according to their putative role in ocular development and function; *HGF, MMP-9*, *MTHFR*, and *MFRP* affect the growth of the axial length, and *CALCRL* is believed to regulate the drainage of aqueous humor. All genes were examined for association with PACG in previous studies, except for the *HGF* gene which we proposed as a candidate gene. The differences noted in associations of the genetic risk among both cohorts may reflect ethnic differences in the disease pathogenesis.

In the Nepalese cohort, our study showed four intronic SNPs in the *HGF* gene to be significantly associated with PACG (rs5745718, rs12536657, rs12540393 and rs17427817). The former two SNPs were recently reported to be associated with hyperopia in an Australian Caucasian population. (Veerappan, Pertile et al. 2010) Interestingly, the risk alleles for hyperopia, rs5745718 (A) and rs12536657 (A), in their study were the same as in our PACG study. This finding indicates a possible common pathway, or similarities between hyperopia and PACG, which are known to share the same biometric feature of short axial length. (Young, Metlapally et al. 2007; Veerappan, Pertile et al. 2010) Interestingly, all four SNPs in our PACG study were significantly associated with PACG independent of spherical equivalent refraction, and there was no significant difference in the refraction between cases and controls in the Nepalese cohort. So the associations here appear to occur through a mechanism beyond an indirect association with hyperopia in this population. Furthermore, the significantly associated haplotype contains the risk alleles of the

four significant associated SNPs with frequency of 18% in patients and 9% in healthy controls. These alleles do not occur on any other common haplotype in this population.

A meta-analysis study in two Chinese cohorts has reported a minor allele of rs3735520 (A) to increase vitreous chamber depth, thus increasing the axial length, so the investigators suggested that *HGF* is probably involved in development of the posterior eye segment, and consequently in spherical error and axial hyperopia. (Chen, Chen et al. 2012) The role of *HGF* in PACG remains unknown. Further work is needed to determine its involvement in the pathogenesis of this blinding disease. The similar findings in hyperopia indicate that it may be involved in influencing the structure of the eye and thus predisposing those with short axial length to the risk of angle-closure. It is unlikely that the tag SNPs assayed here are the functional variants. All four tag SNPs are located in introns of the *HGF* gene and are likely to be in linkage disequilibrium with actual functional variants. The causative variant will likely be found on the background of the GAATGCCAG haplotype.

In *MMP-9*, a significant association of two SNPs, rs17576 and rs3918249, with PACG was identified in the Australian Caucasian population, and this remained statistically significant independent of age and sex. These two SNPs were in strong linkage disequilibrium (r^2=0.98). The minor allele of each SNP (G and C, respectively) was associated with PACG under the allelic model. These risk alleles were split across two haplotypes, only one of which is associated with PACG. Most importantly, the most significantly associated haplotype contains the common allele

at both SNPs and appears to be protective with a haplotype frequency of 69% in controls and only 59% in cases, p=0.006. However rs2274756 was more significantly associated in the combined analysis than in the Australian cohort alone, which may suggest the possibility of a link between this SNP and PACG in the Nepalese population.

Previous study has found an association between rs17576 and acute PACG in Taiwanese populations. (Wang, Chiang et al. 2006) However, other studies on Singaporean and Southern Chinese patients failed to replicate this finding (Aung, Yong et al. 2008; Cong, Guo et al. 2009). Cong and colleagues also identified an association of *MMP-9* SNP rs2550889 with PACG in a Southern Chinese population. (Cong, Guo et al. 2009) This SNP was not included in our study, as it was unable to be genotyped in a multiplex with the other SNPs. However, it is in strong linkage disequilibrium with our two associated tag SNPs (rs17576 and rs3918249, r^2= 0.85 and 0.86 respectively in the HapMap, CEU sample), suggesting a similar finding in the current study. Further replications are required to directly examine the association of rs2550889 with PACG in Australian individuals. Interestingly, all three previous studies in Asian populations showed that the A/A genotype of SNP rs17576 was more common in PACG cases than in normal controls. Thus, the minor A allele conferred risk for PACG. In the current Caucasian study, we found that the A allele conferred protection against PACG and is the more common allele in this population. There is a well-documented difference in allele frequency across populations at this SNP. The frequencies in Asian populations range from 0.22 to 0.30 (Shibata, Ohnuma et al. 2005; Wang, Chiang et al. 2006; Aung, Yong et al.

2008; Hirose, Chiba et al. 2008; Cong, Guo et al. 2009) while the frequency in Caucasians is approximately 0.65. (Rodriguez-Pla, Beaty et al. 2008; Brooks, Kizer et al. 2010; Mossbock, Weger et al. 2010; Pinto, Depner et al. 2010) Similar differences in frequencies are also observed in HapMap.

The opposite association of an allele or genotype of the same SNP with disease could be due to different functional effects among different ethnic groups, or the heterogeneous effect of the same variant such as genetic background or environmental factors. (Lin, Vance et al. 2007) This "flip-flop" association may indicate that rs17576 is not the causative allele despite being a non-synonymous change (p.Gln279Arg), but that the risk variants occur on different genetic backgrounds in different ethnicities. Additionally, the fact that this variant is predicted to be benign or tolerated by both PolyPhen, SIFT and Mutation Taster supports this hypothesis. Examples of such "flip-flop" associations have been previously reported and are well established in ophthalmology for the coding *LOXL1* variant rs1048661 (R141L) SNP associated with pseudo-exfoliation syndrome in opposite directions in Japanese population compared with Caucasians. (Hayashi, Gotoh et al. 2008) Alternatively, the findings could represent type 1 errors that will not replicate in further studies.

In *MTHFR* gene, the c.677C>T polymorphism (rs1801133) affects the homocysteine concentration, and an increase in plasma levels of homocysteine has been detected in Caucasian patients with PACG. (Bleich, Junemann et al. 2002) Elevated homocysteine levels lead to scleral restructuring, and structural remodelling of

connective tissue of the anterior segment (Mujumdar, Tummalapalli et al. 2002) and trabecular meshwork. (Michael, Qamar et al. 2008) Ethnic differences seem to play a role in the reported associations of this polymorphism with various types of glaucoma. A relationship has been reported between *MTHFR* c.677C>T polymorphism and open-angle glaucoma in Caucasians (Junemann, von Ahsen et al. 2005) and normal tension glaucoma in Koreans. (Woo, Kim et al. 2009) However, this variant was not associated with normal tension glaucoma or POAG either in Japanese, (Mabuchi, Tang et al. 2006) or in Central European populations. (Mossbock, Weger et al. 2006)

Recently Michael et al. found a significant association between the TT and AC genotypes of *MTHFR* c.677C>T (rs1801133) and c.1298A>C (rs1801131) polymorphisms with PACG in a Pakistani cohort. (Michael, Qamar et al. 2008; Micheal, Qamar et al. 2009) Our data did not support an association of variants including rs1801133 in the *MTHFR* gene with PACG in either the Australian or Nepalese cohorts. This gene has been studied in a variety of glaucoma phenotypes and ethnic groups with limited overlap of each between studies. The variable results may reflect the study and phenotype differences or could suggest that the gene has a very limited role to play in PACG.

Mutations in the *Membrane frizzled-related protein* (*MFRP*) gene cause autosomal recessive nanophthalmos. Homozygous *MFRP* mutation carriers have a shorter axial length than normal eyes, with an increase in both choroidal and scleral thickness, which in turn leads to axial hyperopia. (Martorina 1988) As both nanophthalmos and

PACG have similar anatomical abnormalities, *MFRP* is a possible candidate gene for PACG. However, studies done on Chinese and Taiwanese patients did not show any coding mutations in this gene. (Aung, Lim et al. 2008; Wang, Lin et al. 2008)
In this study no significant SNPs survived correction for multiple testing in either cohort. It is the first time this gene has been studied for association with PACG in Caucasians, and further investigation in a larger cohort is warranted.

In our study rs1157699 in the *CALCRL* gene failed to be genotyped in a multiplex with the other SNPs. However SNPs rs2063505 and rs6706141, which are in strong linkage disequilibrium with rs1157699 (r^2=1 and 0.96, respectively), did not demonstrate any association in either cohort. Interestingly, the AATACAGAT haplotype did show an association in the Australian cohort (corrected p-value =0.024), which suggests genetic variation at the *CALCRL* gene may play a role in PACG. The examination of haplotypes in candidate gene studies can be superior to investigating individual SNPs when the haplotype tags variation not tagged by the individual SNPs. (Clark 2004) This haplotype appears to be protective in the Australian cohort. It is a relatively rare haplotype and the implication of its association is not yet clear. Alternatively, the associated haplotype is more common in Nepal and the lack of association here may suggest that the Australian cohort result is a false positive finding. Further work is required to assess the potential involvement of this gene with PACG and replication of these results an independent Caucasian cohort is required to confirm the findings of this study.

In conclusion, this is the first report to identify an association between *HGF* and PACG, and to suggest an association between *MMP-9* polymorphisms and PACG in the Australian population. Additionally the underlying genetic aetiology of PACG in people of Nepalese descent has not been previously studied, and limited reports have been made for Caucasian cohorts.

Previous positive associations previously reported at *MTHFR* gene failed to replicate in our study in both Caucasian and Nepalese populations. Polymorphic variation at a nanophthalmos gene (*MFRP)* showed a trend towards association but requires a larger cohort to definitively detect an effect in this complex disease. In addition, haplotypic association at the *CALCRL* gene with PACG in the Australian cohort may implicate this gene further in the pathogenesis of PACG.

Chapter 7

ANALYSES OF THE COMMON VARIATION IN *PRSS56, ENOS, CYP1B1* AND *NTF4* WITH PACG

Introduction

The data presented in this chapter was generated in 2011, by which time additional cases had been recruited for inclusion in the Australian Caucasian cohort but the Nepalese cohort remained the same. The cohorts were used to analyse the association of additional genes which have been more recently suggested as candidates for PACG; *Cytochrome P450* (*CYP1B1*), *Endothelial nitric oxide synthase* (*eNOS*), *Protease serine 56* (*PRSS56*), and *Neurotrophin-4* (*NTF4*). *CYP1B1*, *eNOS*, and *NTF4* genes have been reported to be associated with PACG in humans, and mutation in the *PRSS56* gene was found to cause a phenotype in a mouse model that resembles angle-closure glaucoma in humans. (Nair, Hmani-Aifa et al. 2011)

Mutations in *PRSS56* [OMIM 613858] gene has been recently identified as a cause for an autosomal recessive form of nanophthalmos, (Gal, Rau et al. 2011; Orr, Dube et al. 2011) and we found novel segregating variant in our study as described in **Chapter 3**. Nanophthalmos and PACG share certain clinical features such as narrow anterior chamber angle, short axial length, and hyperopic refractive error. Nair and colleagues have found that mice carrying the *PRSS56* mutation (T to A transversion in exon 11 and disrupts a splice donor site) showed a phenotype that resembles PACG in human. The mutant mice have a narrow anterior chamber angle with a significant decrease of the outflow facility and increase in the IOP compared to the

wild type. Thinning of the nerve fibre layer and destruction of the optic nerve was also observed in the mutant mice. They also showed significant lower axial length with increasing age than wild-type controls, however the lens size was unaffected. (Nair, Hmani-Aifa et al. 2011) This study is the first to look for association of common sequence variations of *PRSS56* with PACG in humans

CYP1B1 [OMIM 601771] is the most common gene known to be involved with the pathogenesis of primary congenital glaucoma. (Stoilov, Akarsu et al. 1997; Sarfarazi, Stoilov et al. 2003) Sarfarazi has hypothesized that *CYP1B1* is involved in the development of the irido-corneal angle of the eye, making it a gene of interest for PACG. (Sarfarazi and Stoilov 2000) Chakrabarti and colleagues have sequenced the coding region of the gene, and found association with PACG in an Indian cohort consisting of 90 cases and 200 controls. (Chakrabarti, Devi et al. 2007) Another study did not report any known or novel polymorphisms or variants in a smaller Middle Eastern cohort of 29 cases with PACG using sequencing methodology. (Abu-Amero, Morales et al. 2007)

Nitric oxide (NO) is synthesized in the vascular endothelium via endothelial nitric oxide synthase 3 (also known as *eNOS*) using the substrate L-arginine. (Karantzoulis-Fegaras, Antoniou et al. 1999) *eNOS* [OMIM 163729] over expression is thought to be neuroprotective by causing vasodilation and increased blood flow in human eye tissues. (Neufeld, Hernandez et al. 1997) Overexpression of *eNOS* was also reported to lower IOP in mouse eyes by increase in the pressure-dependent drainage. (Stamer, Lei et al. 2011) Other factors such as asymmetric

dimethylarginine (ADMA) and symmetric dimethylarginine (SDMA) also play an inhibitory role in the production of NO. Our laboratory found that serum levels of both ADMA and SDMA are significantly elevated in patients with advanced open angle glaucoma. (Javadiyan, Burdon et al. 2012) Furthermore, NO enhances the activity of *Matrix metalloprotinase-9* (*MMP-9).* (Dumont, Loufrani et al. 2007) *MMP-9* was reported to be associated with PACG in our cohort as discussed in **Chapter 6.** (Wang, Chiang et al. 2006; Awadalla, Burdon et al. 2011) Alteration in *MMP-9* activity during eye development may lead to the development of hyperopic refractive error which is a risk factor for development of PACG. (Wang, Chiang et al. 2006) It has been reported that alteration of *eNOS* expression causes impairment of the blood flow and development of angle-closure, and the 27-bp variable number of tandem repeat (VNTR) polymorphism in intron 4 of *eNOS* is believed to alter the production of nitric oxide and cause vascular dysregulation. (Nath, He et al. 2009) This VNTR has also been assessed and found to be associated with PACG in Pakistani cohort. (Ayub, Khan et al. 2010) Conversely, a study of Han Chinese used tag SNPs to look for association of common variants in the *eNOS* gene in 88 patients with PACG, but no associations were observed. (Liao, Wang et al. 2011) In this chapter, we will look for association of *eNOS* with PACG in both the Australian and Nepalese cohorts.

Neurotrophin plays a vital role in the neuronal cell development, survival and differentiation, and it has been suggested that the neurotrophin signalling system prevents neuronal damage in humans including retinal ganglion cells. (Pasutto, Matsumoto et al. 2009) Heterozygous mutations in *NTF4* [OMIM 162662] have been

reported to be responsible for 1.7% of POAG cases of European descent. (Pasutto, Matsumoto et al. 2009) This was followed by studies that looked for association with PACG in both Indian (Rao, Kaur et al. 2010) and European ancestry from the south-eastern United States (Liu, Liu et al. 2010) by sequencing the coding exons, but results failed to detect an association.

Aim

Although the *CYP1B1*, *eNOS*, and *NTF4* genes are plausible candidates, results are not consistent between studies and even less so across ethnicities. In addition this is the first study to look for association of *PRSS56* and PACG in humans. *PRSS56* is a very attractive candidate gene based on its causation of nanophthalmos in humans and an angle-closure glaucoma phenotype in mice. In this study we aimed to investigate the association between tag SNPs of these four candidate genes and PACG in both Australian and Nepalese cohorts.

Methods

Methods in this chapter followed the same protocol as presented in **Section 2.2.** The link between *eNOS* and *MMP-9* with PACG in the Australian cohort was further analysed by comparing the combined risk alleles with the protective one using chi-square test. The results for *MMP-9* were that previously discussed in **Chapter 6**. We selected the significant SNP from each gene *eNOS* rs3793342 and *MMP-9* rs17576. The numbers of tag SNPs chosen in each gene for both cohorts are presented in **Table 7.1**.

Table 7.1. Tag SNPs, chromosome and base position in each gene included in this chapter. "Y" indicates that the tag SNP was selected to represent variation in the specified cohort, "-" tag SNP was not selected for that cohort, "Chr" chromosome.

Chr	Gene	SNP	bp Position	Australia	Nepal
2	*PRSS56*	rs1881494	233372766	Y	Y
		rs17360319	233381606	Y	-
		rs11902035	233386432	Y	Y
		rs733602	233388311	Y	Y
		rs12466358	233397525	Y	Y
		rs3828246	233398215	Y	Y
2	*CYP1B1*	rs2855658	38298203	Y	Y
		rs10916	38297170	Y	-
		rs162562	38297515	-	Y
		rs162561	38298877	-	Y
		rs2551188	38302794	Y	Y
7	*eNOS*	rs3793342	150695195	Y	-
		rs1799983	150696111	Y	Y
		rs3918227	150700946	Y	-
		rs3918186	150702432	-	Y
		rs3918188	150702781	Y	Y
		rs1808593	150708302	Y	Y
		rs7830	150709571	Y	Y
19	*NTF4*	rs12973356	49562738	Y	Y
		rs11669977	49564124	Y	Y
		rs4802546	49570686	Y	Y

Results

All cases in the Nepalese cohort presented with PACG, of which 53 cases were reported to have had an acute attack. In the Australian cohort 71 cases were identified as PACS and 129 cases as PACG (35 with previous history of acute attack). **Table 7.2** shows characteristics and clinical data of cases and controls for each cohort. The Nepalese cohort was well matched to the control group for age, sex and ethnicity, but in the Australian cohort a higher percentage of females was present in the case than the control group (p-value of <0.01). As expected, peak IOP and cup:disc ratio were significantly higher in the cases compared to the controls (p-value <0.01). The Australian cases were more hyperopic with p-value of <0.01, unlike the Nepalese cases (p-value 0.16).

Assuming complete linkage disequilibrium between the disease-causing variant and the marker, we had a power of 94% in the Australian cohort and 79% in the Nepalese cohort to detect a genotypic relative risk of 1.4 with a risk allele frequency of 0.31 under an additive model.

Table 7.2. Characteristics of the Nepalese and the Australian cohorts.

Variables	Australian			Nepalese		
	Case	**Control**	**p-value**	**Case**	**Control**	**p-value**
Number	200	288	-	106	204	-
Sex (% female)	75%	53%	<0.01	76%	75%	0.85
Mean age in years (SD)	70 (8.2)	69 (11.21)	0.28	57.3 (12.30)	60.3 (13.71)	0.07
Mean SE in dioptres (SD)	0.9 (2.15)	0.1 (0.37)	<0.01	-0.3 (1.64)	0.1 (0.31)	0.16
Mean IOP in mmHg (SD)	23.5 (12.9)	14.6 (3.4)	<0.01	21.3 (17.71)	12.8 (2.3)	<0.01
Mean Cup/disc ratio (SD)	0.5 (0.16)	0.2 (0.25)	<0.01	0.8 (0.11)	0.2 (0.12)	<0.01

SD= standard deviation; SE= spherical equivalent; IOP= intra ocular pressure.

Protease serine 56 (PRSS56)

In *PRSS56*, six tag SNPs were selected in and around the gene. SNPs rs11902035 and rs733602 are located in intronic region. SNPs rs2853444 and rs733603 did not fit in the multiplex design, and were replaced by rs1881494 and rs3828246, respectively (r^2=1 for both SNPs). The physical location is presented in **Figure 7.1**. Bonferroni correction for the 6 SNPs was 0.05/6= 0.008.

The allelic frequencies and association p-values of typed SNPs are presented in **Table 7.3.** In the Australian cohort rs11902035, C allele, showed borderline association with p-value of 0.045 (OR 1.7, 95%CI 1.0-3.0) and rs3828246, C allele, with p-value 0.011 (OR 1.4, 95%CI 1.1-1.7). Both SNPs remained significant after adjustment for sex and age (p-value 0.005 and 0.014, respectively); only rs11902035 survived correction for multiple testing (p-value 0.005). In the Nepalese cohort, one SNP rs733602 showed significant association with PACG with a p-value 0.004 (OR 0.2, 95%CI 0.1-0.7) that survived correction for multiple testing, but not after adjustment for sex and age (p-value=0.016).

In the haplotype analysis, only the Australian cohort showed significant global p-value of 0.006. Tag SNPs in around *PRSS56* gene formed one linkage disequilibrium block in the Australian cohort (**Figure 7.2**). TGTTCC showed a nominally significant association with a p-value of 0.046 (OR 1.9, 95%CI 0.9-3.7) (**Table 7.4**). In the Nepalese cohort, the TGTGTT haplotype showed an association with PACG with a p-value of 0.021 (OR 0.2, 95% CI 0.1-0.8), but did not survive correction for multiple testing.

Figure 7.1. *PRSS56* gene ideogram depicting the location of all tag SNPs genotyped. Exons are indicated by solid boxes and joined by introns indicated by lines. Figure adapted from NCBI website (http://www.ncbi.nlm.nih.gov/gene).

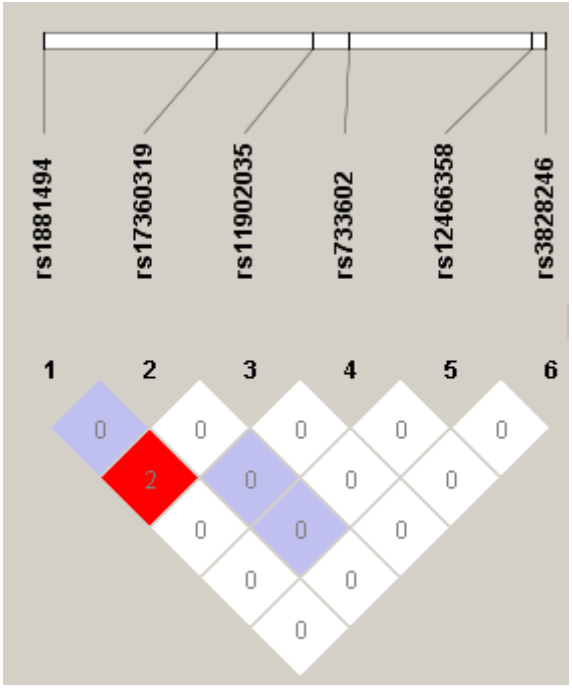

Figure 7.2. LD plot of tag SNPs in *PRSS56* gene. Linkage disequilibrium plot generated in Haploview shows the haplotype block structure using the solid spine definition in the Australian cohort. The number in the box represents the r^2 value.

Table 7.3. Allele frequencies (%) of SNPs in and around the *PRSS56* gene in the Australian and Nepalese cohorts and unadjusted p-value for association under the allelic model with odds ratio (95% CI). Values in bold are considered significant (p<0.05). Table shows the unadjusted p-value, adjusted p-value for sex and age, and combined p-value using Cochran-Mantel- Haenszel 2x2xK test.

N#	SNP	Minor Allele	Australian				Nepalese				Combined p-value
			MAF	p-value	OR (95% CI)	p*	MAF	p-value	OR (95% CI)	p*	
1	rs1881494	C	0.32	0.921	1.0 (0.8-1.3)	0.921	0.31	0.756	1.1 (0.7--1.5)	0.654	0.347
2	rs17360319	A	0.01	0.091	3.5 (0.9-16)	0.153	0.12	0.583	1.2 (0.7-2.0)	0.672	0.654
3	rs11902035	C	0.07	**0.045**	1.7 (1.0-3.0)	**0.005**	0.03	0.947	1.0 (0.4-2.6)	0.938	0.433
4	rs733602	G	0.02	0.302	1.9 (0.6-5.1)	0.291	0.02	**0.004**	0.2 (0.1-0.7)	**0.016**	0.189
5	rs12466358	C	0.20	0.659	1.1 (0.8-1.4)	0.908	0.31	0.697	0.9 (0.6-1.3)	0.689	0.355
6	rs3828246	C	0.44	**0.011**	1.4 (1.1-1.7)	**0.014**	0.35	0.228	1.2 (0.9-1.8)	0.209	0.370

p*= p-value adjusted for sex and age. OR (95% CI) = odds ratio (95% confidence interval). Chr= chromosome. MAF= minor allele frequency.

Table 7.4. Haplotype association between variants across *PRSS56* gene and primary angle-closure glaucoma in Australian and Nepalese cohorts. The nominally associated haplotype is highlighted in bold. The order of SNPs in the haplotype follow the order in Table 7.3.

Haplotype 1 2 3 4 5 6	**Australian**				**Nepalese**			
	Case	**Controls**	**OR (95%CI)**	**p-value**	**Case**	**Controls**	**OR (95%CI)**	**p-value**
T G T T C C	0.06	0.04	1.9 (0.9-3.7)	**0.046**	0.07	0.07	1.0 (0.5-2.0)	1.000
C G T T T C	0.13	0.11	0.5 (0.3-1.0)	0.271	0.06	0.06	0.9 (0.4-2.5)	0.920
T G T T T C	0.21	0.20	0.4 (0.2-0.7)	0.956	0.16	0.16	0.9 (0.5-1.6)	0.935
C G T T C T	0.04	0.04	0.3 (0.1-0.9)	0.555	0.07	0.06	1.8 (0.7-4.4)	0.318
T G T T C T	0.07	0.09	0.3 (0.1-0.6)	0.130	0.17	0.18	0.7 (0.4-1.3)	0.669
T G C T T T	0.03	0.02	0.7 (0.2-1.8)	0.277	-	-	-	-
C G T T T T	0.16	0.17	0.4 (0.2-0.7)	0.268	0.12	0.13	0.7 (0.4-1.3)	0.583
T G T T T T	0.30	0.33	0.4 (0.3-0.7)	0.081	0.30	0.26	1.2 (0.8-1.9)	0.216
T G T G T T	-	-	-	-	0.01	0.05	0.2 (0.1-0.8)	**0.021**
T A T T T T	-	-	-	-	0.04	0.04	1.1 (0.4-2.6)	0.874
	global p-value **0.006**				global p-value 0.103			

OR= odds ratio, 95% CI= 95% confidence interval.

Cytochrome P450 (CYP1B1)

In *CYP1B1*, SNPs rs2855658, rs10916, and rs162562 are located in the 3' untranslated region, while rs162561, and rs2551188 are intronic. The physical location is presented in **Figure 7.3**. Bonferroni correction for the 5 SNPs was 0.05/5= 0.01.

The allelic frequencies and association p-values of typed SNPs in the Nepalese cohort are presented in **Table 7.5**. Two nominally significant SNPs from the *CYP1B1* gene: rs10916, G allele, with odds ratio 2.1 (95%CI 1.1-4.0, p=0.022) and rs162561, A allele, with odds ratio 2.2 (95% CI 1.1-4.3, p=0.014). Both SNPs remained significant after adjustment for sex and age, but none passed correction for multiple testing.

The *CYP1B1* gene formed one linkage disequilibrium block (**Figure 7.4**). It showed a nominally significant haplotypic association in the Nepalese cohort (**Table 7.6**)**.** The AGCAC haplotype showed an association with PACG in the Nepalese cohort with a p-value of 0.019 (odds ratio 2.3, 95% CI 0.8-6.7), but did not survive correction for multiple testing. No significant association was detected in the Australian cohort in either allelic or haplotypic results.

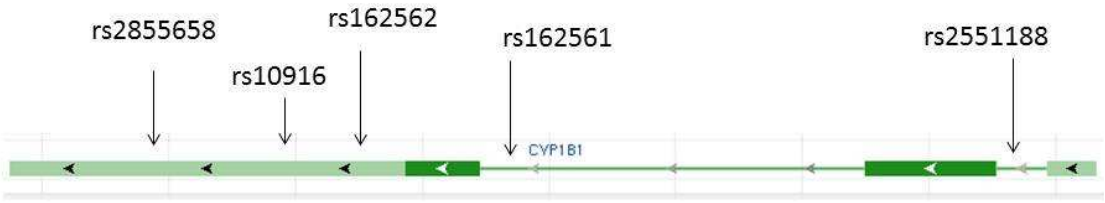

Figure 7.3. *CYP1B1* gene ideogram depicting the location of all tag SNPs genotyped. Exons are indicated by solid boxes and joined by introns indicated by lines. Figure adapted from NCBI website (http://www.ncbi.nlm.nih.gov/gene)

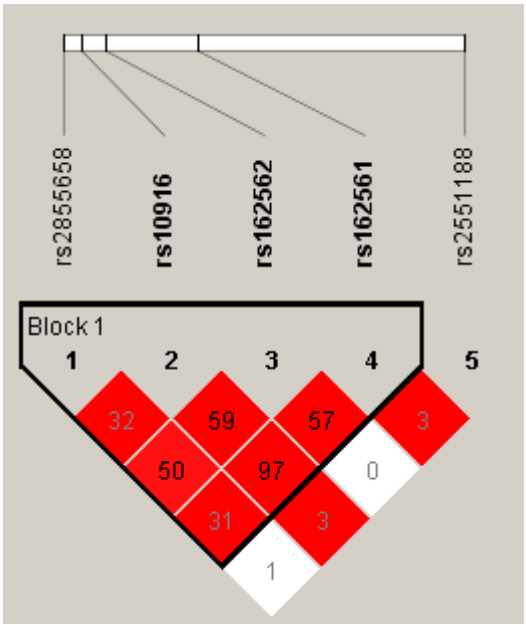

Figure 7.4. LD plot of tag SNPs in *CYP1B1* haplotype. Linkage disequilibrium plot generated in Haploview shows the haplotype block structure using the solid spine definition in the Nepalese cohort. The number in the box represents the r^2 value.

Table 7.5. Allele frequencies (%) of tag SNPs in *CYP1B1* gene in the Australian and Nepalese cohorts and unadjusted p-value for association under the allelic model with odds ratio (95% CI). Values in bold considered significant (p<0.05). Table shows the unadjusted p-value, adjusted p-value for sex and age, and combined p-value using Cochran-Mantel-Haenszel 2x2xK test

N#	SNP	Minor Allele	Australian				Nepalese				Combined
			MAF	p-value	OR (95% CI)	p*	MAF	p-value	OR (95% CI)	p*	
1	rs2855658	A	0.44	0.537	1.1 (0.8-1.4)	0.380	0.19	0.463	1.1 (0.7-1.8)	0.315	0.876
2	rs10916	G	0.21	0.714	1.1 (0.8-1.4)	0.670	0.09	**0.022**	2.1 (1.1-4.0)	**0.023**	0.542
3	rs162562	C	0.21	0.714	1.1 (0.8-1.4)	0.670	0.13	0.095	1.5 (0.9-2.6)	0.075	0.615
4	rs162561	A	0.16	0.641	1.1 (0.8-1.5)	0.800	0.10	**0.014**	2.2 (1.1-4.3)	**0.022**	0.507
5	rs2551188	T	0.28	0.716	1.0 (0.8-1.4)	0.530	0.38	0.542	1.1 (0.7-1.5)	0.625	0.919

p*= p-value adjusted for sex and age. OR (95% CI) = odds ratio (95% confidence interval). Chr= chromosome. MAF= minor allele frequency

Table 7.6. Haplotype association between variants across *CYP1B1* gene and primary angle-closure glaucoma in Australian and Nepalese cohorts. The nominally associated haplotype is highlighted in bold. The order of SNPs in the haplotypes follows the order in Table 7.5.

Haplotype 1 2 3 4 5 6	**Australian**				**Nepalese**			
	Cases	**Controls**	**p-value**	**OR (95% CI)**	**Cases**	**Controls**	**p-value**	**OR (95% CI)**
A T C C C T	-	-	-	-	0.03	0.03	0.759	0.9 (0.3-2.1)
G T A C C T	0.27	0.28	0.689	0.9 (0.7-1.3)	0.34	0.31	0.528	1.1 (0.5-2.7)
A G C C A C	0.16	0.17	0.709	0.9 (0.6-1.5)	0.09	0.04	**0.019**	2.3 (0.8-6.7)
A T A C C C	0.23	0.23	0.76	1.0 (0.7-1.4)	0.05	0.07	0.263	0.7 (0.2-2.1)
G T A C C C	0.28	0.25	0.277	1.1 (0.8-1.6)	0.47	0.52	0.239	0.9 (0.4-2.2)
A G C C C C	0.05	0.05	0.954	1.0 (0.6-1.9)	-	-	-	-
	global p-value 0.874				global p-value 0.116			

OR= odds ratio, 95% CI= 95% confidence interval.

Endothelial nitric oxide synthase (eNOS)

In *eNOS*, typed SNPs are located in the introns, except for rs1799983 and rs3918227, which are in exon 8 and 17, respectively. The physical location is presented in **Figure 7.5**. Bonferroni correction for the seven SNPs was 0.05/7= 0.007.

The minor allele frequencies and allelic association p-values of typed SNPs are presented in **Table 7.7**. In the Australian cohort three SNPs in *eNOS* were found to show significant association with PACG: rs3793342, T allele, with p-value of 0.002 (OR 1.9, 95%CI 1.3-2.8), rs3918188, A allele, with p-value of 0.013 (OR 1.4, 95%CI 1.1-1.8), and rs7830, A allele, p-value=0.011 (OR 1.4, 95%CI 1.1-1.9). Only rs3793342 survived correction for multiple testing, but not after adjustment for age and sex (p-value of 0.01). No significant associations were found in the Nepalese cohort. In the combined analysis we found rs3793342 and rs7830 to be associated with p-values of 0.012 for both SNPs.

The linkage disequilibrium structure is shown in **Figure 7.6**. Two haplotypes in the Australian cohort showed association with PACG, with a global p value of 0.011 (**Table 7.8**). The CGCAATC haplotype conferred risk, with a significant p-value of 0.005 (OR 1.1, 95%CI 0.6-2.3). This haplotype contains the risk alleles of all the three nominally associated SNPs. A second haplotype, TGCACTC with p-value of 0.022, OR 0.3 (95% CI 0.1-0.8) contains only one of the three risk alleles and appears to be protective for PACG.

When we further analysed the association between *eNOS* and *MMP-9* with PACG in the Australian cohort, a significant difference was found between individuals carrying the risk alleles of both SNPs rs17576 in *MMP-9* and rs3793342 in *eNOS* (105 individuals) with those who do carry the protective allele only (264 individuals) with p-value 0.026 (OR 2.5).

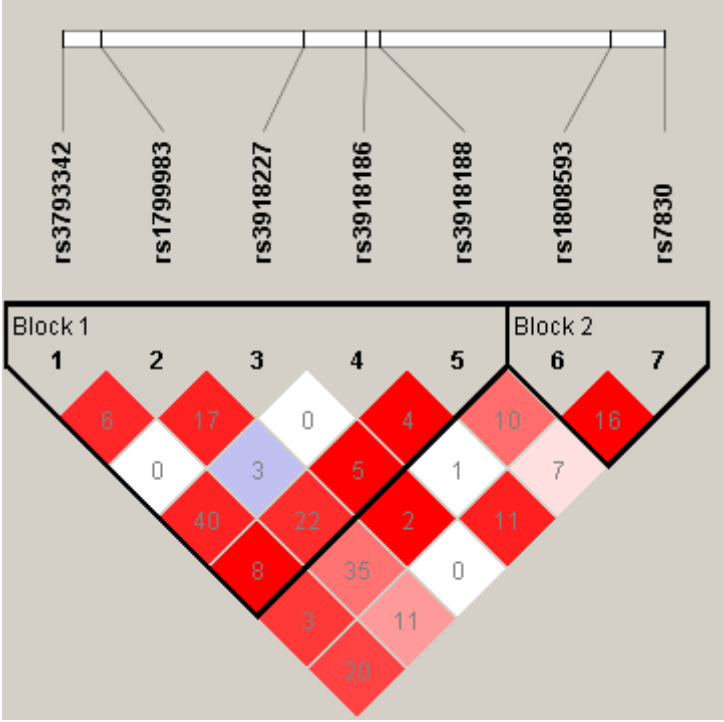

Figure 7.6. LD plot of tag SNPs in *eNOS* haplotype. Linkage disequilibrium plot generated in Haploview shows the haplotype block structure using the solid spine definition in the Australian cohort. The number in the box represents the r^2 value.

Figure 7.5. *eNOS* gene ideogram depicting the location of all tag SNPs genotyped. Exons are indicated by solid boxes and joined by introns indicated by lines. Figure adapted from NCBI website (http://www.ncbi.nlm.nih.gov/gene)

Table 7.7. Allele frequencies (%) of tag SNPs in *eNOS* gene in the Australian and Nepalese cohorts and unadjusted p-value for association under the allelic model with odds ratio (95% CI). Values in bold considered significant (p<0.05). Table shows the unadjusted p-value, adjusted p-value for sex and age, and combined p-value using Cochran-Mantel-Haenszel 2x2xK test

N#	SNP	Minor Allele	Australian				Nepalese				Combined p-value
			MAF	p-value	OR (95% CI)	p*	MAF	p-value	OR (95% CI)	p*	
1	rs3793342	T	0.09	**0.002**	1.9 (1.3-2.8)	**0.010**	0.10	0.99	1.0 (0.5-1.7)	0.95	0.012
2	rs1799983	T	0.34	0.475	1.1 (0.8-1.5)	0.620	0.19	0.73	1.0 (0.7-1.6)	0.76	0.435
3	rs3918227	A	0.10	0.186	1.4 (0.9-2.2)	0.180	0.04	0.17	1.7 (0.8-3.6)	0.22	0.725
4	rs3918186	T	0.06	0.294	1.3 (0.8-2.2)	0.250	0.11	0.92	1.0 (0.6-1.7)	0.9	0.493
5	rs3918188	A	0.41	**0.013**	1.4 (1.1-1.8)	0.080	0.33	0.87	1.0 (0.7-1.5)	0.99	0.067
6	rs1808593	G	0.25	0.334	1.2 (0.9-1.6)	0.460	0.28	0.42	1.1 (0.8-1.7)	0.46	0.214
7	rs7830	A	0.31	**0.011**	1.4 (1.1-1.9)	0.050	0.38	0.39	1.2 (0.8-1.6)	0.41	0.012

p*= p-value adjusted for sex and age. OR (95% CI) = odds ratio (95% confidence interval). Chr= chromosome. MAF= minor allele frequency.

Table 7.8. Haplotype frequencies and association between variants across *eNOS* gene and primary angle-closure glaucoma in Australian and Nepalese cohorts. The significantly associated haplotype is highlighted in bold. The orders of SNPs in the haplotype follow order in Table 7.7.

Haplotype 1 2 3 4 5 6 7	**Australian**				**Nepalese**			
	Cases	**Controls**	**p-value**	**OR (95% CI)**	**Cases**	**Controls**	**p-value**	**OR (95% CI)**
T G C T C T C	0.02	0.02	0.842	0.9 (0.3-2.7)	0.01	0.02	0.79	0.7 (0.1-3.9)
C G C A A T A	0.15	0.16	0.598	0.9 (0.4-2.1)	0.08	0.11	0.23	0.6 (0.3-1.3)
T G C T C T A	0.04	0.07	0.060	0.4 (0.1-1.1)	0.06	0.05	0.54	1.3 (0.5-3.0)
C G C A A T C	0.23	0.13	**0.005**	1.1 (0.6-2.3)	0.12	0.11	0.90	0.9 (0.5-1.6)
C G C A A G C	0.02	0.01	0.717	0.8 (0.2-3.6)	0.14	0.12	0.40	1.2 (0.6-2.1)
T G C A C T C	0.02	0.05	**0.022**	0.3 (0.1-0.8)	-	-	-	-
C T A A C T C	0.08	0.06	0.288	1.0 (0.4-2.4)	0.03	0.04	0.23	0.5 (0.1-1.4)
C G C A C T A	0.09	0.12	0.294	0.7 (0.3-1.5)	0.21	0.25	0.43	0.8 (0.5-1.3)

Table 7.8. Continue.

Haplotype	Australian				Nepalese			
1 2 3 4 5 6 7	**Cases**	**Controls**	**p-value**	**OR (95% CI)**	**Cases**	**Controls**	**p-value**	**OR (95% CI)**
T G C A C T A	0.03	0.05	0.126	0.5 (0.2-1.2)	0.01	0.01	0.69	0.6 (0.1-3.6)
C T C A C G C	0.18	0.15	0.342	1.0 (0.5-2.1)	0.13	0.1	0.34	1.2 (0.8-1.7)
C T C A C T C	0.02	0.03	0.153	0.3 (0.1-1.2)	-	-	-	-
C T C A A T C	0.01	0.01	0.502	1.3 (0.2-7.2)	-	-	-	-
C G C A C T C	0.08	0.10	0.397	0.6 (0.3-1.4)	0.15	0.13	0.41	1.2 (0.7-2.2)
C G C A C G C	0.02	0.02	0.438	0.5 (0.1-1.8)	0.01	0.02	0.73	0.5 (0.1-3.3)
C T A A C T A	0.02	0.02	0.765	0.7 (0.2-2.4)	-	-	-	-
	global p-value **0.011**				global p-value 0.867			

OR= odds ratio, 95% CI= 95% confidence interval.

Neurotrophin-4 (NTF4)

In *NTF4*, the physical location of the selected tag SNPs is presented in **Figure 7.7**. Bonferroni correction for the three SNPs was 0.05/3= 0.016. SNP rs11669977 showed a p-value of 0.042 (OR 1.5, 95%CI 1.0-2.4) in the Nepalese cohort, and a p-value of 0.175 after adjustment for sex and age. This SNP did not survive correction for multiple testing.

No associations were found in *NTF4* with PACG in the Australian cohort in the allelic results (**Table 7.9**). Haplotypic results (**Table 7.10**) showed no significance in either the Australian or the Nepalese cohort.

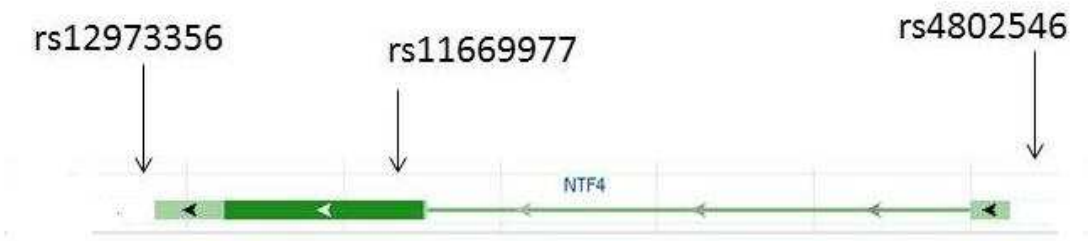

Figure 7.7. *NTF4* gene ideogram depicting the location of all tag SNPs genotyped. Exons are indicated by solid boxes and joined by introns indicated by lines. Figure adapted from NCBI website (http://www.ncbi.nlm.nih.gov/gene)

Table 7.9. Allele frequencies (%) of the tag SNPs in *NTF4* gene in the Australian and Nepalese cohorts and unadjusted p-value for association under the allelic model with odds ratio (95% CI). Values in bold considered significant (p<0.05). Table shows the unadjusted p-value, adjusted p-value for sex and age, and combined p-value using Cochran-Mantel-Haenszel 2x2xK test.

N#	SNP	Minor Allele	Australian				Nepalese				Combined
			MAF	p-value	OR (95% CI)	p*	MAF	p-value	OR (95% CI)	p*	
1	rs12973356	T	0.11	0.289	1.1 (0.9-1.5)	0.230	0.21	0.673	1.1 (0.7-1.5)	0.776	0.270
2	rs11669977	T	0.34	0.479	1.1 (0.8-1.6)	0.360	0.22	**0.042**	1.5 (1.0-2.4)	0.175	0.563
3	rs4802546	T	0.17	0.085	0.8 (0.6-1.0)	0.160	0.52	0.466	1.1 (0.8-1.5)	0.363	0.367

p*= p-value adjusted for sex and age. OR (95% CI) = odds ratio (95% confidence interval). Chr= chromosome. MAF= minor allele frequency.

Table 7.10. Haplotype association between variants across *NTF4* gene and primary angle-closure glaucoma in Australian and Nepalese cohorts. The significantly associated haplotype is highlighted in bold.

Haplotype 1 2 3	**Australian**				**Nepalese**			
	Case	**Control**	**p-value**	**OR (95% CI)**	**Case**	**Control**	**p-value**	**OR 95%CI)**
C A C	0.35	0.38	0.306	0.9 (0.6-1.1)	0.3	0.33	0.573	0.9 (0.6-1.3)
G G C	0.12	0.14	0.283	0.9 (0.6-1.4)	0.22	0.16	0.184	1.5 (0.9-2.3)
C G T	0.17	0.15	0.435	1.2 (0.8-1.8)	0.22	0.22	0.946	1.1 (0.7-1.7)
C G C	0.37	0.33	0.176	1.3 (0.9-1.7)	0.26	0.29	0.382	0.9 (0.6-1.4)
	global p-value 0.289				global p-value 0.340			

OR= odds ratio, 95% CI= 95% confidence interval.

Discussion

In this chapter, we chose four genes targeting different functions in the pathogenesis of glaucoma: development of the axial length (*PRSS56*), development of anterior chamber (*CYP1B1*), retinal ganglion cell development and survival (*NTF4)*, regulation of IOP (*eNOS*). All except for *PRSS56* have previously been implicated in POAG or PCG and have been studied as likely candidates for PACG based on their function.

As discussed in **Chapter 3** *PRSS56* has been recently reported to cause autosomal dominant nanophthalmos, and to develop a phenotype in a mouse model that resembles PACG in human (Gal, Rau et al. 2011; Nair, Hmani-Aifa et al. 2011; Orr, Dube et al. 2011) This study was first to explore this interesting candidate gene for association with PACG in human eyes. Only one rare SNP rs11902035 showed significant association in the Australian cohort. Although the global haplotype p-value was significant, none of the haplotypes showed association with the disease in the Australian cohort. In the Nepalese cohort, rs733602 showed significance with PACG; the protective allele of this SNP is only present in one out of nine haplotypes which showed borderline significance in this population.

CYP1B1 is well known for its association with primary congenital glaucoma (PCG). It is expressed in tissues of the anterior chamber of the eye such as ciliary body, iris and trabecular meshwork. Previous studies have looked for association of rare variants with PACG in an Indian population (Liao, Wang et al. 2011) and in a Middle Eastern cohort using sequencing methodology. (Abu-Amero, Morales et al.

2007) Here we genotyped tag SNPs to look for common variations within the gene. Our study showed a nominal association in the Nepalese cohort under both single SNP and haplotypic analyses. However this SNP was not considered significant when the number of tests conducted in this study were taken into account. Using rs162561 to determine the strength of this association, we had a power of 86% to detect a genotypic relative risk of 2.1 with a risk allele frequency of 0.09 under an additive model. Thus, replication of these results will be required to confirm this putative association. No statistically significant association was found in the Australian cohort.

Variants in *eNOS* showed significant association with PACG in the Australian cohort in both allelic and haplotypic results. Since nitric oxide enhances the activity of *MMP-9*, (Dumont, Loufrani et al. 2007) we looked at the link between *MMP-9* and *eNOS*. Both *eNOS* and *MMP-9* (**Chapter 6**) showed significant association within the same Australian cohort. Interestingly, patients carrying PACG-risk alleles at both *MMP-9* and *eNOS* associated SNPs have double the risk of developing the disease compared to carrying none. This may highlight the presence of a functional link between these two genes in causing PACG in the Australian population.

Due to a low frequency of *NTF4* variants, it has been reported to have a minor contribution in the pathogenesis of POAG. (Chen, Ng et al. 2012). An Indian study has not found associations in *NTF4* with PACG, and has reported that the most prevalent variant (p.Ala88Val) presented at a higher frequency in controls (4.91%) than in cases (2.85%). (Rao, Kaur et al. 2010) This is opposite to the findings in a

large cohort of POAG. (Pasutto, Matsumoto et al. 2009) Our finding looked for common variations of *NTF4*; the Nepalese cohort did not survive correction for multiple testing and no associations were detected in the Australian cohort either. Thus we were not able to confirm the association of *NTF4* with PACG.

In conclusion, each gene is associated differently amongst the two cohorts. This could be due to the changes in the LD structure and allelic frequencies or the variation in the functional effect of the allele or genotype association with a disease. Also heterogeneous effects such as environmental factors and genetic background could play a role in this scenario. The present data indicate involvement of sequence variation in *eNOS* and *PRSS56* with PACG pathogenesis in our cohorts, and this study was the first to explore the association of the *PRSS56* candidate gene with PACG in human eyes.

Chapter 8

REPLICATION OF GENETIC VARIANTS FROM A RECENTLY PUBLISHED GENOME-WIDE ASSOCIATION STUDY

Introduction

Recently in August 2012, a large two-staged GWAS for PACG were published. The discovery stage consisted of 1,854 Asian PACG cases and 9,608 controls recruited from Singapore, Hong Kong, India, Malaysia, and Vietnam. Genome-wide genotyping was performed using the Illumina 610K Quad beadchips (www.illumina.com). The replication stage included 1,917 PACG cases and 8,943 controls recruited from China, Singapore, India, Saudi Arabia and the United Kingdom. The genotyping in this stage was performed using the Sequenom MassArray platform (www.sequenom.com). (Wilkins, Gasteiger et al. 1999).

Three susceptibility loci were detected at genome-wide significance on meta-analysis of all data from both stages: rs11024102 in *PLEKHA7;* rs3753841 in *COL11A1*, and rs1015213 located between *PCMTD1* and *ST18*.

PLEKHA7 [OMIM 612686] (*Pleckstrin homology domain-containing family A member 7*) located on Chromosome 11 is an adherens junction (AJ) protein. (Stewart, Streeten et al. 1991; Khairallah, Messaoud et al. 2002) AJ is required for organization of the epithelial architecture (Nowilaty, Khan et al. 2013) and contributes to tissue homoeostasis. (Hu, Yu et al. 2011) *PLEKHA7* is likely involved in affecting the fluid flow across the inner wall of Schlemm's canal. (Said,

Chouchene et al. 2013) It has been proposed that mutations in *PLEKHA7* could affect the fluid dynamics in the pathophysiology of angle-closure glaucoma. (Wilkins, Gasteiger et al. 1999)

COL11A1 encodes one of the two alpha chains of type Xl collagen [OMIM 120280]. Mutations in *COL11A1* cause type II Stickler and Marshall syndromes (Annunen, Korkko et al. 1999; Macgregor, Zhao et al. 2008; Richards, McNinch et al. 2012), which are congenital conditions that include high myopia and blindness from retinal detachment. (Richards, McNinch et al. 2010) The GWAS data showed the single SNP rs3753841 to be associated with PACG, and the authors have proposed that the causal variants predisposing towards PACG within *COL11A1* may alter its gene expression thus causing a reverse effect (hyperopia) to that observed in myopic eyes.

The third locus, rs1015213, is located on chromosome 8 between two genes *PCMTD1* and *ST18*, but as the associated SNP was found to be in LD with *PCMTD1*, it has been suggested as the most likely candidate gene. (Wilkins, Gasteiger et al. 1999) *PCMTD1* encodes for protein-L-isoaspartate O-methyltransferase domain-containing protein 1. Very little is known about the function of this gene, but it is expressed in ocular tissues including iris and trabecular meshwork which are involved in the pathogenesis of PACG. *PLEKHA7* and *COL11A1* have also been reported to be expressed in most ocular tissues, especially in iris and trabecular meshwork. (Wilkins, Gasteiger et al. 1999)

The GWAS study also reported a fourth locus, rs3788317, which did not reach level of genome-wide significance in the meta-analysis results. It is located in an intron of the *TXNRD2* gene (*Thioredoxin reductase 2* OMIM: 606448) on chromosome 22. Thioredoxin reductase has been recently found in the lens and reported to participate in the repair process of oxidative-damaged lens proteins/enzymes in patients with cataracts. (Yan, Lou et al. 2006) The variations within this gene may participate in the pathogenesis of PACG, since one of the clinical risk factors of PACG is change in thickness and position of the lens.

Aim

To replicate the recent GWAS results in our PACG cohorts (Australia and Nepal).

Methods

As the recent GWAS study was published in August 2012, the candidate gene analyses were conducted on a larger Australian cohort of 232 cases and 288 controls, and 106 Nepalese participants with PACG and 204 controls. All cases included in this chapter were diagnosed as having PACG only to match the phenotype described in the Asian GWAS data. SNPs for inclusion were selected from the published literature. (Wilkins, Gasteiger et al. 1999)

Initially, analyses were conducted for each cohort separately; p-values were adjusted for sex and age using multivariate analysis. Further combined analysis was then conducted using the Cochran-Mantel-Haenszel 2x2xK test to minimize the population stratification. All analyses were conducted using PLINK.

Results

Replication of the recent GWAS results was investigated using independent cohorts with PACG from Australia and Nepal. The top ranked SNPs rs3753841 (*COL11A1*), rs1015213 (located between *PCMTD1* and *ST18*), rs11024102 (*PLEKHA7*), and rs3788317 (*TXNRD2*) were genotyped. (Wilkins, Gasteiger et al. 1999)

Power calculations (Purcell, Cherny et al. 2003) were undertaken to determine if the current cohorts were sufficiently powered to detect effects of similar size to that reported in the previous GWAS. Thus we used the relative risk and allele frequency of SNP rs3753841 (*COL11A1*) from the previous paper. The overall prevalence of PACG is estimated to be 0.4% in European-derived populations. If the genotypic relative risk 1.2 and the risk allele frequency is 39% under an allelic model, we had a power of 82% to detect genetic association with the disease at α=0.05 level assuming complete linkage disequilibrium between the disease-causing variant and the marker in the Australian cohort (232 cases and 288 controls). The Nepalese sample has 106 cases and 204 controls and with a prevalence of 0.43% in this population, we had a power of 75%.

The allelic frequencies and associations were evaluated in each cohort independently as shown in **Table 8.1**. In the Australian cohort, rs3753841 (*COL11A1*) was associated under the allelic model with a p-value of 0.016 (OR 1.3, 95%CI 1.1-1.7). This association remained significant after adjustment for sex and age with p-value of 0.017. No association was observed in the Nepalese cohort for this SNP.

On the other hand, both rs1015213, located between *PCMTD1* and *ST18*, with p-value of 0.010 (OR 2.3, 95% CI 1.2-4.4), and rs11024102, *PLEKHA7* gene, with p-value of 0.041 (OR1.4, 95%CI 1.0-2.0) showed associations with the disease in the Nepalese cohort, and remained significant after adjustment for age and sex with p-values of 0.014 and 0.039, respectively.

The combined analysis of both cohorts (**Table 8.2**) showed the three SNPs were significantly associated with PACG: rs3753841 with a p-value of 0.009 (OR 1.3, 95%CI 1.1-1.6), rs1015213 with a p-value of 0.004 (OR 1.6, 95%CI 1.1-2.3), and rs11024102 with a p-value 0.035 (OR 1.2, 95%CI 1.0-1.5). SNP rs3788317 did not show association with PACG in any analysis.

The differences in the effect size of Australian, Nepalese, combined cohorts and the results from previous GWAS are presented in **Figure 8.1**, showing that the direction of association of these three SNPs is the same as the previous GWAS report.

Table 8.1. Minor allele frequencies (%) of SNPs, and allelic associations of the Australian and Nepalese cohorts with the odds ratio (95% CI). p-values <0.05 is considered significant.

Gene	Chr	SNP	Minor Allele	Australian				Nepalese			
				MAF	p-value	OR(95% CI)	p*	MAF	p-value	OR(95%CI)	p*
COL11A1	1	rs3753841	C	0.43	**0.016**	1.3 (1.1-1.7)	**0.017**	0.35	0.321	1.2 (0.8-1.7)	0.308
PCMTD1-ST18	8	rs1015213	T	0.12	0.105	1.4 (0.9-2.1)	0.157	0.10	**0.010**	2.3 (1.2-4.4)	**0.014**
PLEKHA7	11	rs11024102	C	0.31	0.312	1.1 (0.9-1.5)	0.411	0.50	**0.041**	1.4 (1.0-2.0)	**0.039**
TXNRD2	22	rs3788317	T	0.22	0.824	1.0 (0.8-1.4)	0.750	0.16	0.735	0.9 (0.6-1.4)	0.742

OR= Odds ratio, Chr =chromosome, MAF= minor allele frequency, p*= p-value adjusted for age and sex

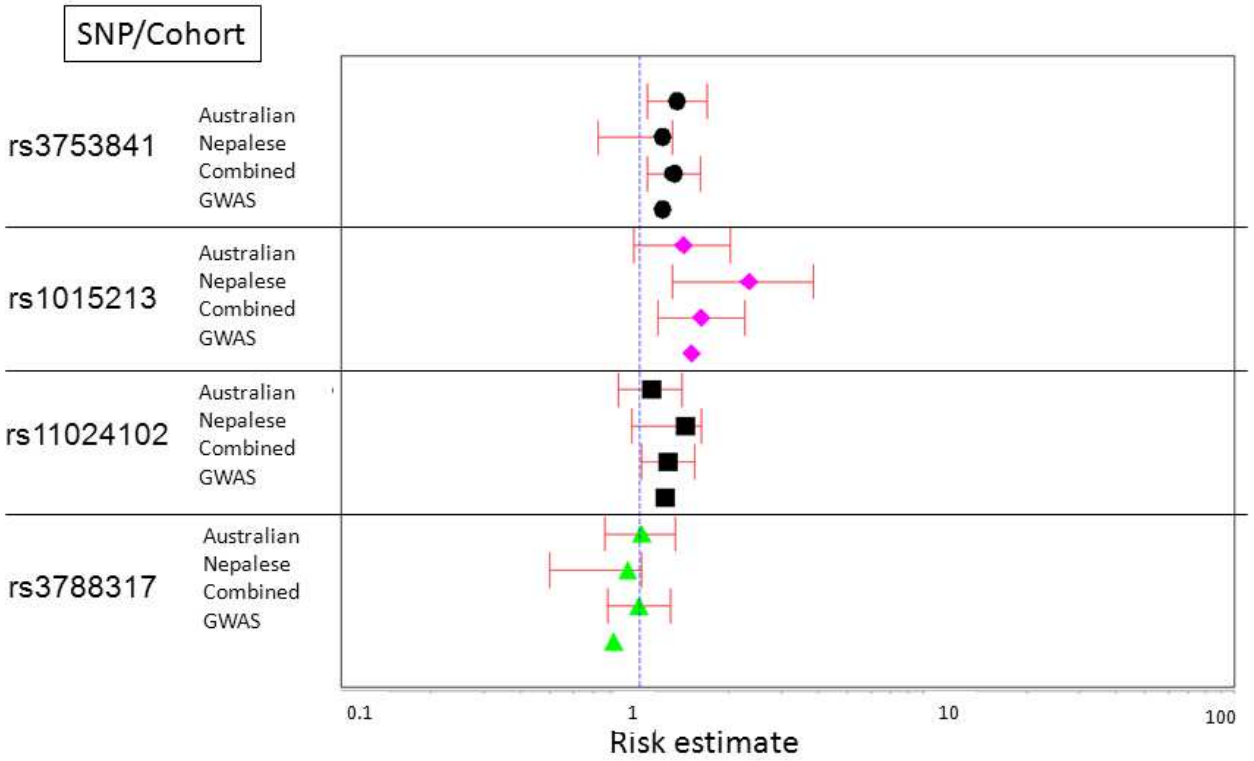

Figure 8.1. Forest plot of GWAS top ranked SNPs. The plot demonstrates the odds ratio and 95% CI of the four typed SNPs in the Australian, the Nepalese, our combined analysis and, the meta-analysis results of previous GWAS.

Table 8.2. Top ranked SNPs in our combined cohort after adjustment for population stratification, showing p-value under the additive model. p-values <0.05 are considered significant.

Gene	SNP	Minor allele	Additive	
			p-value	OR (95%CI)
COL11A1	rs3753841	C	**0.009**	1.3 (1.1-1.6)
PCMTD1-ST18	rs1015213	T	**0.004**	1.6 (1.1-2.3)
PLEKHA7	rs11024102	C	**0.035**	1.2 (1.0-1.5)
TXNRD2	rs3788317	T	0.999	1.0 (0.8-1.3)

OR = odds ratio, Chr = Chromosome, Additive p-value was analysed using Cochran-Mantel-Haenszel

Discussion

The present results support the association of rs3753841, rs1015213, and 11024102 with PACG in our cohorts, and shows that carriers of the minor alleles of these SNPs are as much as 1.5 times more likely to develop PACG. The effect size in our Australian cohort is comparable to the findings in the small UK cohort included in the published GWAS study.

SNP rs3753841 is located in the *COL11A1* gene. It is a missense mutation, situated in a coding region of the gene c.3968C>T (NM_001854.3). The previous GWAS showed the minor risk allele with a meta-analysis p-value of 9.2×10^{-10} (OR 1.20). The variant leads to changing the protein from proline to leucine (p.Pro1284Leu) which is predicted to cause no damage in the protein. This may indicate the SNP is unlikely to be the causative allele despite being a non-synonymous change, but it is

likely tagging another functional variant that is responsible of this disease. Other explanations are that either this variant has an effect at the DNA level that alters expression levels or splicing efficiency or perhaps more likely, that the bioinformatics predictions are not accurate in predicting lack of pathogenicity.

Both rs11024102 and rs3788317 are situated in an intron of the *PLEKHA7* and *TXNRD2* genes respectively. SNP rs11024102 met the criteria for genome-wide significance in the published GWAS (meta-analysis p-value of 5.33×10^{-12}, OR 1.22) and our study replicates the observed association. SNP rs3788317 did not reach genome-wide significance in the GWAS with a meta-analysis p-value of 1.73×10^{-7} (OR 0.82), but failed to replicate in either cohort in our study. We also report rs1015213 (located between *PCMTD1* and *ST18*) to be replicated in our cohorts; however, further work is required to unveil the role of this SNP in the development of PACG. We accessed the ENCODE project data (The Encyclopedia of DNA Elements) to determine if rs1015213 was located in any known regulatory elements. As at December 2012, no such elements were located at this genomic position and there is not much information can obtain from this project. (The ENCODE Project Consortium 2011)

In conclusion, this is the first study to replicate and to confirm the role of *PLEKHA7* and *COL11A1* as likely candidate genes for PACG. However further analysis is still required to identify how rs1015213 contributes to the disease. The results presented show-compelling evidence for progress in the understanding of the molecular basis of angle-closure glaucoma.

Chapter 9

DISCUSSION AND CONCLUSIONS

Understanding the genetic determinants of primary angle-closure glaucoma (PACG) is important to provide a greater understanding of the mechanisms and pathways involved in the development of the disease. It is also vital for developing better screening tests in the future which could determine those at highest risk so that appropriate screening and treatment can be made available before the disease causes blindness. This is crucial for a disease such as PACG, where more than 50% of affected individuals remain undiagnosed in developed countries. At present the complex nature of the disease and our lack in knowledge of PACG genetics, have made it impossible to move research forwards in this direction. To date ocular screening is the only way to diagnose high-risk individuals, and special attention is paid to follow-up of individuals who are angle-closure suspect who have not developed optic neuropathy or significant visual loss. Fortunately only 10% of these patients go on to develop PACG. (Wang, Wu et al. 2002)

Identifying the causative variants requires collaborative efforts as multiple genes are likely to be involved in the pathogenesis of the disease and any identified variant must be rigorously verified in different ethnic cohorts before it can be confirmed as a causative gene. Other factors such as additive effects, incomplete penetrance and environmental variables also contribute to the complexity of PACG.

Nanophthalmos was included in this project, as individuals with the disorder develop blindness at an early age secondary to angle-closure glaucoma. The pathogenesis of both PACG and nanophthalmos have been poorly understood and current established treatments for glaucoma do not reverse the pathological changes but only delay further progression of optic neuropathy and vision loss.

Identifying the genetic factors that cause nanophthalmos and PACG offer the potential not only to clarify the role of genetics as a risk factor but of also discovering new susceptibility loci for both conditions and to better understanding the pathogenesis of the disease. This thesis aimed to explore the genetic risk for the development of PACG, with a particular focus on the rare developmental disorder nanophthalmos.

Prior to this research project commencing, there was no knowledge of the genes involved in autosomal dominant nanophthalmos. We utilized a genome-wide linkage study to narrow down the linkage region, followed by exome sequencing to identify the causative variants amongst hundreds of genes. A novel coding variant in exon 8 of *TMEM98* was thus discovered. This was the first documentation of any gene likely to be causative for the autosomal dominant type of nanophthalmos. It is a potentially significant finding that verifies the original hypothesis that formed the basis of this project; however, this result must be viewed cautiously until further mutations in *TMEM98* are identified in other autosomal dominant pedigrees with nanophthalmos which are rare.

While conducting experiments to identify the novel gene *TMEM98* for autosomal dominant nanophthalmos, we screened additional nanophthalmos families for variants in either *MFRP* or *PRSS56*. We found *PRSS56* contributes to the pathogenesis in Family 2, although the second variant was not yet identified. *MFRP* was found to be mutated in Family 3 who has autosomal recessive nanophthalmos. Identifying the causative genes in only three out of twelve families indicates that *TMEM98*, *MFRP*, and *PRSS56* accounted for a minority of recruited nanophthalmos families. Future studies are required to identify the genetic cause in the remainder of the families and to investigate other candidate genes implicated in microphthalmia and/or anophthalmia (Verma and Fitzpatrick 2007) including *Paired box 6* (*PAX6*) (Glaser, Jepeal et al. 1994) *SRY (sex determining region Y)-box 2* (*SOX2*) (Fantes, Ragge et al. 2003; Williamson, Hever et al. 2006; Schneider, Bardakjian et al. 2009) *Orthodenticle homeobox 2* (*OTX2*) (Ragge, Brown et al. 2005) and *Ceh-10 homeo domain containing homolog* (*CHX10*). (Ferda Percin, Ploder et al. 2000)

Common variants in the three nanophthalmos genes (*PRSS56*, *TMEM98* and *MFRP*) were then analysed for association in an independent cohort of PACG; only *PRSS56* showed significant association that survived correction for multiple testing. The association of a nanophthalmos gene with angle-closure glaucoma pathogenesis highlights the complexity of genetic influence in both conditions. Thus future work to detect the functional role of the gene in affecting the growth and development of the eye is warranted.

Two methodological approaches, candidate gene study and GWAS, were employed

to identify novel genes for PACG in the human population. Using the candidate gene approach to analyze the association of the specific gene with the disease is one of the advantages in this study as certain genes influencing known functional pathways for a disease or trait of interest are selected. (Jorgensen, Ruczinski et al. 2009) Another advantage is the relatively low number of tests, resulting in fewer false positive results and a higher probability of finding the pathogenic variant if SNPs of known functional significance are included. However, the disadvantages of candidate gene methodology are the requirement of intimate knowledge in the relevant molecular pathways and their proteins for appropriate gene selection, and the need for results to be replicated in other cohorts to prove the genetic association with the disease. (Tabor, Risch et al. 2002) Therefore candidate genes analyses are not the optimal way to study complex diseases such as PACG. We planned to overcome this problem through conducting a GWAS as it is more effective, and provides access to the whole genome at once. Whilst we had sufficient power to detect genes of large effect size such as *LOXL1* in pseudoexfoliation syndrome, or *CFH* in age related macular degeneration, it has now been shown that the additional genetic complexity and genetic heterogeneity in angle-closure glaucoma mean that our pooled GWAS analysis had insufficient power to detect association at the genome wide significance level.

Conducting another GWAS on a larger cohort to increase the power is mandatory and currently ongoing. Meanwhile the first GWAS for PACG has been published in late 2012 using a large cohort from multiple ethnicities, predominantly Asians. Three novel susceptible loci have reached the level of genome-wide significance on meta-

analysis of all data from both stages: *PLEKHA7* rs11024102, *COL11A1* rs3753841, and rs1015213 located between *PCMTD1* and *ST18*. Our results supported the association of these three loci in our cohorts and demonstrated that carriers of the minor alleles of these SNPs are approximately 1.5 times more likely to develop PACG. The replication of associated SNPs from a large study suggests that these findings represent a true association.

The differences noted in the genetic risk amongst the two different ethnicities included in this thesis have led to difficulty in establishing specific genetic risk factors for the development of PACG. Few of the SNPs that were identified to be associated with PACG in one of the cohorts also showed association in the combined analyses. This may suggest the lack of association within the other cohort to be due to insufficient power. While most SNPs in this study did not show association in the combined analysis, indicating differences in the genetic substructure and the allelic frequencies among subpopulations. The variation of specific alleles' frequencies and difference in genetic background leads to difference in the genetic risk between ethnic groups, which can explain the variations in prevalence and incidence of the disease in one subgroup not the other. Considering these difficulties, the final chapter in which replicated association occurs in some SNPs across multiple ethnic groups indicates that these genes are likely to be playing an important role in the pathogenesis of angle-closure glaucoma.

Several limitations are inherent in this study, such as the suboptimal power of the

recruited cohorts meaning we had power only to detect association of SNPs with a frequency more than 2%. The relatively low prevalence of PACG among Australian and Nepalese populations made it difficult to build a large cohort in a limited period, as it took more than 3 years to recruit 310 cases in the Australian cohort. It is accepted that replication of all results are required in further large independent cohorts to confirm findings from this study. Another limitation was the failed assay design in a number of SNPs on the Sequenom platform, which was overcome by selecting SNPs in linkage disequilibrium with the failed ones. Blood pooling techniques used in the GWAS study suffer from several sources of error, which were offset by individual genotyping for validation, as validation provides significantly more information, but budget considerations were important in selecting appropriate experiments to further the overall goals of the thesis.

Conclusion

The identification of *TMEM98* as a potential gene for nanophthalmos, coupled with its possible role in causing PACG, is one of the most pertinent findings to arise from this thesis. Not only does it recognize *TMEM98* as a gene worthy of further investigation in terms of its function in the development of nanophthalmos, but it could validate the genetic link between both conditions.

The results obtained from this thesis have identified and refined plausible candidate genes associated with nanophthalmos and PACG. Given the findings of previous candidate genes studies and those of this thesis, it confirms that complex polygenic influences are at play in PACG. Many of the significant genes in this project are likely to have a specific role in causing PACG either through controlling IOP as in *PLEKHA7* and *eNOS* or causing hyperopic changes during ocular development such as for *PRSS56*, *HGF*, *MMP-9*, and *COL11A1*. Other genetic and environmental factors may indirectly exert their effects on PACG by directly influencing the associated risk factors. Upon confirmation of disease susceptibility of these significant genetic markers, the information can be used to predict the genetic risks of PACG by estimating a genetic risk score (GRS). A GRS can act as an independent predictor of the disease, and helps to improve risk classification for the disease. This method has been previously used to predict the genetic risk in different diseases such as age-related macular degeneration (Grassmann, Fritsche et al. 2012) type 2 diabetes (Iwata, Maeda et al. 2012) and cardiovascular diseases. (Paynter, Chasman et al. 2010)

Collaborations for studying the genetics of PACG and nanophthalmos are still ongoing. Research for this project will be continued after the completion of this thesis with the aim of conducting another GWAS on a larger Australian cohort with PACG participants and exploring the functional mechanism of *TMEM98* in causing nanophthalmos, and in screening *TMEM98* for variants in further families with autosomal dominant nanophthalmos. In the future, genetic research into PACG susceptibility will have the potential to make a direct impact on patient management by improving screening regimes in high-risk individuals. Identifying specific genetic markers for those at high risk of developing sight threatening disease could allow for earlier intervention and management, which will be helpful in minimizing the global burden of this blinding disease.

APPENDICES

Appendix 1: Primers for PCR-based amplification of coding regions of the *MFRP* gene

Primer name	Forward Primer 5'→3'	Reverse Primer 5'→3'
Exon 1,2	cccccacacagagacagagt	agccccttctgttgggtatt
Exon 3,4	agctccctggcatggtaac	tcaaggtgcctcttcctcac
Exon 5	gtgaggaagaggcaccttga	cttcctcggttagcccttct
Exon 6,7	cagtttgggggttgagaaaa	gactgagcaggaaatgctga
Exon 8	tttggcccagaacttgtttc	gacccagtgtgggaacatct
Exon 9	caccaatgatgaaagcacca	agctggagaatggaatgtgc
Exon 10,11	cttccatcacctttggcatc	gcagtacggcagtagggttc
Exon 12,13	gattcggtgacttgccaca	ctgctgatgctccttccttt

Appendix 2: Primers for PCR based amplification of coding regions of the *TMEM98* gene

Exon Number	**Forward primer 5`-3`**	**Reverse Primer 5`-3`**
Exon 1	cagggtttcaatgggacagt	tactcctttccccaacttcg
Exon 2, 3	ctggggagcaaattcttctg	ttgcccaacactgaactacg
Exon 4	atggtgtatgtgggcctcag	gctaagtgctctggcaaagg
Exon 5	tcccactctcagtggttggt	ccaagtgtcaagttaaggaaagg
Exon 6	cagctgcgatggaactcac	ggctaccccagcttccag
Exon 7	tgggtttcaggagaggactg	aagctgaggcaggagaatca
Exon 8-1	aagtctatctatttgggcttttgtg	acggtggctcaattttcttg
Exon 8-2	caaactgtggctggtgagtg	tcctcaggattcttaggctctc

Appendix 3.a: *MFRP* SNPs identified in the probands of families with nanophthalmos. Table shows genotype of the identified SNPs in each proband. F indicates the family number.

SNP/ Family	Ref allele	F2	F3	F4	F5	F6	F7	F8	F9	F10	F11	F12
rs883245	C	TT	TT	TT	TT	TT	CT	TT	CC	TT	TT	CT
rs883247	G	AA	AA	AA	AA	AA	AG	AA	GG	AA	AG	AG
rs3814762	G	GG	GA	GG	GG	GG	GA	GG	GG	GA	GG	GA
rs36015759	C	CC	CC	CC	CC	CC	CT	CC	CT	CC	CC	CC
rs2510143	T	CC	CC	CC	CC	CC	CC	CC	CT	CC	CC	CC
rs2509388	G	CC	CC	CC	CC	CC	CC	GG	CC	CC	CC	GG
rs117790326	C	CC	CC	CC	CC	CC	CC	AA	CC	CC	CC	CC
rs145719998	G	GG	GG	GG	GG	GG	GG	TT	GG	GG	GG	GG
rs145881139	G	GG	GG	GG	GG	GG	GG	GG	GT	GG	GG	GG
rs11217241	G	GG	GA	GG	GG	GG	GG	GG	GG	GG	AA	GA

Appendix 3.b: *PRSS56* SNPs identified in the probands of families with nanophthalmos. Table shows genotype of the identified SNPs in each proband. F indicates the family number.

SNP/Family	Ref allele	F2	F3	F4	F5	F6	F7	F8	F9	F10	F11	F12
rs2741294	C	CC	CC	CT	CT	TT	CT	CC	CT	CT	CC	CC
rs1550094	G	AA	GG	AG	AA	AA	AA	AG	AA	AG	AA	AA
rs116445642	C	CT	CC	CC	CC	CC	CC	CC	CC	CC	CC	CC
rs2853444	T	CC	CC	CT	CC	CC	CC	CT	CC	CC	CC	CC
rs2853445	T	TC	TT	TC	TC	TT	TC	TC	TC	TC	TT	TT
rs733603	A	GG	GG	AG	GG	GG	GG	AG	GG	GG	GG	GG
rs733602	C	CT	CC	CC	CC	CC	CT	CC	CT	CC	TT	TT
rs79792358	G	GA	GG	GG	GG	GG	GG	GG	GG	GG	GG	GG
rs285344	A	GG	GG	GA	GG	GG	GG	GA	GG	GA	GG	GG
rs2741299	T	GT	GG	GT	GG	GG	GG	GT	GG	GG	GG	GG

Appendix 4: *TMEM98* SNPs identified in the probands of families with nanophthalmos. Table shows genotype of the identified SNPs in each proband. F indicates the family number.

SNP/Families	Ref allele	F2	F4	F5	F6	F7	F8	F9	F10	F11	F12
rs75168466	-	--	-A	-A	--	--	-A	-A	--	-A	-A
rs9911256	G	GG	GG	GG	AG	GG	GG	GG	GG	GG	GG
rs72817027	G	GG	GG	GG	GG	GC	GG	GG	GG	GG	GG
rs148593533	G	GG	GG	GG	GG	GC	GG	GG	GG	GG	GG
rs29019	C	CC	CC	CC	CT	CC	CC	CC	CC	CC	CC
rs29016	G	GG	GG	GG	GA	GG	GG	GG	GG	GG	GG
rs9894694	C	CC	CC	CC	CC	CC	CC	CC	TT	CT	CT
rs28367276	C	CC	CC	CC	CC	CC	CC	CC	TT	CT	CT
rs28259	C	CC	CC	CC	TC	CC	CC	CC	CC	CC	CC
rs28258	A	AA	AA	AA	AA	AA	AA	AA	AA	AA	AA
rs28919	C	TT	TT	TT	CC	CC	CT	CT	CC	CT	CT
rs9772	C	TT	TT	TT	CC	CC	TC	TC	CC	TC	TC

REFERENCES

Abecasis, G. R., S. S. Cherny, et al. (2002). "Merlin--rapid analysis of dense genetic maps using sparse gene flow trees." Nature Genetics **30**(1): 97-101.

Abu-Amero, K. K., J. Morales, et al. (2007). "Nuclear and mitochondrial analysis of patients with primary angle-closure glaucoma." Invest Ophthalmol Vis Sci **48**(12): 5591-5596.

Adzhubei, I. A., S. Schmidt, et al. (2010). "A method and server for predicting damaging missense mutations." Nat Methods **7**(4): 248-249.

Allan, J. A., A. J. Docherty, et al. (1995). "Binding of gelatinases A and B to type-I collagen and other matrix components." Biochem J **309 (Pt 1)**: 299-306.

Alsbirk, P. H. (1976). "Primary angle-closure glaucoma. Oculometry, epidemiology, and genetics in a high risk population." Acta Ophthalmol Suppl(127): 5-31.

Alsbirk, P. H. (1992). "Anatomical risk factors in primary angle-closure glaucoma. A ten year follow up survey based on limbal and axial anterior chamber depths in a high risk population." Int Ophthalmol **16**(4-5): 265-272.

Alward, W. L., Y. H. Kwon, et al. (2003). "Evaluation of optineurin sequence variations in 1,048 patients with open-angle glaucoma." Am J Ophthalmol **136**(5): 904-910.

Amerasinghe, N., J. Zhang, et al. (2011). "The heritability and sibling risk of angle closure in Asians." Ophthalmology **118**(3): 480-485.

Annunen, S., J. Korkko, et al. (1999). "Splicing mutations of 54-bp exons in the COL11A1 gene cause Marshall syndrome, but other mutations cause overlapping Marshall/Stickler phenotypes." Am J Hum Genet **65**(4): 974-983.

Aung, T., M. C. Lim, et al. (2008). "Molecular analysis of CHX10 and MFRP in Chinese subjects with primary angle closure glaucoma and short axial length eyes." Mol Vis **14**: 1313-1318.

Aung, T., W. P. Nolan, et al. (2005). "Anterior chamber depth and the risk of primary angle closure in 2 East Asian populations." Arch Ophthalmol **123**(4): 527-532.

Aung, T., S. L. Tow, et al. (2000). "Trabeculectomy for acute primary angle closure." Ophthalmology **107**(7): 1298-1302.

Aung, T., V. H. Yong, et al. (2008). "Lack of association between the rs2664538 polymorphism in the MMP-9 gene and primary angle closure glaucoma in Singaporean subjects." J Glaucoma **17**(4): 257-258.

Awadalla, M. S., K. P. Burdon, et al. (2011). "Matrix metalloproteinase-9 genetic variation and primary angle closure glaucoma in a Caucasian population." Mol Vis **17**: 1420-1424.

Ayala-Ramirez, R., F. Graue-Wiechers, et al. (2006). "A new autosomal recessive syndrome consisting of posterior microphthalmos, retinitis pigmentosa, foveoschisis, and optic disc drusen is caused by a MFRP gene mutation." Mol Vis **12**: 1483-1489.

Ayub, H., M. I. Khan, et al. (2010). "Association of eNOS and HSP70 gene polymorphisms with glaucoma in Pakistani cohorts." Mol Vis **16**: 18-25.

Banyai, L. and L. Patthy (1991). "Evidence for the involvement of type II domains in collagen binding by 72 kDa type IV procollagenase." FEBS Lett **282**(1): 23-25.

Barrett, J. C., B. Fry, et al. (2005). "Haploview: analysis and visualization of LD and

haplotype maps." Bioinformatics **21**(2): 263-265.
Bell, J. R. (2008). "A Simple Way to Treat PCR Products Prior to Sequencing Using ExoSAP-IT®." Biotechniques **44**(6): 834.
Bleich, L., A. Junemann, et al. (2002). "Homocysteine and risk of open angle glaucoma." J Neural Transm **109**: 1499-1504.
Boland, M. V., L. Zhang, et al. (2008). "Comparison of optic nerve head topography and visual field in eyes with open-angle and angle-closure glaucoma." Ophthalmology **115**(2): 239-245 e232.
Bonomi, L., G. Marchini, et al. (2000). "Epidemiology of angle-closure glaucoma: prevalence, clinical types, and association with peripheral anterior chamber depth in the Egna-Neumarket Glaucoma Study." Ophthalmology **107**(5): 998-1003.
Bosse, Y., F. Bacot, et al. (2009). "Identification of susceptibility genes for complex diseases using pooling-based genome-wide association scans." Hum Genet **125**(3): 305-318.
Brooks, R., N. Kizer, et al. (2010). "Polymorphisms in MMP9 and SIPA1 are associated with increased risk of nodal metastases in early-stage cervical cancer." Gynecol Oncol **116**(3): 539-543.
Burdon, K. P., S. Macgregor, et al. (2011). "Association of polymorphisms in the hepatocyte growth factor gene promoter with keratoconus." Invest Ophthalmol Vis Sci **52**(11): 8514-8519.
Burdon, K. P., S. Macgregor, et al. (2011). "Genome-wide association study identifies susceptibility loci for open angle glaucoma at TMCO1 and CDKN2B-AS1." Nat Genet **43**(6): 574-578.
Cao, D., X. Liu, et al. (2009). "Investigation of the association between CALCRL polymorphisms and primary angle closure glaucoma." Mol Vis **15**: 2202-2208.
Casson, R. J. (2008). "Anterior chamber depth and primary angle-closure glaucoma: an evolutionary perspective." Clin Experiment Ophthalmol **36**(1): 70-77.
Casson, R. J., G. Chidlow, et al. (2012). "Translational neuroprotection research in glaucoma: a review of definitions and principles." Clin Experiment Ophthalmol **40**(4): 350-357.
Chakrabarti, S., K. R. Devi, et al. (2007). "Glaucoma-associated CYP1B1 mutations share similar haplotype backgrounds in POAG and PACG phenotypes." Invest Ophthalmol Vis Sci **48**(12): 5439-5444.
Chen, J. H., H. Chen, et al. (2012). "Endophenotyping reveals differential phenotype-genotype correlations between myopia-associated polymorphisms and eye biometric parameters." Mol Vis **18**: 765-778.
Chen, L. J., T. K. Ng, et al. (2012). "Evaluation of NTF4 as a causative gene for primary open-angle glaucoma." Mol Vis **18**: 1763-1772.
Clark, A. G. (2004). "The role of haplotypes in candidate gene studies." Genet Epidemiol **27**(4): 321-333.
Cong, Y., X. Guo, et al. (2009). "Association of the single nucleotide polymorphisms in the extracellular matrix metalloprotease-9 gene with PACG in southern China." Mol Vis **15**: 1412-1417.
Craig, J. E., A. W. Hewitt, et al. (2006). "The role of the Met98Lys optineurin variant in inherited optic nerve diseases." Br J Ophthalmol **90**(11): 1420-1424.

Craig, J. E., A. W. Hewitt, et al. (2009). "Rapid inexpensive genome-wide association using pooled whole blood." Genome Res **19**(11): 2075-2080.

Crespi, J., J. A. Buil, et al. (2008). "A novel mutation confirms MFRP as the gene causing the syndrome of nanophthalmos-renititis pigmentosa-foveoschisis-optic disk drusen." Am J Ophthalmol **146**(2): 323-328.

Day, A. C., G. Baio, et al. (2012). "The prevalence of primary angle closure glaucoma in European derived populations: a systematic review." Br J Ophthalmol **96**(9): 1162-1167.

Dumont, O., L. Loufrani, et al. (2007). "Key role of the NO-pathway and matrix metalloprotease-9 in high blood flow-induced remodeling of rat resistance arteries." Arterioscler Thromb Vasc Biol **27**(2): 317-324.

Edwards, A. O., B. L. Fridley, et al. (2008). "Evaluation of clustering and genotype distribution for replication in genome wide association studies: the age-related eye disease study." PLoS One **3**(11): e3813.

Elaine K. Woo, E. K., C. J. Pavlin, et al. (1999). "Ultrasound Biomicroscopic Quantitative Analysis of Light-Dark Changes Associated With Pupillary Block." Am J Ophthalmol **127**: 43-47.

Eurocat work group (2010). "Surveillance of anophthalmia/microphthalmia in Europe 2004 –2010."

Fan, B. J., D. Y. Wang, et al. (2006). "Gene mapping for primary open angle glaucoma." Clin Biochem **39**(3): 249-258.

Fantes, J., N. K. Ragge, et al. (2003). "Mutations in SOX2 cause anophthalmia." Nature Genetics **33**(4): 461-463.

Ferda Percin, E., L. A. Ploder, et al. (2000). "Human microphthalmia associated with mutations in the retinal homeobox gene CHX10." Nature Genetics **25**(4): 397-401.

Fingert, J. H., E. Heon, et al. (1999). "Analysis of myocilin mutations in 1703 glaucoma patients from five different populations." Hum Mol Genet **8**(5): 899-905.

Flanagan, J. (1998). "Glaucoma update: epidemiology and new approaches to medical management." Ophthalmic Physiol Opt **18**(2): 126-132.

Foster, P. J., R. Buhrmann, et al. (2002). "The definition and classification of glaucoma in prevalence surveys." Br J Ophthalmol **86**: 238-242.

Foster, P. J. and G. J. Johnson (2001). "Glaucoma in China: how big is the problem?" Br J Ophthalmol **85**: 1277-1282.

Gabriel, S. B., S. F. Schaffner, et al. (2002). "The structure of haplotype blocks in the human genome." Science **296**(5576): 2225-2229.

Gal, A., I. Rau, et al. (2011). "Autosomal-recessive posterior microphthalmos is caused by mutations in PRSS56, a gene encoding a trypsin-like serine protease." Am J Hum Genet **88**(3): 382-390.

Ghazouani, L., N. Abboud, et al. (2009). "Homocysteine and methylenetetrahydrofolate reductase C677T and A1298C polymorphisms in Tunisian patients with severe coronary artery disease." J Thromb Thrombolysis **27**(2): 191-197.

Glaser, T., L. Jepeal, et al. (1994). "PAX6 gene dosage effect in a family with congenital cataracts, aniridia, anophthalmia and central nervous system defects." Nature Genetics **7**(4): 463-471.

Grassmann, F., L. G. Fritsche, et al. (2012). "Modelling the genetic risk in age-

related macular degeneration." PLoS One **7**(5): e37979.
Green, C. M., L. S. Kearns, et al. (2007). "How significant is a family history of glaucoma? Experience from the Glaucoma Inheritance Study in Tasmania." Clin Experiment Ophthalmol **35**(9): 793-799.
Han, W., M. K. Yap, et al. (2006). "Family-based association analysis of hepatocyte growth factor (HGF) gene polymorphisms in high myopia." Invest Ophthalmol Vis Sci **47**(6): 2291-2299.
Hayashi, H., N. Gotoh, et al. (2008). "Lysyl oxidase-like 1 polymorphisms and exfoliation syndrome in the Japanese population." Am J Ophthalmol **145**(3): 582-585.
He, P. M., S. He, et al. (1998). "Retinal pigment epithelial cells secrete and respond to hepatocyte growth factor." Biochem Biophys Res Commun **249**(1): 253-257.
Hewitt, A. W., D. P. Dimasi, et al. (2006). "A Glaucoma Case-control Study of the WDR36 Gene D658G sequence variant." Am J Ophthalmol **142**(2): 324-325.
Hirose, Y., K. Chiba, et al. (2008). "A functional polymorphism in THBS2 that affects alternative splicing and MMP binding is associated with lumbar-disc herniation." Am J Hum Genet **82**(5): 1122-1129.
Hmani-Aifa, M., S. Ben Salem, et al. (2009). "A genome-wide linkage scan in Tunisian families identifies a novel locus for non-syndromic posterior microphthalmia to chromosome 2q37.1." Hum Genet **126**(4): 575-587.
Hu, C., J. Q. Han, et al. (2001). "[Effects of baicalin on hepatocyte apoptosis induced by TNF-alpha and act D in rats]." Zhongguo Zhong Yao Za Zhi **26**(2): 124-127.
Hu, D. N. and R. Ritch (2001). "Hepatocyte growth factor is increased in the aqueous humor of glaucomatous eyes." J Glaucoma **10**(3): 152-157.
Hu, Z., C. Yu, et al. (2011). "A novel locus for congenital simple microphthalmia family mapping to 17p12-q12." Invest Ophthalmol Vis Sci **52**(6): 3425-3429.
Huang, E. C. and V. H. Barocas (2004). "Active iris mechanisms and pupillary block: steady-state analysis and comparison with anatomical risk factors." Ann Biomed Eng **32**: 1276-1285.
Hung, P. T. and L. H. Chou (1979). "Provocation and mechanism of angle-closure glaucoma after iridectomy." Arch Ophthalmol **97**(10): 1862-1864.
International Clearing House for Birth Defects Surveillance and Research (2010). Annual Report 2010 with data for 2008. Rome.
Ivanisevic, M., M. Erceg, et al. (2002). "The incidence and seasonal variations of acute primary angle-closure glaucoma." Coll Antropol **26**(1): 41-45.
Iwata, M., S. Maeda, et al. (2012). "Genetic risk score constructed using 14 susceptibility alleles for type 2 diabetes is associated with the early onset of diabetes and may predict the future requirement of insulin injections among Japanese individuals." Diabetes Care **35**(8): 1763-1770.
Javadiyan, S., K. P. Burdon, et al. (2012). "Elevation of serum asymmetrical and symmetrical dimethylarginine in patients with advanced glaucoma." Invest Ophthalmol Vis Sci **53**(4): 1923-1927.
Jorgensen, T. J., I. Ruczinski, et al. (2009). "Hypothesis-driven candidate gene association studies: practical design and analytical considerations." Am J Epidemiol **170**(8): 986-993.
Junemann, A. G., N. von Ahsen, et al. (2005). "C677T variant in the

methylentetrahydrofolate reductase gene is a genetic risk factor for primary open-angle glaucoma." Am J Ophthalmol **139**(4): 721-723.
Kallen, B., E. Robert, et al. (1996). "The descriptive epidemiology of anophthalmia and microphthalmia." Int J Epidemiol **25**(5): 1009-1016.
Kanski, J. (2007). Clinical Ophthalmology. London, Edinburgh : Elsevier Butterworth-Heinemann.
Karantzoulis-Fegaras, F., H. Antoniou, et al. (1999). "Characterization of the human endothelial nitric-oxide synthase promoter." J Biol Chem **274**(5): 3076-3093.
Katoh, M. (2001). "Molecular cloning and characterization of MFRP, a novel gene encoding a membrane-type frizzled-related protien." Biochem Biophys Res Commun **282**: 116-123.
Keenan, T. D., J. F. Salmon, et al. (2009). "Trends in rates of primary angle closure glaucoma and cataract surgery in England from 1968 to 2004." J Glaucoma **18**(3): 201-205.
Khairallah, M., R. Messaoud, et al. (2002). "Posterior segment changes associated with posterior microphthalmos." Ophthalmology **109**(3): 569-574.
Khan, A. O. (2006). "Recognizing posterior microphthalmos." Ophthalmology **113**(4): 718.
Khan, A. O., M. A. Aldahmesh, et al. (2007). "Recessive congenital total cataract with microcornea and heterozygote carrier signs caused by a novel missense CRYAA mutation (R54C)." Am J Ophthalmol **144**(6): 949-952.
Klein, R. J., C. Zeiss, et al. (2005). "Complement factor H polymorphism in age-related macular degeneration." Science **308**(5720): 385-389.
Knaski, J. (2008). Clinical Ophthalmology. London, Butterworth Heinemann.
Krumbiegel, M., F. Pasutto, et al. (2011). "Genome-wide association study with DNA pooling identifies variants at CNTNAP2 associated with pseudoexfoliation syndrome." Eur J Hum Genet **19**(2): 186-193.
Kumar, R. S., V. Tantisevi, et al. (2009). "Plateau iris in Asian subjects with primary angle closure glaucoma." Arch Ophthalmol **127**(10): 1269-1272.
Lam, D. S., J. S. Lai, et al. (1998). "Immediate argon laser peripheral iridoplasty as treatment for acute attack of primary angle-closure glaucoma: a preliminary study." Ophthalmology **105**(12): 2231-2236.
Li, H., J. X. Wang, et al. (2008). "Localization of a novel gene for congenital nonsyndromic simple microphthalmia to chromosome 2q11-14." Hum Genet **122**(6): 589-593.
Li, Q., J. Weng, et al. (1996). "Hepatocyte growth factor and hepatocyte growth factor receptor in the lacrimal gland, tears, and cornea." Invest Ophthalmol Vis Sci **37**(5): 727-739.
Liao, Q., D. H. Wang, et al. (2011). "Association of genetic polymorphisms of eNOS with glaucoma." Mol Vis **17**: 153-158.
Lin, P. I., J. M. Vance, et al. (2007). "No Gene Is an Island: The Flip-Flop Phenomenon." American Journal of Human Genetics **80**(3): 531-538.
Lipton, S. A., W. K. Kim, et al. (1997). "Neurotoxicity associated with dual actions of homocysteine at the N-methyl-D-aspartate receptor." Proc Natl Acad Sci U S A **94**(11): 5923-5928.
Litt, M., P. Kramer, et al. (1998). "Autosomal dominant congenital cataract associated with a missense mutation in the human alpha crystallin gene CRYAA." Hum Mol Genet **7**(3): 471-474.

Liu, Y., W. Liu, et al. (2010). "No evidence of association of heterozygous NTF4 mutations in patients with primary open-angle glaucoma." Am J Hum Genet **86**(3): 498-499; author reply 500.

Lowe, R. F. (1972). "Primary angle-closure glaucoma. Inheritance and environment." Br J Ophthalmol **56**(1): 13-20.

Mabuchi, F., S. Tang, et al. (2006). "Methylenetetrahydrofolate reductase gene polymorphisms c.677C/T and c.1298A/C are not associated with open angle glaucoma." Mol Vis **12**: 735-739.

Macgregor, S., Z. Z. Zhao, et al. (2008). "Highly cost-efficient genome-wide association studies using DNA pools and dense SNP arrays." Nucleic Acids Res **36**(6): e35.

Mandal, M. N., V. Vasireddy, et al. (2006). "Spatial and temporal expression of MFRP and its interaction with CTRP5." Invest Ophthalmol Vis Sci **47**(12): 5514-5521.

Mantzioros, N. (2006, Feb 2006). "The history of the meaning of the world glaucoma." Galucoma Australia, from http://www.glaucoma.org.au/History.pdf.

Martorina, M. (1988). "Familial nanophthalmos." J Fr Ophtalmol **11**: 357-361.

McLatchie, L. M., N. J. Fraser, et al. (1998). "RAMPs regulate the transport and ligand specificity of the calcitonin-receptor-like receptor." nature **393**: 333-339.

Michael, S., R. Qamar, et al. (2008). "C677T polymorphism in the methylenetetrahydrofolate reductase gene is associated with primary closed angle glaucoma." Mol Vis **14**: 661-665.

Micheal, S., R. Qamar, et al. (2009). "MTHFR gene C677T and A1298C polymorphisms and homocysteine levels in primary open angle and primary closed angle glaucoma." Mol Vis **15**: 2268-2278.

Monemi, S., G. Spaeth, et al. (2005). "Identification of a novel adult-onset primary open-angle glaucoma (POAG) gene on 5q22.1." Hum Mol Genet **14**(6): 725-733.

Morrison, J. and I. Pollack (2003). Glaucoma: Science and Practice. New york, Theime.

Mossbock, G., M. Weger, et al. (2006). "Methylenetetrehydrofolate reductase MTHFR 677C>T polymorphism and open angle glaucoma." Mol Vis **12**(356-9).

Mossbock, G., M. Weger, et al. (2010). "Role of functional single nucleotide polymorphisms of MMP1, MMP2, and MMP9 in open angle glaucomas." Mol Vis **16**: 1764-1770.

Mujumdar, V. S., C. M. Tummalapalli, et al. (2002). "Mechanism of constrictive vascular remodeling by homocysteine: role of PPAR." Am J Physiol Cell physiol **282**: C1009-1015.

Mukhopadhyay, N., L. Almasy, et al. (2005). "Mega2: data-handling for facilitating genetic linkage and association analyses." Bioinformatics **21**(10): 2556-2557.

Mukhopadhyay, R., P. I. Sergouniotis, et al. (2010). "A detailed phenotypic assessment of individuals affected by MFRP-related oculopathy." Mol Vis **16**: 540-548.

Nair, K. S., M. Hmani-Aifa, et al. (2011). "Alteration of the serine protease PRSS56 causes angle-closure glaucoma in mice and posterior microphthalmia in

humans and mice." Nat Genet **43**(6): 579-584.
Nath, S. D., X. He, et al. (2009). "The 27-bp repeat polymorphism in intron 4 (27 bp-VNTR) of endothelial nitric oxide synthase (eNOS) gene is associated with albumin to creatinine ratio in Mexican Americans." Mol Cell Biochem **331**(1-2): 201-205.
Natividad, A., G. Cooke, et al. (2006). "A coding polymorphism in matrix metalloproteinase 9 reduces risk of scarring sequelae of ocular Chlamydia trachomatis infection." BMC Med Genet **7**: 40.
Neufeld, A. H., M. R. Hernandez, et al. (1997). "Nitric oxide synthase in the human glaucomatous optic nerve head." Arch Ophthalmol **115**(4): 497-503.
Ng, P. C. and S. Henikoff (2001). "Predicting deleterious amino acid substitutions." Genome Res **11**(5): 863-874.
Ningli, W., Z. Wenbin, et al. (1997). "Studies of primary angle closure glaucoma in China." Yan Ke Xue Bao **13**(3): 120-124.
Nowilaty, S. R., A. O. Khan, et al. (2013). "Biometric and molecular characterization of clinically diagnosed posterior microphthalmos." Am J Ophthalmol **155**(2): 361-372 e367.
Orr, A., M. P. Dube, et al. (2011). "Mutations in a novel serine protease PRSS56 in families with nanophthalmos." Mol Vis **17**: 1850-1861.
Othman, M. I., S. A. Sullivan, et al. (1998). "Autosomal dominant nanophthalmos (NNO1) with high hyperopia and angle-closure glaucoma maps to chromosome 11." Am J Hum Genet **63**(5): 1411-1418.
Paper, W., M. Kroeber, et al. (2008). "Elevated amounts of myocilin in the aqueous humor of transgenic mice cause significant changes in ocular gene expression." Exp Eye Res **87**(3): 257-267.
Pasutto, F., T. Matsumoto, et al. (2009). "Heterozygous NTF4 mutations impairing neurotrophin-4 signaling in patients with primary open-angle glaucoma." Am J Hum Genet **85**(4): 447-456.
Pavlin, C. J., M. Easterbrook, et al. (1993). "An ultrasound biomicroscopic analysis of angle-closure glaucoma secondary to ciliochoroidal effusion in IgA nephropathy." Am J Ophthalmol **116**(3): 341-345.
Paynter, N. P., D. I. Chasman, et al. (2010). "Association between a literature-based genetic risk score and cardiovascular events in women." JAMA **303**(7): 631-637.
Pearson, J. V., M. J. Huentelman, et al. (2007). "Identification of the genetic basis for complex disorders by use of pooling-based genomewide single-nucleotide-polymorphism association studies." Am J Hum Genet **80**(1): 126-139.
Pinto, L. A., M. Depner, et al. (2010). "MMP-9 gene variants increase the risk for non-atopic asthma in children." Respir Res **11**(1): 23.
Polansky, J. R., D. J. Fauss, et al. (1997). "Cellular pharmacology and molecular biology of the trabecular meshwork inducible glucocorticoid response gene product." Ophthalmologica **211**(3): 126-139.
Purcell, S., S. S. Cherny, et al. (2003). "Genetic Power Calculator: design of linkage and association genetic mapping studies of complex traits." Bioinformatics **19**(1): 149-150.
Purcell, S., B. Neale, et al. (2007). "PLINK: a tool set for whole-genome association and population-based linkage analyses." Am J Hum Genet **81**(3): 559-575.
Quigley, H., N. Congdon, et al. (2001). "Glaucoma in China (and worldwide) :

changes in established thinking will decrease preventable blindness." Br J Ophthalmol **85**: 1271-1272.

Quigley, H. A. and A. T. Broman (2006). "the number of people with glaucoma world wide in 2010 and 2020." Br J Ophthalmol **90**(3): 262-267.

Ragge, N. K., A. G. Brown, et al. (2005). "Heterozygous mutations of OTX2 cause severe ocular malformations." American journal of human genetics **76**(6): 1008-1022.

Ramdas, W. D., L. M. van Koolwijk, et al. (2010). "A genome-wide association study of optic disc parameters." PLoS Genet **6**(6): e1000978.

Rao, K. N., I. Kaur, et al. (2010). "Variations in NTF4, VAV2, and VAV3 genes are not involved with primary open-angle and primary angle-closure glaucomas in an indian population." Invest Ophthalmol Vis Sci **51**(10): 4937-4941.

Richards, A. J., A. McNinch, et al. (2010). "Stickler syndrome and the vitreous phenotype: mutations in COL2A1 and COL11A1." Hum Mutat **31**(6): E1461-1471.

Richards, A. J., A. McNinch, et al. (2012). "Splicing analysis of unclassified variants in COL2A1 and COL11A1 identifies deep intronic pathogenic mutations." Eur J Hum Genet **20**(5): 552-558.

Rivera, A., S. A. Fisher, et al. (2005). "Hypothetical LOC387715 is a second major susceptibility gene for age-related macular degeneration, contributing independently of complement factor H to disease risk." Hum Mol Genet **14**(21): 3227-3236.

Rodriguez-Pla, A., T. H. Beaty, et al. (2008). "Association of a nonsynonymous single-nucleotide polymorphism of matrix metalloproteinase 9 with giant cell arteritis." Arthritis Rheum **58**(6): 1849-1853.

Said, M. B., E. Chouchene, et al. (2013). "Posterior microphthalmia and nanophthalmia in Tunisia caused by a founder c.1059_1066insC mutation of the PRSS56 gene." Gene.

Salmon, J. F. (1999). "Predisposing factors for chronic angle-closure glaucoma." Prog Retin Eye Res **18**(1): 121-132.

Sarfarazi, M., A. Child, et al. (1998). "Localization of the fourth locus (GLC1E) for adult-onset primary open-angle glaucoma to the 10p15-p14 region." Am J Hum Genet **62**(3): 641-652.

Sarfarazi, M. and I. Stoilov (2000). "Molecular genetics of primary congenital glaucoma." Eye (Lond) **14 (Pt 3B)**: 422-428.

Sarfarazi, M., I. Stoilov, et al. (2003). "Genetics and biochemistry of primary congenital glaucoma." Ophthalmol Clin North Am **16**(4): 543-554, vi.

Schneider, A., T. Bardakjian, et al. (2009). "Novel SOX2 mutations and genotype-phenotype correlation in anophthalmia and microphthalmia." American journal of medical genetics. Part A **149A**(12): 2706-2715.

Schwarz, J. M., C. Rodelsperger, et al. (2010). "MutationTaster evaluates disease-causing potential of sequence alterations." Nat Methods **7**(8): 575-576.

Shaffer, R. N. (1973). "A suggested anatomic classification to define the pupillary block glaucomas." Invest Ophthalmol **12**(7): 540-542.

Sharma, S., K. P. Burdon, et al. (2012). "Association of genetic variants in the TMCO1 gene with clinical parameters related to glaucoma and characterization of the protein in the eye." Invest Ophthalmol Vis Sci **53**(8): 4917-4925.

Sharmini, A. T., N. Y. Yin, et al. (2009). "Mean target intraocular pressure and progression rates in chronic angle-closure glaucoma." J Ocul Pharmacol Ther **25**(1): 71-75.

Shepard, A. R., N. Jacobson, et al. (2007). "Glaucoma-causing myocilin mutants require the Peroxisomal targeting signal-1 receptor (PTS1R) to elevate intraocular pressure." Hum Mol Genet **16**(6): 609-617.

Shibata, N., T. Ohnuma, et al. (2005). "Genetic association between matrix metalloproteinase MMP-9 and MMP-3 polymorphisms and Japanese sporadic Alzheimer's disease." Neurobiol Aging **26**(7): 1011-1014.

Sihota, R. and H. C. Agarwal (1998). "Profile of the subtypes of angle closure glaucoma in a tertiary hospital in north India." Indian J Ophthalmol **46**(1): 25-29.

Sihota, R., N. C. Lakshmaiah, et al. (2000). "Ocular parameters in the subgroups of angle closure glaucoma." Clin Experiment Ophthalmol **28**(4): 253-258.

Singh, O. S., R. J. Simmons, et al. (1982). "Nanophthalmos: a perspective on identification and therapy." Ophthalmology **89**(9): 1006-1012.

Sobel, E. and K. Lange (1996). "Descent graphs in pedigree analysis: applications to haplotyping, location scores, and marker-sharing statistics." American journal of human genetics **58**(6): 1323-1337.

Souzeau, E., I. Goldberg, et al. (2011). "Australian and New Zealand Registry of Advanced Glaucoma: methodology and recruitment." Clin Experiment Ophthalmol **40**(6): 569-575.

Spitznas, M., E. Gerke, et al. (1983). "Hereditary posterior microphthalmos with papillomacular fold and high hyperopia." Arch Ophthalmol **101**(3): 413-417.

Stamer, W. D., Y. Lei, et al. (2011). "eNOS, a pressure-dependent regulator of intraocular pressure." Invest Ophthalmol Vis Sci **52**(13): 9438-9444.

Stewart, D. H., 3rd, B. W. Streeten, et al. (1991). "Abnormal scleral collagen in nanophthalmos. An ultrastructural study." Arch Ophthalmol **109**(7): 1017-1025.

Stoilov, I., A. N. Akarsu, et al. (1997). "Identification of three different truncating mutations in cytochrome P4501B1 (CYP1B1) as the principal cause of primary congenital glaucoma (Buphthalmos) in families linked to the GLC3A locus on chromosome 2p21." Hum Mol Genet **6**(4): 641-647.

Stone, E. M., J. H. Fingert, et al. (1997). "Identification of a gene that causes primary open angle glaucoma." Science **275**(5300): 668-670.

Sundin, O. H., S. Dharmaraj, et al. (2008). "Developmental basis of nanophthalmos: MFRP is required for both prenatal ocular growth and postnatal emmotropization." Ophthalmic Genet **29**: 1-9.

Sundin, O. H., G. S. Leppert, et al. (2005). "Extreme hyperopia is the result of null mutations in MFRP, which encodes a Frizzled-related protein." Proceedings of the National Academy of Sciences of the United States of America **102**(27): 9553-9558.

Sundin, O. H., G. S. Leppert, et al. (2005). "Extreme hyperopia is the result of null mutations in MFRP, which encodes a Frizzled-related protein." Proc Natl Acad Sci U S A **102**(27): 9553-9558.

Tabor, H. K., N. J. Risch, et al. (2002). "Candidate-gene approaches for studying complex genetic traits: practical considerations." Nat Rev Genet **3**(5): 391-397.

Taniguchi, T., K. Kawase, et al. (1999). "Ocular effects of adrenomedullin." Experimental Eye Research **69**(5): 467-474.

Tarongoy, P., C. L. Ho, et al. (2009). "Angle-closure glaucoma: the role of the lens in the pathogenesis, prevention, and treatment." Surv Ophthalmol **54**(2): 211-225.

Tham, C. C., J. S. Lai, et al. (1999). "Immediate argon laser peripheral iridoplasty for acute attack of PACG (addendum to previous report)." Ophthalmology **106**(6): 1042-1043.

Thapa, S. S., I. Paudyal, et al. (2012). "A population-based survey of the prevalence and types of glaucoma in Nepal: the Bhaktapur Glaucoma Study." Ophthalmology **119**(4): 759-764.

Thapa, S. S., P. P. Rana, et al. (2011). "Rationale, methods and baseline demographics of the Bhaktapur Glaucoma Study." Clin Experiment Ophthalmol **39**(2): 126-134.

The ENCODE Project Consortium (2011). "A user's guide to the encyclopedia of DNA elements (ENCODE)." PLoS Biol **9**(4): e1001046.

Thorleifsson, G., K. P. Magnusson, et al. (2007). "Common sequence variants in the LOXL1 gene confer susceptibility to exfoliation glaucoma." Science **317**(5843): 1397-1400.

Thorleifsson, G., G. B. Walters, et al. (2010). "Common variants near CAV1 and CAV2 are associated with primary open-angle glaucoma." Nat Genet **42**(10): 906-909.

Tyagi, S. C. (1998). "Homocysteine redox receptor and regulation of extracellular matrix components in vascular cells." Am J Physiol **274**(2 Pt 1): C396-405.

Van Der Put, N. M., F. Gabreels, et al. (1998). "A second common mutation in the methylenetetrahydrofolate reductase gene: an additional risk factor for neural-tube defects?" Am J Hum Genet **62**(5): 1044-1051.

Veerappan, S., K. K. Pertile, et al. (2010). "Role of the hepatocyte growth factor gene in refractive error." Ophthalmology **117**(2): 239-245 e231-232.

Verma, A. S. and D. R. Fitzpatrick (2007). "Anophthalmia and microphthalmia." Orphanet journal of rare diseases **2**: 47.

Vijaya, L., R. George, et al. (2008). "Prevalence of primary angle-closure disease in an urban south Indian population and comparison with a rural population. The Chennai Glaucoma Study." Ophthalmology **115**(4): 655-660 e651.

Vingolo, E. M., K. Steindl, et al. (1994). "Autosomal dominant simple microphthalmos." J Med Genet **31**(9): 721-725.

Walland, M. J. (2004). "Glaucoma treatment in Australia: changing patterns of therapy" Clin Exp Ophthal **32**(6): 590-596.

Wang, I. J., T. H. Chiang, et al. (2006). "The association of single nucleotide polymorphisms in the MMP-9 genes with susceptibility to acute primary angle closure glaucoma in Taiwanese patients." Mol Vis **12**: 1223-1232.

Wang, I. J., S. Lin, et al. (2008). "The association of membrane frizzled-related protein (MFRP) gene with acute angle-closure glaucoma--a pilot study." Mol Vis **14**: 1673-1679.

Wang, N., H. Wu, et al. (2002). "Primary angle closure glaucoma in Chinese and Western populations." Chin Med J (Engl) **115**(11): 1706-1715.

Weisberg, I. S., P. F. Jacques, et al. (2001). "The 1298A-->C polymorphism in methylenetetrahydrofolate reductase (MTHFR): in vitro expression and

association with homocysteine." Atherosclerosis **156**(2): 409-415.
Weng, J., Q. Liang, et al. (1997). "Hepatocyte growth factor, keratinocyte growth factor, and other growth factor-receptor systems in the lens." Invest Ophthalmol Vis Sci **38**(8): 1543-1554.
Wiggs, J. L., R. R. Allingham, et al. (1998). "Prevalence of mutations in TIGR/Myocilin in patients with adult and juvenile primary open-angle glaucoma." Am J Hum Genet **63**(5): 1549-1552.
Wiggs, J. L., J. H. Kang, et al. (2011). "Common variants near CAV1 and CAV2 are associated with primary open-angle glaucoma in Caucasians from the USA." Hum Mol Genet **20**(23): 4707-4713.
Wiggs, J. L., B. L. Yaspan, et al. (2012). "Common variants at 9p21 and 8q22 are associated with increased susceptibility to optic nerve degeneration in glaucoma." PLoS Genet **8**(4): e1002654.
Wilkins, M. R., E. Gasteiger, et al. (1999). "Protein identification and analysis tools in the ExPASy server." Methods Mol Biol **112**: 531-552.
Williamson, K. A., A. M. Hever, et al. (2006). "Mutations in SOX2 cause anophthalmia-esophageal-genital (AEG) syndrome." Human molecular genetics **15**(9): 1413-1422.
Wong, T. T., C. Sethi, et al. (2002). "Matrix metalloproteinases in disease and repair processes in the anterior segment." Surv Ophthalmol **47**(3): 239-256.
Woo, S. J., J. Y. Kim, et al. (2009). "Investigation of the association between 677C>T and 1298A>C 5,10 methylenetetrahydrofolate reductase gene polymorphisms and normal tension glaucoma" Eye **23**: 17-24.
Wordinger, R. J., A. F. Clark, et al. (1998). "Cultured human trabecular meshwork cells express functional growth factor receptors." Invest Ophthalmol Vis Sci **39**(9): 1575-1589.
Yamada, K., Z. Chen, et al. (2001). "Effects of common polymorphisms on the properties of recombinant human methylenetetrahydrofolate reductase." Proc Natl Acad Sci U S A **98**(26): 14853-14858.
Yan, H., M. F. Lou, et al. (2006). "Thioredoxin, thioredoxin reductase, and alpha-crystallin revive inactivated glyceraldehyde 3-phosphate dehydrogenase in human aged and cataract lens extracts." Mol Vis **12**: 1153-1159.
Yanovitch, T., Y. J. Li, et al. (2009). "Hepatocyte growth factor and myopia: genetic association analyses in a Caucasian population." Mol Vis **15**: 1028-1035.
Yong, H. K., H. F. John, et al. (2009). "Mechanism of disease.Primary open angle glaucoma." N Eng J Med **360**: 1113-1124.
Young, T. L., R. Metlapally, et al. (2007). "Complex trait genetics of refractive error." Arch Ophthalmol **125**(1): 38-48.
Yousufzai, S. Y., N. Ali, et al. (1999). "Effects of adrenomedullin on cyclic AMP formation and on relaxation in iris sphincter smooth muscle." Invest Ophthalmol Vis Sci **40**(13): 3245-3253.
Yu, C., Z. Hu, et al. (2009). "Clinical and genetic features of a dominantly-inherited microphthalmia pedigree from China." Molecular vision **15**: 949-954.
Zenteno, J. C., B. Buentello-Volante, et al. (2009). "Compound heterozygosity for a novel and a recurrent MFRP gene mutation in a family with the nanophthalmos-retinitis pigmentosa complex." Mol Vis **15**: 1794-1798.